

Survey of period variations of superhumps in SU UMa-type dwarf novae. VIII. The eighth year (2015–2016)

Taichi KATO,^{1,*} Franz-Josef HAMBSCH,^{2,3,4} Berto MONARD,^{5,6}
Tonny VANMUNSTER,⁷ Yutaka MAEDA,⁸ Ian MILLER,⁹ Hiroshi ITOH,¹⁰
Seiichiro KIYOTA,¹¹ Keisuke ISOGAI,¹ Mariko KIMURA,¹ Akira IMADA,¹²
Tamás TORDAI,¹³ Hidehiko AKAZAWA,¹⁴ Kenji TANABE,¹⁴ Noritoshi OTANI,¹⁴
Minako OGI,¹⁴ Kazuko ANDO,¹⁴ Naoki TAKIGAWA,¹⁴ Pavol A. DUBOVSKY,¹⁵
Igor KUDZEJ,¹⁵ Sergey Yu. SHUGAROV,^{16,17} Natalia KATYSHEVA,¹⁶
Polina GOLYSHEVA,¹⁶ Natalia GLADILINA,¹⁸ Drahomir CHOCHOL,¹⁷
Peter STARR,¹⁹ Kiyoshi KASAI,²⁰ Roger D. PICKARD,^{21,22}
Enrique de MIGUEL,^{23,24} Naoto KOJIGUCHI,²⁵ Yuki SUGIURA,²⁵
Daiki FUKUSHIMA,²⁵ Eiji YAMADA,²⁵ Yusuke UTO,²⁵ Taku KAMIBETSUNAWA,²⁵
Taiki TATSUMI,²⁵ Nao TAKEDA,²⁵ Katsura MATSUMOTO,²⁵ Lewis M. COOK,²⁶
Elena P. PAVLENKO,²⁷ Julia V. BABINA,²⁷ Nikolaj V. PIT,²⁷
Oksana I. ANTONYUK,²⁷ Kirill A. ANTONYUK,²⁷ Aleksei A. SOSNOVSKIJ,²⁷
Aleksei V. BAKLANOV,²⁷ Stella KAFKA,²⁸ William STEIN,²⁹
Irina B. VOLOSHINA,¹⁶ Javier RUIZ,^{30,31,32} Richard SABO,³³ Shawn DVORAK,³⁴
Geoff STONE,²⁸ Maksim V. ANDREEV,^{35,36} Sergey V. ANTIPIN,^{16,18}
Alexandra M. ZUBAREVA,^{18,16} Anna M. ZAOSTROJNYKH,³⁷
Michael RICHMOND,³⁸ Jeremy SHEARS,^{21,39} Franky DUBOIS,⁴⁰
Ludwig LOGIE,⁴⁰ Steve RAU,⁴⁰ Siegfried VANAVERBEKE,⁴⁰ Andrei SIMON,⁴¹
Arto OKSANEN,⁴² William N. GOFF,⁴³ Greg BOLT,⁴⁴ Bartłomiej DĘBSKI,⁴⁵
Christopher S. KOCHANEK,⁴⁶ Benjamin SHAPPEE,⁴⁶ Krzysztof Z. STANEK,⁴⁶
José L. PRIETO,^{47,48} Rod STUBBINGS,⁴⁹ Eddy MUYLLAERT,⁵⁰
Mitsutaka HIRAGA,⁵¹ Tsuneo HORIE,⁵² Patrick SCHMEER,⁵³
and Kenji HIROSAWA⁵⁴

¹Department of Astronomy, Kyoto University, Kyoto 606-8502, Japan

²Groupe Européen d'Observations Stellaires (GEOS), 23 Parc de Levesville, 28300 Bailleul l'Évêque, France

³Bundesdeutsche Arbeitsgemeinschaft für Veränderliche Sterne (BAV), Munsterdamm 90, 12169 Berlin, Germany

⁴Vereniging Voor Sterrenkunde (VVS), Oude Bleken 12, 2400 Mol, Belgium

⁵Bronberg Observatory, Center for Backyard Astrophysics Pretoria, PO Box 11426, Tiegterpoort 0056, South Africa

⁶Klein Karoo Observatory, Center for Backyard Astrophysics Klein Karoo, St Helena 1B, PO Box 281, Calitzdorp 6660, South Africa

⁷Center for Backyard Astrophysics Belgium, Walhostraat 1A, B-3401 Landen, Belgium

⁸Kaminishiyamamachi 12-14, Nagasaki, Nagasaki 850-0006, Japan

- ⁹Furzehill House, Ilston, Swansea, SA2 7LE, UK
- ¹⁰Variable Star Observers League in Japan (VSOLJ), 1001-105 Nishiterakata, Hachioji, Tokyo 192-0153, Japan
- ¹¹VSOLJ, 7-1 Kitahatsutomi, Kamagaya, Chiba 273-0126, Japan
- ¹²Kwasan and Hida Observatories, Kyoto University, Yamashina, Kyoto 607-8471, Japan
- ¹³Polaris Observatory, Hungarian Astronomical Association, Laborc utca 2/c, 1037 Budapest, Hungary
- ¹⁴Department of Biosphere-Geosphere System Science, Faculty of Informatics, Okayama University of Science, 1-1 Ridai-cho, Okayama, Okayama 700-0005, Japan
- ¹⁵Vihorlat Observatory, Mierova 4, 06601 Humenne, Slovakia
- ¹⁶Sternberg Astronomical Institute, Lomonosov Moscow State University, Universitetsky Ave., 13, Moscow 119992, Russia
- ¹⁷Astronomical Institute of the Slovak Academy of Sciences, 05960 Tatranska Lomnica, Slovakia
- ¹⁸Institute of Astronomy, Russian Academy of Sciences, Moscow 119017, Russia
- ¹⁹Warrumbungle Observatory, Tenby, 841 Timor Rd, Coonabarabran NSW 2357, Australia
- ²⁰Baselstrasse 133D, CH-4132 Muttenz, Switzerland
- ²¹The British Astronomical Association, Variable Star Section (BAA VSS), Burlington House, Piccadilly, London, W1J 0DU, UK
- ²²The Birches, Shobdon, Leominster, Herefordshire, HR6 9NG, UK
- ²³Departamento de Física Aplicada, Facultad de Ciencias Experimentales, Universidad de Huelva, 21071 Huelva, Spain
- ²⁴Center for Backyard Astrophysics, Observatorio del CIECEM, Parque Dunar, Matalascañas, 21760 Almonte, Huelva, Spain
- ²⁵Osaka Kyoiku University, 4-698-1 Asahigaoka, Osaka 582-8582, Japan
- ²⁶Center for Backyard Astrophysics Concord, 1730 Helix Ct. Concord, CA 94518, USA
- ²⁷Federal State Budget Scientific Institution “Crimean Astrophysical Observatory of RAS”, Nauchny, 298409, Republic of Crimea
- ²⁸American Association of Variable Star Observers, 49 Bay State Rd., Cambridge, MA 02138, USA
- ²⁹6025 Calle Paraiso, Las Cruces, NM 88012, USA
- ³⁰Observatorio de Cantabria, Ctra. de Rocamundo s/n, Valderredible, 39220 Cantabria, Spain
- ³¹Instituto de Física de Cantabria (CSIC-UC), Avenida Los Castros s/n, E-39005 Santander, Cantabria, Spain
- ³²Agrupación Astronómica Cantabria, Apartado 573, 39080, Santander, Spain
- ³³2336 Trailcrest Dr., Bozeman, MT 59718, USA
- ³⁴Rolling Hills Observatory, 1643 Nightfall Drive, Clermont, FL 34711, USA
- ³⁵Terskol Branch of Institute of Astronomy, Russian Academy of Sciences, 361605, Peak Terskol, Kabardino-Balkaria Republic, Russia
- ³⁶International Center for Astronomical, Medical and Ecological Research of NASU, Ukraine 27 Akademika Zabolotnoho Str. 03680 Kyiv, Ukraine
- ³⁷Institute of Physics, Kazan Federal University, Ulitsa Kremlevskaya 16a, Kazan 420008, Russia
- ³⁸Physics Department, Rochester Institute of Technology, Rochester, NY 14623, USA
- ³⁹“Pemberton”, School Lane, Bunbury, Tarporley, Cheshire, CW6 9NR, UK
- ⁴⁰Public observatory Astrolab Iris, Verbrandemolenstraat 5, B 8901 Zillebeke, Belgium
- ⁴¹Taras Shevchenko National University of Kyiv, the Faculty of Physics, Astronomy and Space Physics Department, 64/13, Volodymyrska Street, Kyiv 01601, Ukraine
- ⁴²Hankasalmi observatory, Jyvaskylan Sirius ry, Verkkoniementie 30, FI-40950 Muurame, Finland
- ⁴³13508 Monitor Ln., Sutter Creek, CA 95685, USA
- ⁴⁴Camberwarra Drive, Craigie, Western Australia 6025, Australia
- ⁴⁵Astronomical Observatory, Jagiellonian University, ul. Orła 171 30-244 Kraków, Poland
- ⁴⁶Department of Astronomy, the Ohio State University, Columbia, OH 43210, USA
- ⁴⁷Núcleo de Astronomía de la Facultad de Ingeniería, Universidad Diego Portales, Av. Ejército 441, Santiago, Chile
- ⁴⁸Department of Astrophysical Sciences, Princeton University, NJ 08544, USA

⁴⁹Tetoora Observatory, 2643 Warragul-Korumburra Road, Tetoora Road, VIC 3821, Australia

⁵⁰Vereniging Voor Sterrenkunde (VVS), Moffelstraat 13 3370 Boutersem, Belgium

⁵¹19-27 Higashikannon-cho, Shimonoseki, Yamaguchi 752-0906, Japan

⁵²759-10 Tokawa, Hadano-shi, Kanagawa 259-1306, Japan

⁵³Bischmisheim, Am Probstbaum 10, 66132 Saarbrücken, Germany

⁵⁴216-4 Maeda, Inazawa-cho, Inazawa-shi, Aichi 492-8217, Japan

*E-mail: tkato@kustastro.kyoto-u.ac.jp

Received 2016 April 5; Accepted 2016 May 20

Abstract

Continuing the project described by Kato et al. (2009, PASJ, 61, S395), we collected times of superhump maxima for 128 SU UMa-type dwarf novae observed mainly during the 2015–2016 season and characterized these objects. The data have improved the distribution of orbital periods, the relation between the orbital period and the variation of superhumps, and the relation between period variations and the rebrightening type in WZ Sge-type objects. Coupled with new measurements of mass ratios using growing stages of superhumps, we now have a clearer and statistically greatly improved evolutionary path near the terminal stage of evolution of cataclysmic variables. Three objects (V452 Cas, KK Tel, and ASASSN-15cl) appear to have slowly growing superhumps, which is proposed to reflect the slow growth of the 3:1 resonance near the stability border. ASASSN-15sl, ASASSN-15ux, SDSS J074859.55+312512.6, and CRTS J200331.3–284941 are newly identified eclipsing SU UMa-type (or WZ Sge-type) dwarf novae. ASASSN-15cy has a short (~ 0.050 d) superhump period and appears to belong to EI Psc-type objects with compact secondaries having an evolved core. ASASSN-15gn, ASASSN-15hn, ASASSN-15kh, and ASASSN-16bu are candidate period bouncers with superhump periods longer than 0.06 d. We have newly obtained superhump periods for 79 objects and 13 orbital periods, including periods from early superhumps. In order that future observations will be more astrophysically beneficial and rewarding to observers, we propose guidelines on how to organize observations of various superoutbursts.

Key words: accretion, accretion disks — novae, cataclysmic variables — stars: dwarf novae

1 Introduction

This paper is one of a series of papers (Kato et al. 2009, 2010, 2012, 2013a, 2014a, 2014b, 2015a) dealing with superhumps in SU UMa-type dwarf novae (DNe). SU UMa-type dwarf novae are a class of cataclysmic variables (CVs) which are close binary systems transferring matter from a low-mass dwarf secondary to a white dwarf, forming an accretion disk. In SU UMa-type dwarf novae, two types of outbursts are seen: normal outbursts and superoutbursts. During superoutbursts, small-amplitude variations with periods of a few percent longer than the orbital period (P_{orb}), called superhumps, are observed. These superhumps are considered to be a result of the precession of the eccentric (or flexing) disk deformed by the tidal instability at the 3:1 resonance (see e.g., Whitehurst 1988; Hirose & Osaki 1990; Lubow 1991; Wood et al. 2011;

for general information of CVs, DNe, SU UMa-type dwarf novae and superhumps, see e.g., Warner 1995a).

In recent years, it has been demonstrated that the periods of superhumps systematically vary during superoutburst, and Kato et al. (2009) introduced superhump stages (stages A, B, and C): the initial growing stage with a long period (stage A), the fully developed stage with a systematically varying period (stage B), and the later stage (stage C) with a shorter, almost constant period (see figure 1). Although the origin of these stages was unknown at the time of Kato et al. (2009), the phenomenon has been repeatedly confirmed by observations reported in Kato et al. (2010, 2012, 2013a, 2014a, 2014b, 2015a). Quite recently, partly with the help of Kepler (Koch et al. 2010) observations, Osaki and Kato (2013b) proposed that stage A superhumps reflect

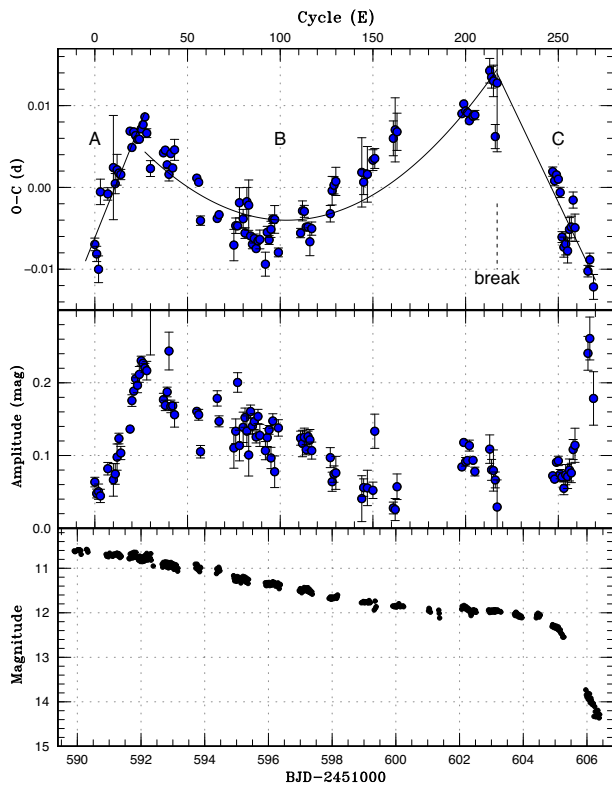


Fig. 1. Representative $O-C$ diagram showing three stages (A–C) of $O-C$ variation. The data were taken from the 2000 superoutburst of SWUMa. Upper: $O-C$ diagram. Three distinct stages (A: evolutionary stage with a longer superhump period; B: middle stage; C: stage after transition to a shorter period) and the location of the period break between stages B and C are shown. Middle: Amplitude of superhumps. During stage A, the amplitude of the superhumps grew. Lower: Light curve. (Reproduction of figure 1 in Kato & Osaki 2013b.) (Color online)

the dynamical precession rate at the 3:1 resonance radius and that the rapid decrease of the period (stage B) reflects the pressure effect which has an effect of retrograde precession (Lubow 1992; Hirose & Osaki 1993; Murray 1998; Montgomery 2001; Pearson 2006). Kato and Osaki (2013b) further extended this interpretation and confirmed that stage A superhumps indeed reflect the dynamical precession rate at the 3:1 resonance radius by using objects with mass ratios (q) established by eclipse observations. After this physical identification of the superhump stages, observations of superhumps during superoutbursts became an important tool not only for diagnosing the accretion disk but also for obtaining q values, which are most essential in understanding the nature of binaries and their evolutions. Applications of the stage A superhump method have been numerous: e.g., Kato et al. (2013b, 2014c), Nakata et al. (2013, 2014), and Ohshima et al. (2014).

Outbursts and superoutbursts in SUUMa-type dwarf novae are considered to be a result of the combination of thermal and tidal instabilities [thermal–tidal instability

(TTI) model by Osaki (1989, 1996)]. Although there have been claims for other mechanisms [the enhanced mass-transfer model (Smak 1991) and pure thermal instability model (Cannizzo et al. 2010)], it has been demonstrated using Kepler observations of V1504 Cyg and V344 Lyr that the TTI model is the best one to explain the observations (Osaki & Kato 2013a; see also Osaki & Kato 2014).

In this paper, we report observations of superhumps and associated phenomena in SUUMa-type dwarf novae whose superoutbursts were observed mainly in 2015–2016. We present basic observational materials and discussions in relation to individual objects. Starting from Kato et al. (2014b), we have intended these series of papers to also be a source of compiled information, including historical, of individual dwarf novae.

The material and methods of analysis are given in section 2, the observations and analysis of individual objects are given in section 3, including discussions particular to the objects, the general discussion is given in section 4, and the summary is given in section 5. Some tables and figures are only available online.

2 Observation and analysis

The data were obtained under campaigns led by the VSNET Collaboration (Kato et al. 2004b). We also used the public data for some objects from the AAVSO International Database.¹ Outburst detections heavily relied on the ASAS-SN CV patrol (Davis et al. 2015),² and the Catalina Real-time Transient Survey (CRTS: Drake et al. 2009),³ in addition to outburst detections reported to VSNET, AAVSO,⁴ BAAVSS alert,⁵ and cvnet-outburst.⁶ There were some detections by the MASTER network (Gorbovskey et al. 2013).

The majority of the data were acquired by time-resolved CCD photometry by using 30-cm class telescopes located world-wide. The details of these observations will be presented in future papers dealing with the analysis and discussion of individual objects of interest. The list of outbursts and observers is summarized in table 1. The data analysis was performed in the same way as described in Kato et al. (2009, 2014b) and we mainly used R software for data analysis.⁷ In de-trending the data, we used both lower (1st–3rd order) polynomial fitting and locally

¹ (<http://www.aavso.org/data-download>).

² (<http://cv.asasn.astronomy.ohio-state.edu/>).

³ (<http://nesssi.cacr.caltech.edu/catalina/>). For the information of the individual Catalina CVs, see (<http://nesssi.cacr.caltech.edu/catalina/AllCV.html>).

⁴ (<https://www.aavso.org/>).

⁵ (<https://groups.yahoo.com/neo/groups/baavss-alert/info>).

⁶ (<https://groups.yahoo.com/neo/groups/cvnet-outburst/info>).

⁷ The R Foundation for StatisticAL Computing (<http://cran.r-project.org/>).

Table 1. List of superoutbursts.

Subsection	Object	Year	Observers or references*	ID [†]
3.1	KV And	2015	DPV, RPc, Rui	
3.2	EG Aqr	2015	Aka, Kis	
3.3	NN Cam	2015	DPV, NKa, Aka, Trt	
3.5	V452 Cas	2016	RPc, IMi, Trt	
3.6	V1040 Cen	2015	HaC	
3.4	PU CMa	2016	GBo, Aka, Kis, SPE	
3.7	AL Com	2015	Kimura et al. (2016a)	
3.8	VW CrB	2015	Kis, Dub	
3.9	V550 Cyg	2015	Mdy	
–	V1006 Cyg	2015	Kato et al. (2016a)	
3.10	V1028 Cyg	2016	Aka, RPc, Trt	
3.11	V1113 Cyg	2015	Trt, Ter, Kai, Shu, COO, DPV, IMi, Kis, Rui	
3.12	HO Del	2015	Trt	
3.13	AQ Eri	2016	Aka, Kis, Mdy, AAVSO	
3.14	AX For	2015	HaC, Aka	
3.15	V844 Her	2015	OKU, DPV, IMi	
3.17	RZ Leo	2016	Kis, deM, HaC, Aka, AAVSO, CRI, Mdy, IMi, SWI, DKS, SRI, SGE, Trt, RPc	
3.16	MM Hya	2015	COO	
3.18	V585 Lyr	2015	RPc, DPV, OKU	
3.19	V2051 Oph	2015	HaC, Kis, Aka	
3.20	V368 Peg	2015	Trt	
3.21	V650 Peg	2015	HaC, Shu, Mdy, Aka, Kai, Trt, Ioh	
3.24	TY Psc	2015	Trt, Deb, Kis	
3.22	PU Per	2015	KU, Mdy, Vol, IMi, Kis	
3.22	QY Per	2015	Trt, Shu	
3.25	V493 Ser	2015	DPV, HaC, IMi	
3.26	V1212 Tau	2016	Mdy	
3.27	KK Tel	2015	HaC, SPE	
3.28	CI UMa	2016	SGE, Trt	
3.29	KS UMa	2015	Kis, Ioh, AAVSO, Aka, Kai	
3.30	MR UMa	2015	DPV	
3.31	NSV 2026	2015	AAVSO, IMi	
		2016	JSh, RPc, IMi, KU, Dub, AAVSO	
3.32	ASASSN-13ah	2016	Van, IMi	
3.33	ASASSN-13ak	2015	deM, KU, RPc, IMi	
3.34	ASASSN-13az	2016	Van	
3.35	ASASSN-14ca	2015	IMi	
–	ASASSN-14cc	2014	Kato, Hamsch, and Monard (2015b)	
3.36	ASASSN-14dh	2015	HaC, Mdy, Ioh	
3.37	ASASSN-14fz	2015	HaC	
3.38	ASASSN-14le	2014	KU	
3.39	ASASSN-15cl	2016	Kis, HaC, Ioh	
3.40	ASASSN-15cy	2015	MLF, HaC, deM, Kis	
3.41	ASASSN-15dh	2015	Van, SWI	
3.42	ASASSN-15dp	2015	DPV, Van, Trt, IMi, SWI	
3.43	ASASSN-15dr	2015	HaC, MLF	
3.44	ASASSN-15ea	2015	deM, Van	
3.45	ASASSN-15ee	2015	MLF, HaC, SPE	
3.46	ASASSN-15eh	2015	MLF	
3.47	ASASSN-15ev	2015	MLF, HaC	
3.48	ASASSN-15fo	2015	MLF, HaC	
3.49	ASASSN-15fu	2015	MLF, HaC	

Table 1. (Continued)

Subsection	Object	Year	Observers or references*	ID [†]
3.50	ASASSN-15gf	2015	Van, Kai	
3.51	ASASSN-15gh	2015	HaC, MLF	
3.52	ASASSN-15gi	2015	MLF, HaC	
3.53	ASASSN-15gn	2015	MLF, HaC, COO	
3.54	ASASSN-15gq	2015	Van, IMi, COO	
3.55	ASASSN-15gs	2015	MLF	
3.56	ASASSN-15hd	2015	Van, OKU, RIT, DPV, IMi, Kai, Ioh, deM, CRI, Trt, GFB, HMB, SRI, COO, DKS, HaC	
3.57	ASASSN-15hl	2015	MLF	
3.58	ASASSN-15hm	2015	HaC, Kis, COO	
3.59	ASASSN-15hn	2015	MLF, HaC, Ioh, COO, Kis, KU, deM	
3.60	ASASSN-15ia	2015	HaC	
3.61	ASASSN-15ie	2015	HaC	
3.62	ASASSN-15iv	2015	HaC	
3.63	ASASSN-15iz	2015	HaC	
–	ASASSN-15jd	2015	Kimura et al. (2016b)	
3.64	ASASSN-15jj	2015	HaC, MLF	
3.65	ASASSN-15kf	2015	MLF, HaC	
3.66	ASASSN-15kh	2015	MLF, HaC, SPE	
3.67	ASASSN-15le	2015	Van, HaC	
3.68	ASASSN-15lt	2015	HaC, SPE	
3.69	ASASSN-15mb	2015	HaC	
3.70	ASASSN-15mt	2015	Kis, Shu, Ant, Ioh, COO, IMi	
3.71	ASASSN-15na	2015	MLF, HaC	
3.72	ASASSN-15ni	2015	OKU, DPV, IMi, Van, Kis, Shu, SPE, Ioh, Trt, AAVSO	
3.73	ASASSN-15nl	2015	Shu, Van, Trt	
3.74	ASASSN-15ob	2015	CRI, HaC	
3.75	ASASSN-15oj	2015	MLF	
3.76	ASASSN-15ok	2015	MLF, HaC	
3.77	ASASSN-15pi	2015	Van	
–	ASASSN-15po	2015	Namekata et al. (2016)	
3.78	ASASSN-15pu	2015	MLF, SPE, HaC	
3.79	ASASSN-15qe	2015	KU, Mdy, Van, Ioh	
3.80	ASASSN-15ql	2015	HaC	
3.81	ASASSN-15qo	2015	IMi, Van, Ioh	
3.82	ASASSN-15qq	2015	MLF, HaC	
3.83	ASASSN-15rf	2015	HaC	
3.84	ASASSN-15rj	2015	Mdy, KU, CRI	
3.85	ASASSN-15ro	2015	Mdy	
3.86	ASASSN-15rr	2015	MLF	
3.87	ASASSN-15rs	2015	Mdy, Ioh, Trt, Kis	
3.88	ASASSN-15ry	2015	Kis, OUS, Ioh	
3.89	ASASSN-15sc	2015	Ioh, Rui, Mdy, SWI, DPV, Van, CRI, Kis, OUS, Les, Kai, IMi	
3.90	ASASSN-15sd	2015	HaC, MLF	
3.91	ASASSN-15se	2015	OKU, Van, Kis, Rui, IMi, HaC	
3.92	ASASSN-15sl	2015	Shu, Ioh, Trt, Van, IMi, CRI	
3.93	ASASSN-15sn	2015	Kai, Mdy	
3.94	ASASSN-15sp	2015	HaC	
3.95	ASASSN-15su	2015	Trt	
3.96	ASASSN-15sv	2015	Kai, Shu	
3.97	ASASSN-15ud	2015	Mdy	
3.98	ASASSN-15uj	2015	MLF, HaC, SPE	

Table 1. (Continued)

Subsection	Object	Year	Observers or references*	ID [†]
3.99	ASASSN-15ux	2015	deM, Ioh, KU, Mdy, Van, Kis, Shu, IMi	
3.100	ASASSN-16af	2016	Mdy, Van, HaC, Ioh	
3.101	ASASSN-16ag	2016	Mdy, IMi, Van, Ioh	
3.102	ASASSN-16ao	2016	MLF	
3.103	ASASSN-16aq	2016	IMi	
3.104	ASASSN-16bh	2016	MLF, SPE, DKS, Kis, Mdy, HaC, Ioh	
3.105	ASASSN-16bi	2016	MLF, SPE, HaC	
3.106	ASASSN-16bu	2016	OKU, Ioh, Kis, IMi, Van, Mdy, deM	
3.107	ASASSN-16de	2016	Van, HaC	
3.108	CRTS J081936	2015	Kai	CRTS J081936.1+191540
3.109	CRTS J095926	2015	MLF, HaC	CRTS J095926.4–160147
3.110	CRTS J120052	2011	Kato et al. (2012)	CRTS J120052.9–152620
		2016	OKU, HaC	
3.111	CRTS J163120	2015	RIT	CRTS J163120.9+103134
3.112	CRTS J200331	2015	HaC	CRTS J200331.3–284941
3.113	CRTS J212521	2015	Shu, Ter	CRTS J212521.8–102627
3.114	CRTS J214738	2015	Ioh	CRTS J214738.4+244554
3.115	CSS J221822	2015	Mdy, Van, Vol	CSS120812:221823+344509
3.116	DDE 26	2015	Kai, Ioh, Mdy	
3.117	IPHAS J230538	2015	CRI, IMi, Van	IPHAS J230538.39+652158.7
3.118	MASTER J003831	2016	HaC	MASTER OT J003831.10–640313.7
3.119	MASTER J073325	2016	Mdy, Van, DPV, R _{Pc} , N _{Ka}	MASTER OT J073325.52+373744.9
3.120	MASTER J120251	2015	MLF, HaC, SPE	MASTER OT J120251.56–454116.7
3.121	MASTER J131320	2016	Van, SGE	MASTER OT J131320.24+692649.1
3.122	MASTER J181523	2015	Van	MASTER OT J181523.78+692037.4
3.123	MASTER J212624	2015	Shu, Ioh	MASTER OT J212624.16+253827.2
3.124	N080829A	2015	KU, Mdy, OUS, SWI, Vol, Ioh	
3.125	OT J191443	2015	Mdy, OKU	OT J191443.6+605214
–	PM J03338+3320	2015	Kato et al. (2016b)	
3.126	SDSS J074859	2015	Mdy, R _{Pc} , Kis	SDSS J074859.55+312512.6
3.127	SDSS J145758	2015	Vol, JSh, AAVSO, Shu, IMi, SRI, Han, deM, Mdy, R _{Pc} , Ioh	SDSS J145758.21+514807.9
3.128	SDSS J164248	2016	HaC, Van	SDSS J164248.52+134751.4

*Key to observers: Aka (H. Akazawa, OUS), Ant (S. Antipin and A. Zubareva team), COO (L. Cook), CRI (Crimean Astrophys. Obs.), Deb (B. Debski), deM (E. de Miguel), DKS[‡] (S. Dvorak), DPV (P. Dubovsky), Dub (F. Dubois team), GBo (G. Bolt), GFB[‡] (W. Goff), HMB (F.-J. Hamsch), HaC (F.-J. Hamsch, remote obs. in Chile), Han (Hankasalmi Obs., by A. Oksanen), IMi[‡] (I. Miller), Ioh (H. Itoh), JSh[‡] (J. Shears), KU (Kyoto Univ., campus obs.), Kai (K. Kasai), Kis (S. Kiyota), Les (Lesniki Obs.), MLF (B. Monard), Mdy (Y. Maeda), N_{Ka} (N. Katysheva and S. Shugarov), OKU (Osaya Kyoiku Univ.), OUS (Okayama Univ. of Science), RIT (M. Richmond), R_{Pc}[‡] (R. Pickard), Rui (J. Ruiz), SGE[‡] (G. Stone), SPE[‡] (P. Starr), SRI[‡] (R. Sabo), SWI[‡] (W. Stein), Shu (S. Shugarov team), Ter (Terskol Obs.), Trt (T. Tordai), Van (T. Vanmunster), Vol (I. Voloshina), AAVSO (AAVSO database).

[†]Original identifications, discoverers, or data source.

[‡]Inclusive of observations from the AAVSO database.

weighted polynomial regression (LOWESS: Cleveland 1979). The times of superhumps maxima were determined by the template fitting method as described in Kato et al. (2009). The times of all observations are expressed in barycentric Julian days (BJD).

The abbreviations used in this paper are the same as in Kato et al. (2014b): P_{orb} means the orbital period and $\epsilon \equiv P_{\text{SH}}/P_{\text{orb}} - 1$ for the fractional superhump excess. Following Osaki and Kato (2013a), the alternative fractional superhump excess in the frequency unit $\epsilon^* \equiv 1 - P_{\text{orb}}/P_{\text{SH}} - 1 = \epsilon/(1 + \epsilon)$ has been introduced because this

fractional superhump excess is a direct measure of the precession rate. We therefore used ϵ^* in discussing the precession rate.

We used phase dispersion minimization (PDM: Stellingwerf 1978) for period analysis and 1σ errors for the PDM analysis was estimated by the methods of Fernie (1989) and Kato et al. (2010). We introduced a variety of bootstrapping in estimating the robustness of the result of the PDM analysis since Kato et al. (2012). We typically analyzed 100 samples which randomly contain 50% of observations, and performed PDM analysis for these samples.

Table 2. Superhump periods and period derivatives.

Object	Year	P_1 (d)*	Err	E_1 †	P_{dot} ‡	Err‡	P_2 (d)*	Err	E_2 †	P_{orb} (d)§	Q		
KV And	2015	0.074283	0.000011	15	56	0.0	2.6	0.074108	0.000054	66	96	–	B
EG Aqr	2015	0.078688	0.000122	51	65	–	–	–	–	–	–	–	C
NN Cam	2015	0.074226	0.000037	0	43	11.6	7.8	0.073768	0.000035	67	150	0.0717	B
V452 Cas	2016	0.088828	0.000088	11	57	–	–	–	–	–	–	–	C
V1040 Cen	2015	0.062244	0.000024	0	67	–	–	–	–	–	–	0.06049	CG2
PUCMa	2016	0.057968	0.000018	0	107	6.9	1.7	–	–	–	–	0.056694	B
AL Com	2015	0.057293	0.000010	0	128	1.6	0.8	–	–	–	–	0.056669	B
VW CrB	2015	0.072820	0.000038	0	112	3.6	3.1	–	–	–	–	–	C
V1006 Cyg	2015	0.105407	0.000044	36	94	20.8	2.0	0.104437	0.000050	102	200	0.09903	B
V1028 Cyg	2016	0.062009	0.000055	0	58	11.8	8.3	–	–	–	–	–	C
V1113 Cyg	2015	0.078937	0.000018	0	107	–4.3	1.3	–	–	–	–	–	BG
HO Del	2015	0.064326	0.000018	0	33	–	–	–	–	–	–	0.06266	C
AQ Eri	2016	0.062432	0.000030	0	83	10.8	2.5	–	–	–	–	0.06094	C
AX For	2015	–	–	–	–	–	–	0.081041	0.000073	0	26	–	C
V844 Her	2015	0.055902	0.000025	32	120	10.4	2.6	0.055819	0.000047	174	228	0.054643	C
RZ Leo	2016	0.078675	0.000035	0	48	15.6	5.9	0.078229	0.000022	53	138	0.076030	A
V585 Lyr	2015	0.060360	0.000018	11	84	9.9	2.4	–	–	–	–	–	C
V2051 Oph	2015	0.064708	0.000088	0	16	–	–	0.064144	0.000044	40	72	0.062428	Ce
V650 Peg	2015	0.069777	0.000020	0	125	6.7	0.9	0.069271	0.000029	135	210	–	C
PU Per	2015	–	–	–	–	–	–	0.067975	0.000020	0	51	–	C
QY Per	2015	0.078593	0.000032	0	40	14.7	2.8	–	–	–	–	–	C
TY Psc	2015	0.070093	0.000330	0	10	–	–	–	–	–	–	0.068348	C
V493 Ser	2015	0.082793	0.000062	39	76	–	–	0.082576	0.000033	87	173	0.08001	B
KK Tel	2015	0.087606	0.000023	42	136	0.8	1.9	–	–	–	–	–	B
CIUMa	2016	0.063283	0.000354	0	5	–	–	–	–	–	–	–	C
KS UMa	2015	0.069948	0.000058	0	19	–	–	0.069763	0.000086	75	93	0.06796	C
NSV 2026	2015	0.069829	0.000015	0	102	0.4	1.5	–	–	–	–	–	CG
NSV 2026	2016	0.069795	0.000013	0	130	–0.4	1.1	–	–	–	–	–	CG
ASASSN-13ah	2016	0.066141	0.000013	0	33	–	–	–	–	–	–	–	C
ASASSN-13ak	2015	0.086655	0.000040	0	34	–	–	–	–	–	–	–	C
ASASSN-14cc	2014	0.015610	0.000010	–	–	–	–	–	–	–	–	–	C
ASASSN-14dh	2015	–	–	–	–	–	–	0.073629	0.000031	0	91	–	C
ASASSN-14fz	2015	0.078028	0.000030	13	103	–2.9	3.0	–	–	–	–	–	CG
ASASSN-15cl	2016	0.094633	0.000104	22	33	–	–	0.093907	0.000071	43	96	–	B
ASASSN-15cy	2015	0.049955	0.000009	0	122	3.4	1.2	–	–	–	–	–	C
ASASSN-15dh	2015	0.088014	0.000087	0	19	–103.2	14.1	–	–	–	–	–	CG
ASASSN-15dp	2015	0.060005	0.000015	49	200	0.4	1.1	–	–	–	–	–	B
ASASSN-15dr	2015	0.056387	0.000045	25	80	–	–	–	–	–	–	–	C
ASASSN-15ea	2015	0.095225	0.000034	–	–	–	–	–	–	–	–	–	CU
ASASSN-15ee	2015	0.057136	0.000018	15	120	8.1	1.2	–	–	–	–	–	B
ASASSN-15eh	2015	0.085665	0.000033	0	60	–10.3	2.4	–	–	–	–	–	CG
ASASSN-15ev	2015	0.058015	0.000041	0	20	–	–	–	–	–	–	–	C
ASASSN-15fo	2015	0.0630	0.0030	0	4	–	–	–	–	–	–	–	C
ASASSN-15fu	2015	0.074770	0.000062	0	44	–	–	0.074001	0.000228	43	71	–	C
ASASSN-15gf	2015	0.06690	0.00012	0	15	–	–	–	–	–	–	–	CU
ASASSN-15gh	2015	0.05905	0.00030	0	68	–	–	–	–	–	–	–	CU
ASASSN-15gi	2015	0.061270	0.000050	0	66	15.5	8.1	0.060928	0.000038	64	130	–	C
ASASSN-15gn	2015	0.063641	0.000033	18	112	–3.2	3.8	–	–	–	–	–	C
ASASSN-15gq	2015	0.066726	0.000034	15	120	11.9	0.8	–	–	–	–	0.06490	BE
ASASSN-15hd	2015	0.056105	0.000007	22	273	1.5	0.3	–	–	–	–	0.05541	BE
ASASSN-15hl	2015	0.067947	0.000035	0	89	–5.9	3.6	–	–	–	–	–	CG
ASASSN-15hm	2015	0.056165	0.000031	34	159	5.4	2.0	–	–	–	–	–	C
ASASSN-15hn	2015	0.061831	0.000018	32	178	–0.5	1.5	–	–	–	–	–	B

Table 2. (Continued)

Object	Year	P_1 (d)*	Err	E_1^\dagger	P_{dot}^\ddagger	Err ‡	P_2 (d)*	Err	E_2^\dagger	P_{orb} (d) §	Q $^\parallel$		
ASASSN-15ia	2015	0.070281	0.000072	0	29	–	–	0.069882	0.000059	28	72	–	C
ASASSN-15ie	2015	0.058616	0.000022	35	224	4.0	0.9	–	–	–	–	–	C
ASASSN-15iv	2015	0.067435	0.000051	0	89	17.4	2.9	0.067099	0.000068	87	149	–	C
ASASSN-15iz	2015	0.081434	0.000049	0	61	–	–	–	–	–	–	–	CU
ASASSN-15jd	2015	0.064981	0.000008	24	90	9.9	4.2	–	–	–	–	–	C
ASASSN-15jj	2015	0.062388	0.000025	0	146	8.1	0.6	0.062124	0.000067	161	209	–	B
ASASSN-15kf	2015	0.019251	0.000097	0	3	–	–	–	–	–	–	–	C
ASASSN-15kh	2015	0.060480	0.000017	43	175	1.2	1.6	–	–	–	–	–	B
ASASSN-15le	2015	0.078000	0.000053	0	43	–	–	–	–	–	–	–	CU
ASASSN-15lt	2015	0.059815	0.000024	49	189	–	–	0.059633	0.000053	188	266	–	CM
ASASSN-15mb	2015	–	–	–	–	–	–	0.068838	0.000056	43	203	–	CU
ASASSN-15mt	2015	0.076342	0.000020	0	31	–	–	0.076032	0.000041	42	97	–	B
ASASSN-15na	2015	0.063720	0.000027	0	111	3.1	2.6	–	–	–	–	0.06297	CE
ASASSN-15ni	2015	0.055854	0.000009	32	205	3.4	0.6	–	–	–	–	0.05517	BE
ASASSN-15nl	2015	0.060095	0.000098	0	33	–	–	–	–	–	–	–	C
ASASSN-15ob	2015	0.060525	0.000060	0	83	15.1	2.8	–	–	–	–	–	C
ASASSN-15ok	2015	0.078931	0.000122	0	25	–	–	0.078476	0.000022	25	115	–	C
ASASSN-15pi	2015	0.078307	0.000300	0	4	–	–	–	–	–	–	–	C
ASASSN-15po	2015	0.050916	0.000002	49	329	1.1	0.1	–	–	–	–	0.050457	AE
ASASSN-15pu	2015	0.058254	0.000024	34	146	3.3	2.1	–	–	–	–	0.05757	BE
ASASSN-15qe	2015	0.061092	0.000017	0	62	–	–	–	–	–	–	–	C
ASASSN-15qq	2015	0.077131	0.000026	0	81	–1.0	2.6	–	–	–	–	–	CG2
ASASSN-15rj	2015	0.092463	0.000164	0	15	–	–	–	–	–	–	–	C
ASASSN-15ro	2015	0.072909	0.000088	0	29	–	–	–	–	–	–	–	C
ASASSN-15rr	2015	0.054938	0.000039	0	75	–	–	–	–	–	–	–	CU
ASASSN-15rs	2015	0.097854	0.000207	0	22	–	–	–	–	–	–	–	C
ASASSN-15ry	2015	0.060876	0.000270	0	3	–	–	–	–	–	–	–	C
ASASSN-15sc	2015	0.057735	0.000015	21	208	5.8	0.3	–	–	–	–	–	A
ASASSN-15sd	2015	–	–	–	–	–	–	0.068894	0.000028	0	93	–	C
ASASSN-15se	2015	0.063312	0.000042	10	58	–	–	–	–	–	–	–	C
ASASSN-15sl	2015	0.091065	0.000066	0	97	9.1	2.6	–	–	–	–	0.087048	CGe
ASASSN-15sn	2015	0.064684	0.000090	0	48	–50.5	11.5	–	–	–	–	–	C
ASASSN-15sp	2015	0.058366	0.000018	33	138	7.7	0.9	0.058292	0.000040	–	–	–	B
ASASSN-15ud	2015	0.05649	0.00023	0	3	–	–	–	–	–	–	–	C
ASASSN-15uj	2015	0.055805	0.000012	35	129	–1.1	1.6	–	–	–	–	0.055266	BE
ASASSN-15ux	2015	0.056857	0.000012	73	131	–	–	–	–	–	–	0.056109	Ce
ASASSN-16af	2016	0.064204	0.000025	0	75	13.0	2.8	–	–	–	–	–	B
ASASSN-16ag	2016	0.058479	0.000071	0	96	–	–	–	–	–	–	–	C
ASASSN-16bh	2016	0.054027	0.000006	32	206	3.7	0.3	–	–	–	–	0.05346	AE
ASASSN-16bu	2016	0.060513	0.000071	42	82	–	–	–	–	–	–	0.05934	BE
CRTS J095926	2015	0.089428	0.000041	10	67	–4.4	5.0	–	–	–	–	–	C
CRTS J120052	2016	0.088950	0.000038	0	85	–5.5	3.2	–	–	–	–	–	CG2
CRTS J163120	2015	0.0645	0.0005	0	3	–	–	–	–	–	–	–	C
CRTS J200331	2015	0.059720	0.000088	49	84	–	–	–	–	–	–	0.058705	Ce
CRTS J212521	2015	0.079090	0.000119	0	26	–	–	–	–	–	–	–	C
CSS J221822	2015	0.069294	0.000035	0	50	–	–	–	–	–	–	–	C
DDE 26	2015	0.088617	0.000042	0	49	10.3	2.5	–	–	–	–	–	C
IPHAS J230538	2015	0.072772	0.000017	15	83	4.6	2.4	0.072493	0.000060	82	125	–	C
MASTER J003831	2016	0.061605	0.000038	0	114	11.5	0.9	0.061310	0.000038	114	179	–	B
MASTER J073325	2016	0.061218	0.000027	32	162	5.5	1.1	–	–	–	–	–	C
MASTER J120251	2015	0.063372	0.000018	0	131	–1.7	3.1	–	–	–	–	–	CGM
MASTER J131320	2016	0.069709	0.000044	0	34	–	–	–	–	–	–	–	CU
MASTER J181523	2015	0.058512	0.000056	0	20	–	–	–	–	–	–	–	C
MASTER J212624	2015	0.091193	0.000148	0	31	–	–	–	–	–	–	–	C

Table 2. (Continued)

Object	Year	P_1 (d)*	Err	E_1 [†]	P_{dot} [‡]	Err [‡]	P_2 (d)*	Err	E_2 [†]	P_{orb} (d) [§]	Q		
N 080829A	2015	0.064282	0.000027	0	100	11.4	2.4	–	–	–	B		
PM J03338	2015	0.069013	0.000021	70	115	–12.7	4.7	0.068629	0.000020	115	246	0.06663	A
SDSS J074859	2015	0.05958	0.00030	–	–	–	–	–	–	–	–	0.058311	Ce
SDSS J145758	2015	0.054912	0.000018	0	128	2.2	2.9	–	–	–	–	0.054087	C
SDSS J164248	2016	0.079327	0.000093	0	54	–	–	–	–	–	–	–	CG

* P_1 and P_2 are mean periods of stage B and C superhumps, respectively.

[†]Interval used for calculating the period (corresponding to E in the individual tables in section 3).

[‡] $P_{\text{dot}} = \dot{P}/P$ for stage B superhumps, unit 10^{-5} .

[§]NN Cam (D. Denissenko 2007, vsnet-alert 9557), V1040 Cen (P. Longa-Peña et al. 2009, see subsection 3.6), PU CMa (Thorstensen, Fenton 2003), AL Com (Kato et al. 2014b), V1006 Cyg (Sheets et al. 2007), HO Del (Patterson et al. 2003), AQ Eri (Thorstensen et al. 1996), V844 Her (Thorstensen et al. 2002), RZ Leo (Dai et al. 2016; improved by this work), V2051 Oph (this work), TY Psc (Thorstensen et al. 1996), V493 Ser (Kato et al. 2009), KS UMa (Patterson et al. 2003), PM J03338 (Skinner et al. 2014), SDSS J145758 (Uthas 2011), ASASSN-15gq, ASASSN-15hd, ASASSN-15na, ASASSN-15ni, ASASSN-15pu, ASASSN-15sc, ASASSN-15uj, ASASSN-15ux, ASASSN-16bh, ASASSN-16bi, ASASSN-16bu, CRTS J095926, CRTS J200331 (this work), ASASSN-15po (Namekata et al. 2016).

^{||}Data quality and comments. A: excellent; B: partial coverage or slightly low quality; C: insufficient coverage or observations with large scatter; G: P_{dot} denotes global P_{dot} ; M: observational gap in middle stage, U: uncertainty in alias selection; 2: late-stage coverage; the listed period may refer to P_2 ; E: P_{orb} refers to the period of early superhumps; e: eclipsing system.

The bootstrap result is shown as a form of 90% confidence intervals in the resultant PDM θ statistics.

If this paper provides the first solid presentation of a new SUUMa-type classification, we provide the result of PDM period analysis and averaged superhump profile.

The resultant P_{SH} , P_{dot} , and other parameters are listed in table 2 in same format as in Kato et al. (2009). The definitions of parameters P_1 , P_2 , E_1 , E_2 , and P_{dot} are the same as in Kato et al. (2009): P_1 and P_2 represent periods in stages B and C, respectively, and E_1 and E_2 represent intervals (in cycle numbers) to determine P_1 and P_2 , respectively.⁸ Comparisons of $O - C$ diagrams between different superoutbursts are also presented whenever available, since this comparison was one of the main motivations in this series of papers. In drawing combined $O - C$ diagrams, we usually used $E = 0$ for the start of the superoutburst, which usually refers to the first positive detection of the outburst. This epoch usually has an accuracy of ~ 1 d for well-observed objects, and if the outburst was not sufficiently observed, we mentioned in the figure caption how to estimate E in such an outburst. In some cases, this $E = 0$ is defined as the appearance of superhumps. This treatment is necessary since some objects have a long waiting time before appearance of superhumps. Combined $O - C$ diagrams also help identifying superhump stages particularly when observations are insufficient. We also note that there is sometimes an ambiguity in selecting the true period among aliases. In some cases, this can be resolved by the help of the $O - C$ analysis. The procedure and example are shown in subsection 2.2 in Kato et al. (2015a).

⁸ The intervals (E_1 and E_2) for the stages B and C given in the table sometimes overlap because there is sometimes observational ambiguity (usually due to a lack of observations) in determining the stages.

We also present $O - C$ diagrams and light curves especially for WZ Sge-type dwarf novae. WZ Sge-type dwarf novae are a subclass of SUUMa-type dwarf novae characterized by the presence of early superhumps. They are seen during the early stages of superoutburst, and have period close to the orbital periods (Kato et al. 1996a; Kato 2002, 2015; Osaki & Meyer 2002). These early superhumps are considered to be a result of the 2:1 resonance (Osaki & Meyer 2002). These objects usually show very rare outbursts (once in several years to decades) and often have complex light curves (Kato 2015) and are of special astrophysical interest since the origin of the complex light curves, including repetitive rebrightenings, is not well understood. They receive special attention since they are considered to represent the terminal stage of CV evolution and they may have brown-dwarf secondaries. We used the period of early superhumps as the approximate orbital period (Kato et al. 2014b; Kato 2015).

In the figures, the points are accompanied by 1σ error bars whenever available, which are omitted when the error is smaller than the plot mark.

We used the same terminology of superhumps as summarized in Kato et al. (2012). We especially call attention to the term “late superhumps.” Although this term has been used to express various phenomena, we only used the concept of “traditional” late superhumps when there is an ~ 0.5 phase shift [Vogt 1983; see also table 1 in Kato et al. (2012) for various types of superhumps], since we suspect that many of the past claims of detections of “late superhumps” were likely stage C superhumps before it became apparent that there are complex structures in the $O - C$ diagrams of superhumps (see discussion in Kato et al. 2009).

Table 3. Coordinates of objects without coordinate-based names.

Object	Right ascension	Declination	Source*	SDSS <i>g</i>	GALEX NUV
ASASSN-13ah	18 ^h 32 ^m 11 ^s .37	+61°55′05″.6	IGSL	–	20.6(2)
ASASSN-13ak	17 ^h 48 ^m 27 ^s .88	+50°50′39″.7	SDSS	19.9	–
ASASSN-13az	18 ^h 42 ^m 58 ^s .18	+73°42′28″.4	ASAS-SN [†]	–	20.9(3)
ASASSN-14ca	23 ^h 53 ^m 13 ^s .22	+27°42′01″.8	SDSS [†]	20.6	–
ASASSN-14dh	21 ^h 23 ^m 25 ^s .65	–15°39′54″.3	IGSL	–	19.7(1)
ASASSN-14fz	19 ^h 00 ^m 05 ^s .25	–49°30′34″.4	IGSL	–	–
ASASSN-14le	21 ^h 43 ^m 21 ^s .84	+73°41′12″.9	SDSS	22.4	–
ASASSN-15cl	07 ^h 39 ^m 51 ^s .35	–15°41′00″.3	IGSL	–	–
ASASSN-15cy	08 ^h 11 ^m 50 ^s .53	–12°27′51″.5	Kis [†]	–	–
ASASSN-15dh	04 ^h 59 ^m 55 ^s .75	+77°11′17″.9	IGSL	–	17.44(3)
ASASSN-15dp	04 ^h 49 ^m 32 ^s .28	+36°05′14″.0	GSC2.3.2	–	–
ASASSN-15dr	11 ^h 05 ^m 49 ^s .38	–42°41′15″.9	IGSL	–	–
ASASSN-15ea	18 ^h 50 ^m 50 ^s .59	+40°44′06″.0	deM	–	–
ASASSN-15ee	06 ^h 36 ^m 17 ^s .49	–31°14′43″.6	IGSL	–	–
ASASSN-15eh	17 ^h 53 ^m 51 ^s .25	–64°17′40″.2	GSC2.3.2	–	–
ASASSN-15ev	07 ^h 38 ^m 19 ^s .36	–82°50′40″.2	IGSL	–	–
ASASSN-15fo	12 ^h 39 ^m 56 ^s .28	–47°16′23″.9	IGSL	–	–
ASASSN-15fu	11 ^h 10 ^m 46 ^s .21	–23°37′44″.2	IGSL	–	21.6(2)
ASASSN-15gf	06 ^h 10 ^m 04 ^s .01	+12°40′08″.5	IPHAS DR2	–	–
ASASSN-15gh	17 ^h 48 ^m 16 ^s .13	–57°33′16″.3	ASAS-SN	–	–
ASASSN-15gi	09 ^h 11 ^m 51 ^s .74	–77°56′33″.8	IGSL	–	–
ASASSN-15gn	15 ^h 19 ^m 29 ^s .60	–24°40′00″.7	GSC2.3.2	–	–
ASASSN-15gq	10 ^h 15 ^m 11 ^s .32	+81°24′17″.5	ASAS-SN [†]	21.6?	–
ASASSN-15gs	13 ^h 59 ^m 17 ^s .48	–37°52′42″.2	GSC2.3.2	–	–
ASASSN-15hd	17 ^h 31 ^m 25 ^s .45	+27°54′28″.5	SDSS	21.4–21.9	–
ASASSN-15hl	05 ^h 53 ^m 30 ^s .40	–48°06′23″.2	GSC2.3.2	–	–
ASASSN-15hm	11 ^h 00 ^m 38 ^s .05	–11°56′46″.4	IGSL	–	21.7(3)
ASASSN-15hn	09 ^h 07 ^m 05 ^s .42	–10°42′45″.4	GSC2.3.2	–	–
ASASSN-15ia	18 ^h 10 ^m 33 ^s .83	–53°49′45″.9	IGSL	–	21.1(3)
ASASSN-15ie	20 ^h 36 ^m 44 ^s .20	–13°11′56″.5	IGSL	–	21.4(2)
ASASSN-15iv	14 ^h 36 ^m 15 ^s .50	–36°04′17″.0	IGSL	–	–
ASASSN-15iz	13 ^h 12 ^m 13 ^s .26	–42°18′00″.4	ASAS-SN	–	–
ASASSN-15jj	19 ^h 17 ^m 56 ^s .80	–56°57′58″.1	IGSL	–	–
ASASSN-15kf	15 ^h 38 ^m 38 ^s .23	–30°35′49″.4	IGSL	–	–
ASASSN-15kh	10 ^h 38 ^m 59 ^s .93	–36°54′41″.5	ASAS-SN	–	–
ASASSN-15le	18 ^h 21 ^m 13 ^s .93	+17°09′16″.2	IGSL	–	19.5(1)
ASASSN-15lt	20 ^h 03 ^m 59 ^s .59	–39°28′30″.7	IGSL	–	20.6(2)
ASASSN-15mb	02 ^h 52 ^m 48 ^s .21	–39°59′11″.3	IGSL	–	–
ASASSN-15mt	19 ^h 12 ^m 35 ^s .54	+50°34′31″.3	IGSL	–	–
ASASSN-15na	19 ^h 19 ^m 08 ^s .77	–49°45′41″.7	IGSL	–	21.0(2)
ASASSN-15ni	18 ^h 39 ^m 57 ^s .96	+22°21′18″.7	ASAS-SN	–	–
ASASSN-15nl	14 ^h 14 ^m 59 ^s .70	+38°35′47″.8	SDSS	19.3	20.1(1)
ASASSN-15ob	16 ^h 50 ^m 59 ^s .48	+01°20′06″.5	SDSS	21.1	–
ASASSN-15oj	13 ^h 45 ^m 18 ^s .90	–36°30′15″.0	IGSL	–	–
ASASSN-15ok	00 ^h 24 ^m 30 ^s .76	–66°35′52″.7	2MASS	–	20.7(2)
ASASSN-15pi	18 ^h 50 ^m 22 ^s .29	+74°56′03″.3	ASAS-SN	–	–
ASASSN-15pu	21 ^h 11 ^m 04 ^s .70	–39°56′33″.9	GSC2.3.2	–	–
ASASSN-15qe	22 ^h 53 ^m 44 ^s .43	+35°53′54″.4	GSC2.3.2	–	–
ASASSN-15ql	20 ^h 21 ^m 56 ^s .11	–85°59′09″.5	IGSL	–	–
ASASSN-15qo	18 ^h 11 ^m 22 ^s .86	+22°42′06″.7	SDSS	22.0	–
ASASSN-15qq	22 ^h 54 ^m 35 ^s .69	–36°12′27″.6	IGSL	–	21.0(2)
ASASSN-15rf	21 ^h 57 ^m 23 ^s .06	+10°49′59″.3	SDSS	20.7–20.8	21.6(2)
ASASSN-15rj	02 ^h 59 ^m 38 ^s .33	+44°57′04″.7	SDSS	21.3	–
ASASSN-15ro	01 ^h 33 ^m 07 ^s .56	+41°07′18″.6	SDSS	21.6	–
ASASSN-15rr	19 ^h 08 ^m 47 ^s .24	–58°31′06″.8	GSC2.3.2	–	–

Table 3. (Continued)

Object	Right ascension	Declination	Source*	SDSS <i>g</i>	GALEX NUV
ASASSN-15rs	04 ^h 46 ^m 33 ^s .68	+48°57′55″.6	2MASS	–	17.89(4)
ASASSN-15ry	05 ^h 28 ^m 55 ^s .66	+36°18′38″.9	IGSL	–	–
ASASSN-15sc	02 ^h 21 ^m 11 ^s .94	+60°19′49″.2	ASAS-SN [†]	–	–
ASASSN-15sd	23 ^h 18 ^m 33 ^s .27	–35°37′22″.7	IGSL	–	18.75(5)
ASASSN-15se	09 ^h 33 ^m 09 ^s .37	+10°28′02″.1	SDSS	20.5–20.6	–
ASASSN-15sl	07 ^h 23 ^m 12 ^s .73	+50°50′07″.7	IGSL	–	21.6(4)
ASASSN-15sn	20 ^h 04 ^m 23 ^s .09	+44°20′30″.2	KIC	–	–
ASASSN-15sp	07 ^h 58 ^m 08 ^s .47	–57°22′41″.9	IGSL	–	–
ASASSN-15su	05 ^h 05 ^m 03 ^s .08	+22°25′30″.3	IGSL	–	–
ASASSN-15sv	00 ^h 39 ^m 00 ^s .55	+27°13′45″.6	SDSS	22.1–22.6	–
ASASSN-15ud	08 ^h 52 ^m 28 ^s .59	–08°44′11″.4	GSC2.3.2	–	–
ASASSN-15uj	04 ^h 36 ^m 21 ^s .63	–55°25′07″.4	IGSL	–	–
ASASSN-15ux	06 ^h 52 ^m 26 ^s .66	+47°10′56″.5	ASAS-SN	–	–
ASASSN-16af	09 ^h 06 ^m 06 ^s .44	+00°04′34″.7	SDSS	21.1–21.9	–
ASASSN-16ag	01 ^h 34 ^m 38 ^s .24	+52°06′16″.5	SDSS	19.7	21.0(3)
ASASSN-16ao	04 ^h 40 ^m 47 ^s .12	–58°07′28″.5	GSC2.3.2	–	21.8(3)
ASASSN-16aq	16 ^h 55 ^m 25 ^s .06	+37°21′36″.8	SDSS	22.2	22.1(4)
ASASSN-16bh	13 ^h 24 ^m 57 ^s .23	–27°56′10″.6	GSC2.3.2	–	21.5(4)
ASASSN-16bi	07 ^h 46 ^m 22 ^s .50	–77°47′16″.7	Gaia	–	–
ASASSN-16bu	07 ^h 27 ^m 31 ^s .65	+33°46′35″.1	SDSS	22.1	22.8(5)
ASASSN-16de	18 ^h 42 ^m 34 ^s .00	+17°41′22″.7	USNO-A2.0	–	–
DDE 26	22 ^h 03 ^m 28 ^s .22	+30°56′36″.4	SDSS	19.6	–
N080829A	21 ^h 42 ^m 54 ^s .30	+15°36′42″.3	SDSS	22.6	–

*Source of the coordinates: 2MASS (2MASS All-Sky Catalog of Point Sources; Cutri et al. 2003), ASAS-SN (ASAS-SN measurements), Gaia (Gaia measurements), GSC2.3.2 (The Guide Star Catalog, Version 2.3.2, Lasker et al. 2007), IGSL (The Initial Gaia Source List 3, Smart 2013), IPHAS DR2 (INT/WFC Photometric H α Survey, Witham et al. 2008), KIC (The Kepler Input Catalog, Kepler Mission Team 2009), SDSS (The SDSS Photometric Catalog, Release 9, Ahn et al. 2012), USNO-A2.0 (The USNO-A2.0 Catalogue, Monet et al. 1998), the others are observers' symbols (see table 1).

[†]See text for more details.

For objects detected in CRTS, we preferably used the names provided in Drake et al. (2014). If these names are not yet available, we used the International Astronomical Union (IAU)-format names provided by the CRTS team in the public data release.⁹ As in Kato et al. (2009), we have used coordinate-based optical transient (OT) designations for some objects, such as apparent dwarf nova candidates reported in the Transient Objects Confirmation Page of the Central Bureau for Astronomical Telegrams and CRTS objects without registered designations in Drake et al. (2014) or in the CRTS public data release and listed the original identifiers in table 1.¹⁰

We provided coordinates from astrometric catalogs for ASAS-SN (Shappee et al. 2014) CVs and two objects without coordinate-based names other than listed in the General Catalog of Variable Stars (Kholopov et al. 1985) in table 3. We used the Sloan Digital Sky Survey (SDSS: Ahn et al. 2012), the Initial Gaia Source List (IGSL: Smart 2013) and Guide Star Catalog 2.3.2 (GSC 2.3.2: Lasker et al. 2007) and some other catalogs. The coordinates used

in this paper are J2000.0. We also supplied SDSS *g* magnitudes and GALEX NUV magnitudes when counterparts are present.

3 Individual objects

3.1 KV Andromedae

KV And was discovered as dwarf nova by Kurochkin (1977). Since Kurochkin (1977) reported very faint (22.5 mag) quiescent magnitude, this object was suspected to be a dwarf nova with a very large outburst amplitude. Later it turned out that Kurochkin (1977) underestimated the quiescent brightness since they used the paper print of the Palomar Observatory Sky Survey, and the true quiescent magnitude is now considered to be around 20. Kato et al. (1994) and Kato (1995) reported superhump observations in 1993 and 1994, respectively. Although this object was recognized as an SU UMa-type dwarf nova relatively early, none of observations sufficiently recorded the development of superhumps. Yet another superoutburst in 2002 (Kato et al. 2009) suffered from rather low signal-to-noise quality.

⁹ (<http://nesssi.cacr.caltech.edu/DataRelease/>).

¹⁰ (<http://www.cbat.eps.harvard.edu/unconf/tocp.html>).

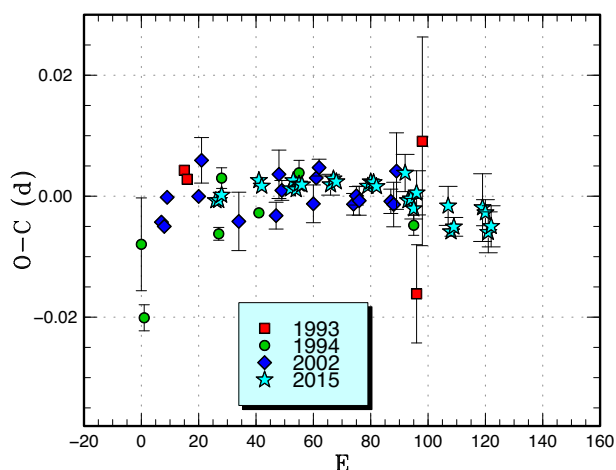


Fig. 2. Comparison of $O - C$ diagrams of KV And between different superoutbursts. A period of 0.07428 d was used to draw this figure. Approximate cycle counts (E) after the outburst detections were used. The actual starts of the outbursts were unknown. Since most of observations recorded large-amplitude superhumps, these observations probably recorded the early phases of the superoutbursts. (Color online)

The 2015 superoutburst was visually detected by P. Dubovsky on August 25 (vsnet-alert 19005). Subsequent observations detected superhumps (vsnet-alert 19011, 19020, 19022). The times of superhump maxima are listed in e-table 1.¹¹ The $O - C$ data suggest that the maxima for $E \leq 2$ probably recorded the final part of stage A. Although we give a comparison of the $O - C$ diagrams in figure 2, the starts of these superoutbursts were not well determined because this object has not been regularly monitored by visual observations. Since most of the observations recorded large-amplitude superhumps, these observations probably recorded the early phases of the superoutbursts and we treated these $O - C$ data as if the initial outburst detection refers to the start of the outburst. It is likely that the 1994 observation partly recorded stage A, which is compatible with low superhump amplitudes on the first two nights (the data quality was very poor, however).

3.2 EG Aquarii

EG Aqr was discovered as a blue eruptive object (BV number 3) in Luyten and Haro (1959), who reported a photographic magnitude of 14.8 on 1951 August 6. Haro and Chavira (1960) reported full photographic data, who gave a maximum of 14.0 mag (photographic) on 1958 November 5. The date in Luyten and Haro (1959) appears to have been a result of confusion. Vogt and Bateson (1982) did not detect any further outburst. Szkody and Howell (1992) obtained a K-type spectrum without emission lines, which was probably due to mis-identification.

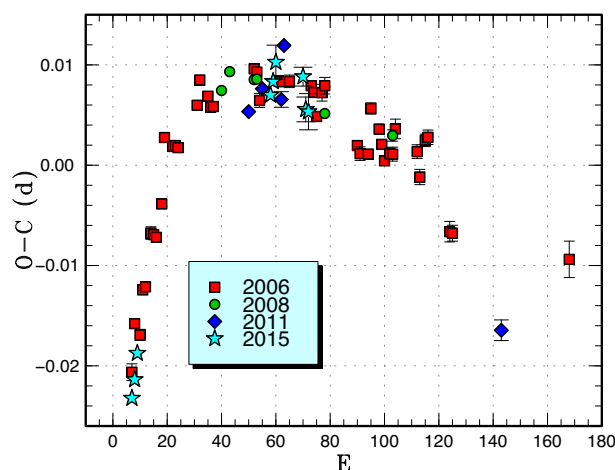


Fig. 3. Comparison of $O - C$ diagrams of EG Aqr between different superoutbursts. A period of 0.07885 d was used to draw this figure. Approximate cycle counts (E) after the start of the superoutburst were used. Since the starts of the 2008, 2011, and 2015 superoutbursts were not well constrained, we shifted the $O - C$ diagrams to best fit the best-recorded 2006 one. (Color online)

The first well-confirmed outburst since the discovery was detected by R. Stubbings on 2006 November 8 at a visual magnitude of 12.4 (vsnet-alert 9103). In vsnet-alert 9105, P. Schmeer reported a CCD detection of the outburst earlier than R. Stubbings. This 2006 superoutburst was well studied by Imada et al. (2008). The 2008 and 2011 superoutbursts were also observed and analyzed in Kato et al. (2009, 2013a), respectively. There was also a normal outburst on 2013 October 1 at $V = 15.0$ (ASAS-SN and R. Stubbings; vsnet-obs 76596, vsnet-outburst 16054). Although there was a bright outburst reaching a visual magnitude of 13.0 (R. Stubbings) on 2014 July 21, the nature of this outburst was unclear.

The 2015 superoutburst was visually detected by R. Stubbings at a magnitude of 12.1 on August 21 (vsnet-alert 18998). This outburst detection was sufficiently early and growing phase of superhumps was recorded (vsnet-alert 19003). There was, however, a long gap after the initial CCD observations and the outburst was not well covered by observations. The times of superhump maxima are listed in e-table 2. The maxima for $E \leq 2$ correspond to stage A superhumps (figure 3). The object showed a rebrightening on September 8 at $V = 16.37$ (ASAS-SN detection, vsnet-alert 19038).

3.3 NN Camelopardalis

NNCam = NSV 1485 was recognized as a dwarf nova by Khruslov (2005). For more history, see Kato et al. (2015a). The 2015 superoutburst was detected visually on August 11 by P. Dubovsky (vsnet-alert 18965). Although

¹¹ E-tables are available only on online edition as Supporting Information.

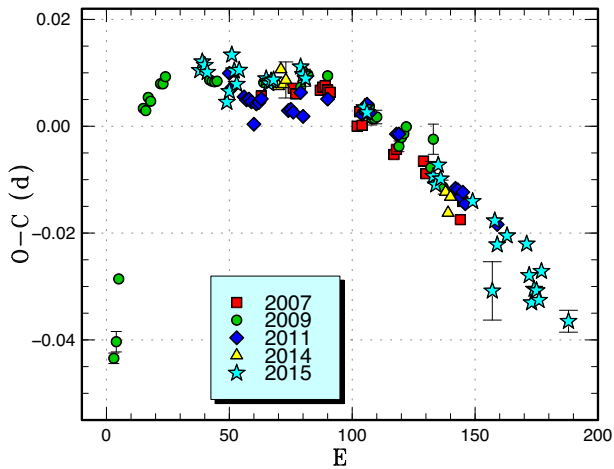


Fig. 4. Comparison of $O-C$ diagrams of NN Cam between different superoutbursts. A period of 0.07425 d was used to draw this figure. Approximate cycle counts (E) after the start of the superoutburst were used. (Color online)

there were possible low-amplitude superhump-like modulations on the next night (vsnet-alert 18972), we could not determine the period. On August 13, the superhumps were already in stage B (vsnet-alert 18977, 18984). The times of superhump maxima are listed in e-table 3. The maxima for $E \geq 133$ refer to a rapidly fading part of the superoutburst. The $O-C$ behavior was similar to that of past superoutbursts (figure 4). There was no indication of a phase jump as expected for traditional late superhumps.

3.4 PU Canis Majoris

This object was originally selected as a ROSAT source (RX J0640–24 = 1RXS J064047.8–242305; Voges et al. 1999). The object was classified as a dwarf nova based on the detection at magnitude 11 on one ESO B plate (cf. Downes et al. 1997). The dwarf nova-type nature was established by monitoring by P. Schmeer with a CCD attached to the 50-cm reflector at the Iowa Robotic Observatory. The object underwent an outburst in 2000 January and February. The rapid fading recorded in the 2000 January outburst suggested a normal outburst in an SUUMa-type dwarf nova (Kato et al. 2003b). Thorstensen and Fenton (2003) obtained an orbital period of 0.05669(4) d by a radial-velocity study. Using the data during superoutbursts in 2003, 2005, and 2008, Kato et al. (2009) established the superhump period. The 2008 superoutburst was preceded by a precursor outburst during which a long superhump period (now known as stage A) was recorded (Kato et al. 2009). The 2009 superoutburst was reported in Kato et al. (2010). Kato and Osaki (2013b) estimated the mass ratio $q = 0.110(11)$ by using stage A superhumps.

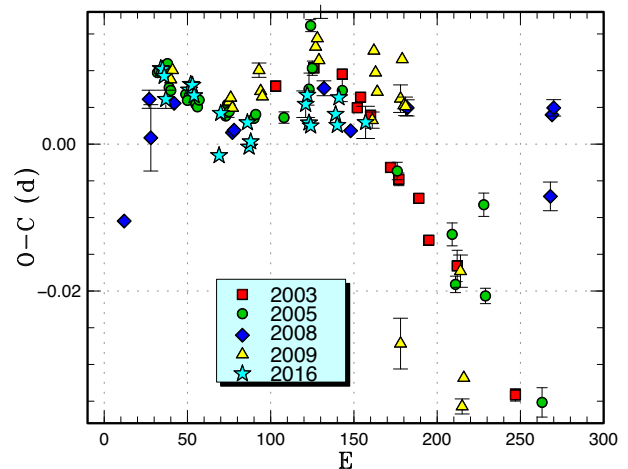


Fig. 5. Comparison of $O-C$ diagrams of PU CMa between different superoutbursts. A period of 0.05801 d was used to draw this figure. Approximate cycle counts (E) after the start of the superoutburst were used. (Color online)

The 2016 superoutburst was visually detected by T. Horie and R. Stubbings on February 29 (vsnet-alert 19543). The object showed a precursor on March 1, as in the 2008 superoutburst. Due to the 1-d gap between observations on March 1 and 2, we could not determine the period of stage A superhumps. The times of superhump maxima are listed in e-table 4. The evolution of the $O-C$ variation was similar to the past superoutbursts (figure 5).

3.5 V452 Cassiopeiae

V452 Cas was discovered as a dwarf nova (= S 10453) with a photographic range of 14–17.5 by Richter (1969). The SUUMa-type nature was confirmed by T. Vanmunster in 2000 (vsnet-alert 3698, 3707). Shears et al. (2009) studied this object between 2005 and 2008, and obtained supercycle lengths of 146 ± 16 d. For more history, see Kato et al. (2014b).

The 2016 superoutburst was detected on February 9 by M. Hiraga at an unfiltered CCD magnitude of 15.5 (cf. vsnet-alert 19486). This outburst was also detected by I. Miller on February 10 and subsequent observations detected superhumps (vsnet-alert 19486). The times of superhump maxima are listed in e-table 5. The initial part ($E < 11$) probably refers to stage A. A comparison of $O-C$ diagrams (figure 6) suggests that V452 Cas has long-lasting stage A, which has been recently established in long- P_{orb} systems such as V1006 Cyg (Kato et al. 2014b, 2016a; subsection 4.4). Having a long superhumps period, V452 Cas is an excellent candidate for this class of objects. Since stage A superhumps appear to be easily observable, determination of the orbital period and the period of stage A superhumps by systematic observations will lead to an

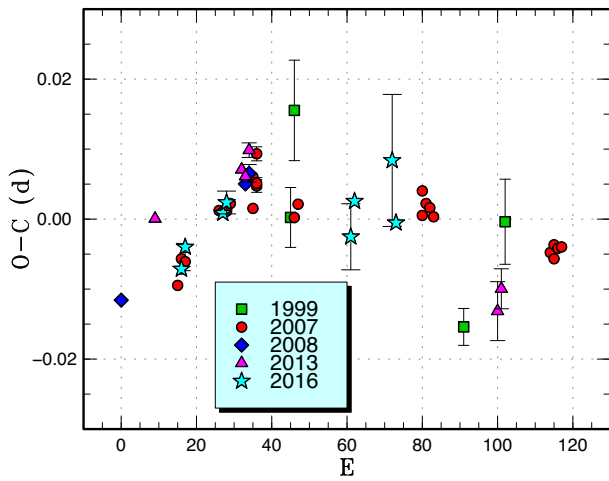


Fig. 6. Comparison of $O-C$ diagrams of V452 Cas between different superoutbursts. A period of 0.08880 d was used to draw this figure. Approximate cycle counts (E) after the start of the superoutburst were used. Since the start of the 2016 superoutburst was well observed, the 2007 $O-C$ diagram has been shifted by 15 cycles to match the 2016 one. (Color online)

estimation of q via the stage A superhump method (Kato & Osaki 2013b).

3.6 V1040 Centauri

This object was originally selected as an X-ray source (RX J1155.4–5641; Motch et al. 1998). After monitoring since 1999, B. Monard detected an outburst on 2000 July 4 (vsnet-alert 5064). The variable star name V1040 Cen was given based on this observation (Kazarovets et al. 2003). The 2002 superoutburst was relatively well observed. Patterson et al. (2003) reported a superhump period of 0.06215(10) d and an orbital signal with a period of 0.06028(6) d. Using the available data (part of the data used in Patterson et al. 2003), Kato et al. (2009) studied the evolution of superhumps and identified a period of 0.060296(8) d during the post-superoutburst phase. This period has been listed as the orbital period in Ritter and Kolb (2003). However, this period was not confirmed during the quiescent phase in 2008 (Kato et al. 2009). Woudt and Warner (2010) studied this object on three nights in 2008 when the object was returning to quiescence from a normal outburst. Although Woudt and Warner (2010) reported dwarf nova oscillations (DNOs) and quasi-periodic oscillations (QPOs), there was no information about the orbital variation. P. Longa-Peña et al. (2009) found a spectroscopic orbital period of 0.06049(10) d.¹²

¹² Longa-Peña, P., & Unda-Sanzana, E. 2009, poster presentation at 14th North American Workshop on Cataclysmic Variable Stars (<http://www.noao.edu/meetings/wildstars2/posters/monday/p-longa-poster.png>).

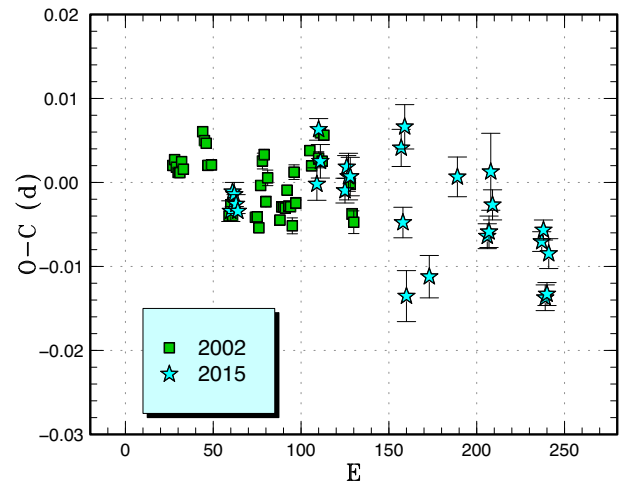


Fig. 7. Comparison of $O-C$ diagrams of V1040 Cen between different superoutbursts. A period of 0.06218 d was used to draw this figure. Approximate cycle counts (E) after the start of the superoutburst were used. Since there was a separate precursor outburst in 2015, we shifted the $O-C$ diagram so that it best matches the 2002 one. The maxima for $E > 150$ for the 2015 superoutburst probably refer to the secondary maxima (see text for details). (Color online)

Rutkowski et al. (2011) studied this object in 2009 in quiescence and two normal outbursts. Rutkowski et al. (2011) derived an orbital period of 0.060458(80) d using their photometric data.

The 2015 superoutburst was detected by R. Stubbings on April 4 at a visual magnitude of 12.0 (vsnet-outburst 18159). This observation later turned out to be a precursor outburst. The object faded once and the rising branch of the main superoutburst was recorded in April 7 at $V = 13.49$ by P. Starr. The object took another 2 d to reach the maximum around $V = 11.4$. Our time-resolved photometry started 1 d after this peak and immediately detected superhumps (vsnet-alert 18532, 18560). The times of superhump maxima are listed in e-table 6. The maxima after $E = 129$ are post-superoutburst superhumps. There was no phase jump around the termination of the superoutburst. A comparison of the $O-C$ diagrams (figure 7) suggests that the $O-C$ diagrams between the 2002 and 2015 observations do not agree if we assume that superhumps immediately started evolving around the precursor outburst. This comparison suggests that superhumps started to develop ~ 40 cycles (~ 2.5 d) following the peak of the precursor outburst. This epoch corresponds to 0.5 d before the rising phase to the main superoutburst. This observation gives support to the suggestion that it can take a long time to fully develop stage B superhumps when the precursor occurred well before the main superoutburst and the system stayed in low state for a long time before the main superoutburst starts [see subsection 5.4 in Kato et al. (2016b); the case of CYUMa in Kato et al. (2015a) might have been similar].

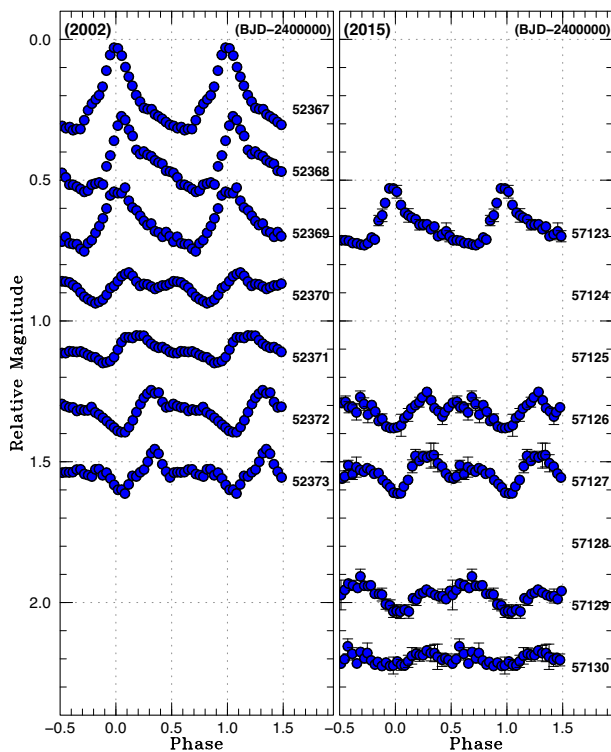


Fig. 8. Evolution of superhumps in V1040 Cen during the 2002 and 2015 superoutbursts. A period of 0.06190 d was used to draw this figure. The 2015 data were shifted by 2 d to reflect the shift in the cycle count in figure 7. (Color online)

The evolutionary phase of superhumps also match well between the 2002 and 2015 superoutburst if it is assumed that superhumps started to develop ~ 40 cycles following the peak of the precursor outburst (figure 8). Secondary maxima of superhumps are relatively prominent in this system and they became stronger than the original maxima during the later course of the superoutburst. The same feature was recorded in the Kepler data of V344 Lyr, which was considered to arise from the accretion stream resulting a bright spot that sweeps around the rim of the non-axisymmetric disk (Wood et al. 2011). The maxima for $E \geq 97$ in e-table 6 correspond to these secondary maxima, and are excluded from the process of obtaining the period in table 3. The interpretation in Wood et al. (2011) would suggest a high mass-transfer rate, and indeed “traditional” late superhumps with an ~ 0.5 phase jump are seen only in systems with frequent outbursts (e.g., Kato et al. 2013a). V1040 Cen, however, lacks frequent normal outbursts which are expected for a high mass-transfer rate. The small outburst amplitude (~ 3.0 mag for superoutbursts) of this systems suggests a bright disk in quiescence, which may in turn suggest a high mass-transfer rate. Normal outbursts in this system may be somehow suppressed. The duration of superoutbursts are somewhat short for a short

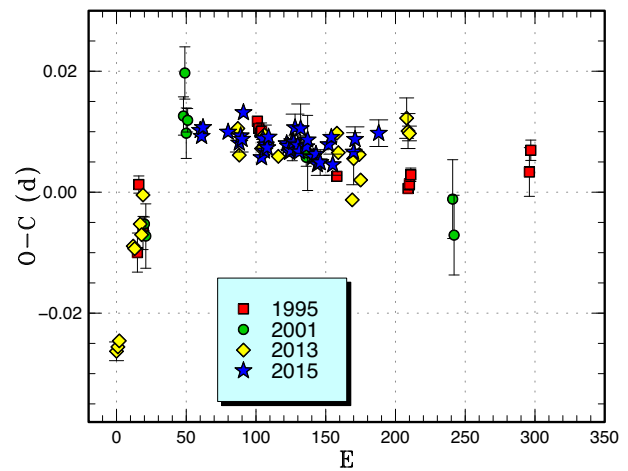


Fig. 9. Comparison of $O-C$ diagrams of ALCom between different superoutbursts. A period of 0.05732 d was used to draw this figure. Approximate cycle counts (E) after the emergence of the superhump were used. Assuming that stage A was best observed in 2013, the 1995 and 2001 $O-C$ diagrams were shifted within 20 cycles to best match the stage A–B transition in 2013. The 2015 $O-C$ diagram was shifted by 60 cycles to best match the others. (Color online)

P_{orb} object (the duration of the plateau phase was ~ 8 d in 2015).

3.7 AL Comae Berenices

We provide the table of superhumps maxima during the 2015 superoutburst which was not presented in Kimura et al. (2016a) in e-table 7. The maxima for $E \leq 20$ were not included in Kimura et al. (2016a) and some maxima with poor statistics have been removed. The resultant updated P_{dot} was $+1.6(0.8) \times 10^{-5}$. The main conclusions in Kimura et al. (2016a) are unchanged.

A comparison of $O-C$ diagrams between different superoutbursts is shown in figure 9. In order to match the other $O-C$ diagrams, the 2015 one had to be shifted by 60 cycles. This implies that stage A superhumps started to appear ~ 3 d before the initial superhump observation on BJD 2457087 (2015 March 6). Since the object was detected on the rise on March 4, superhumps should have already started to appear when the object was on the rise to the superoutburst maximum. This is consistent with the lack of stage A superhumps in Kimura et al. (2016a), in which the earliest part of the superoutburst was not well observed.

3.8 VW Coronae Borealis

VW CrB was discovered as a dwarf nova (Antipin Var 21) by Antipin (1996a). The observations by Antipin (1996a) indicated the presence of two types of outbursts, which was already suggestive of an SUUMa-type dwarf nova. During the 1997 superoutburst, Novák (1997) observed this object

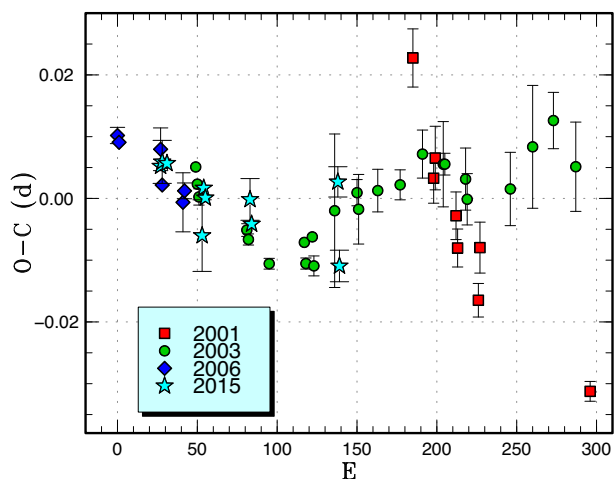


Fig. 10. Comparison of $O-C$ diagrams of VWCrB between different superoutbursts. A period of 0.07290 d was used to draw this figure. Approximate cycle counts (E) after the start of the superoutburst were used. (Color online)

on one night and detected superhumps. Liu et al. (1999) obtained a spectrum in outburst ($B = 15.8$). This observation was made approximately one month after the superoutburst observed in Novák (1997), and was likely a normal outburst. Nogami et al. (2004) reported observations of two superoutbursts in 2001 and 2003, and detected a positive P_{dot} despite the relatively long superhump period. These observations and the 2006 superoutburst were analyzed in Kato et al. (2009).

The 2015 superoutburst was detected by D. Denisenko using the MASTER network (vsnet-alert 18577). Subsequent observations detected superhumps (vsnet-alert 18583). The times of superhump maxima are listed in e-table 8. A comparison of $O-C$ diagrams between different superoutbursts is shown in figure 10. The 2015 observation most likely covered stage B.

3.9 V550 Cygni

V550 Cyg was discovered by Hoffmeister (1949) as a dwarf nova (= S3847) with a photographic range of 15 to fainter than 18 mag. Ahnert-Rohlf (1952) reported a photographic range of 14.8 to fainter than 16.3. Although the finding chart was provided by Hoffmeister (1957) (Nr. 291), the scale was insufficient to identify the object in quiescence. Pinto and Romano (1972) recorded an outburst at a photographic magnitude of 14.2 on 1961 September 20. Skiff (1999) was the first to identify the object in 1999 and two outbursts were detected in 2000 (vsnet-alert 3993, 5191). During the 2000 August outburst, superhumps were detected (Kato et al. 2009).

The 2015 outburst was detected by E. Muylaert on October 11 at an unfiltered CCD magnitude of 15.12

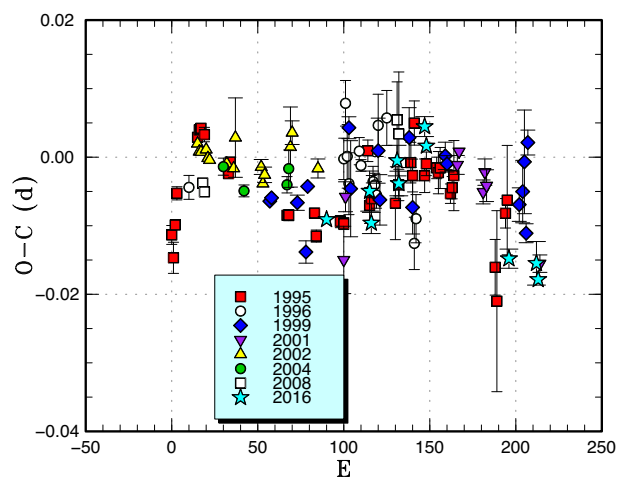


Fig. 11. Comparison of $O-C$ diagrams of V1028 Cyg between different superoutbursts. A period of 0.06178 d was used to draw this figure. Approximate cycle counts (E) after the start of the superoutburst (the start of the main superoutburst when preceded by a precursor) were used. The E for the 2008 superoutburst was somewhat uncertain due to the lack of observations at the early stage. The 2016 superoutburst was shifted by 90 cycles to match the best observed 1995 one. (Color online)

(cf. vsnet-alert 19156). Only single-night observations (vsnet-alert 19173) yielded two superhump maxima: BJD 2457313.0659(5) ($N = 137$) and 2457313.1256(18) ($N = 87$).

3.10 V1028 Cygni

V1028 Cyg was discovered as a dwarf nova (= S7854) by Hoffmeister (1963a). The object has been famous for the low frequency of outbursts (see e.g., Mayall 1968, 1970). Early observations (Tchäpe 1963) were already indicative of an SUUMa-type dwarf nova. Bruch and Schimpke (1992) reported a typical dwarf nova-type spectrum in quiescence. The 1995 superoutburst was the best recorded (cf. vsnet-alert 166, 168, 169, 172, 175, 177, 192, 193, 205). This superoutburst was one of the first examples showing positive P_{dot} , although the publication of results took some time (Baba et al. 2000). Other superoutbursts (not well observed) in 1996, 1999, 2001, 2002, 2004 and 2008 were reported in Kato et al. (2009).

The 2016 outburst was detected on March 14 probably on the rising phase ($V = 14.8$) by the ASAS-SN team and M. Hiraga (vsnet-alert 19601). Since the initial detection magnitude was faint, the outburst did not receive attention. The initial time-resolved photometry started on March 18 when the superoutburst state was confirmed. Superhumps were soon recorded (vsnet-alert 19632). The times of superhump maxima are listed in e-table 9. The $O-C$ analysis (figure 11) clearly indicates that the present observation recorded the later part of stage B and stage C. The period of stage C superhumps was not determined due to the lack

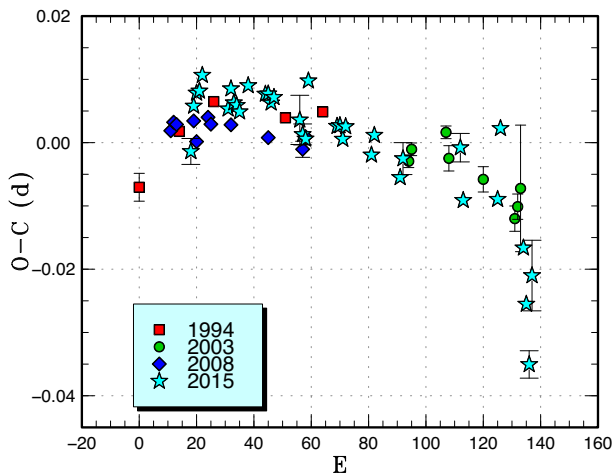


Fig. 12. Comparison of $O-C$ diagrams of V1113Cyg between different superoutbursts. A period of 0.07911 d was used to draw this figure. Approximate cycle counts (E) after the start of the superoutburst were used. (Color online)

of data. In figure 11, we had to shift 90 cycles to match the $O-C$ curve to the 1995 one, although initial superhump observations started ~ 60 cycles after the outburst detection. It may have been that the 2016 superoutburst was shorter than other ones, or it had a separate precursor during which superhumps already started to develop.

3.11 V1113Cygini

V1113 Cyg was discovered as a dwarf nova (= S 9382) by Hoffmeister (1966). Kato et al. (1996b) reported the detection of superhumps. Kato (2001b) reported a mean supercycle of 189.8 d and that the number of normal outbursts is too small for this short supercycle. Bakowska et al. (2010) studied the 2003 and 2005 superoutbursts, and also confirmed the low frequency of normal outbursts. Although Bakowska et al. (2010) reported large negative P_{dot} , they probably recorded stage B–C transition (Kato et al. 2010).

The 2015 superoutburst was detected by the ASAS-SN team on August 28 at $V=13.95$ (cf. vsnet-alert 19014). Subsequent observations detected superhumps (vsnet-alert 19018, 19019, 19023). The times of superhump maxima are listed in e-table 10. The stages are not distinct (see also figure 12) and we adopt a globally averaged period, excluding the rapidly fading part, in table 3.

3.12 HO Delphini

HO Del (= S 10066) was discovered as a dwarf nova by Hoffmeister (1967). Hoffmeister (1967) recorded two outbursts in 1963 October and 1966 September. The coordinates of this object were wrongly given in Hoffmeister (1967) and were only corrected in the third volume of

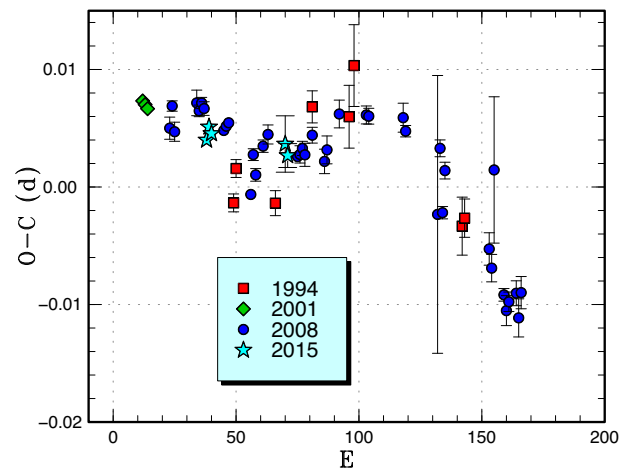


Fig. 13. Comparison of $O-C$ diagrams of HO Del between different superoutbursts. A period of 0.06437 d was used to draw this figure. Approximate cycle counts (E) after the start of the superoutburst were used. The 1994 superoutburst was artificially shifted to match the others. (Color online)

the fourth edition of the GCVS (Kholopov et al. 1985) (the correct identification was found by T.K. in 1990 while preparing charts by comparison with the Palomar Sky Survey; the observations made by the VSOLJ members since 1990 refer to the correct object). Munari and Zwitter (1998) confirmed the dwarf nova-type nature by recording relatively strong Balmer and He I emission lines. Observations of superhumps during the 1994, 1996 and 2001 superoutbursts were analyzed in Kato et al. (2003a). Patterson et al. (2003) also reported the 1996 superoutburst and the spectroscopic orbital period. In Kato et al. (2003a), HO Del was chosen as a prototypical object showing the brightening trend near the end of the plateau phase. This phenomenon was later identified as the emergence of stage C superhumps (Kato et al. 2009). The 2008 superoutburst was also reported in Kato et al. (2009).

The 2015 outburst was detected by R. Stubbings and ASAS-SN on July 18 (vsnet-alert 18865). Superhumps were detected by observations which started 2 d later (vsnet-alert 18871). The times of superhump maxima are listed in e-table 11. The superhump period indicates that these observations were already in stage B. A comparison of $O-C$ diagrams between different superoutbursts is shown in figure 13. It is likely that stage A is short in this system since stage B superhumps appeared 2 d after the outburst detection despite that the outburst was detected sufficiently early, at least in 2001.

3.13 AQ Eridani

AQ Eri was discovered as a dwarf nova (= AN 431.1934) by Morgenroth (1934). Hoppe (1935) studied this object

using 232 plates and concluded that it was unlikely to be a Mira variable since it was invisible most of the time. Hoppe (1935) derived a possible period of 78 d using three observed maxima (outbursts). Petit (1960) listed the object as a U Gem-type object with a cycle length of 78 d. Bond (1978) obtained a spectrum and recorded diffuse (broad) hydrogen emission lines superposed on a blue continuum. Vogt and Bateson (1982) also listed the object as a U Gem-type variable. Kholopov et al. (1985) (printed version) listed the object as a possible Z Cam-type dwarf nova based on Bateson (1982). Photometric observations in quiescence, however, suggested a short orbital period (Szkody 1987).

Based on historical instances in which superoutbursts were confused with Z Cam-type standstills, Kato, Fujino, and Iida (1989) studied this object during a long, bright outburst in 1987 November both in photographic and visual observations. The detection of superhumps confirmed the SUUMa-type nature.

Kato (1991, 2001a) reported observations of superhumps using a CCD in 1991 and 1992, respectively. Kato and Matsumoto (1999b) also reported observations of a normal outburst in 1998 December. The spectroscopic orbital period was determined by Mennicken and Vogt (1993) and by Thorstensen et al. (1996). Tappert et al. (2003) reported a line-profile analysis. Further superoutbursts were observed and reported in Kato et al. (2009) (the 2006, 2008 superoutbursts), Kato et al. (2010) (the 2010 superoutburst), Kato et al. (2013a) (the 2011 superoutburst), and Kato et al. (2014a) (the 2012 superoutburst).

The 2016 superoutburst was visually detected by R. Stubbings on January 24 (vsnet-alert 19438). Subsequent observations detected superhumps (vsnet-alert 19444). The times of superhump maxima are listed in e-table 12. We observed stage B and the initial part of stage C as inferred from figure 14.

3.14 AX Fornacis

This object was cataloged as 2QZ J021927.9–304545 in the 2dF QSO Redshift Survey (Boyle et al. 2000). B. Monard began monitoring this object in 2005 January and detected a bright outburst (unfiltered CCD magnitude 11.9) on 2005 July 2 (vsnet-alert 8521). There were several past outbursts in the ASAS-3 (Pojmański 2002) data (vsnet-alert 8523). The object was then established to be an SUUMa-type dwarf nova by the detection of superhumps (Imada et al. 2006). These two superoutbursts were studied further in Kato et al. (2009). The object was given a permanent name of AX For in Kazarovets et al. (2011).

The 2015 superoutburst was visually detected by R. Stubbings at a magnitude of 12.0 on November 10 (cf. vsnet-alert 19255). The times of superhump maxima

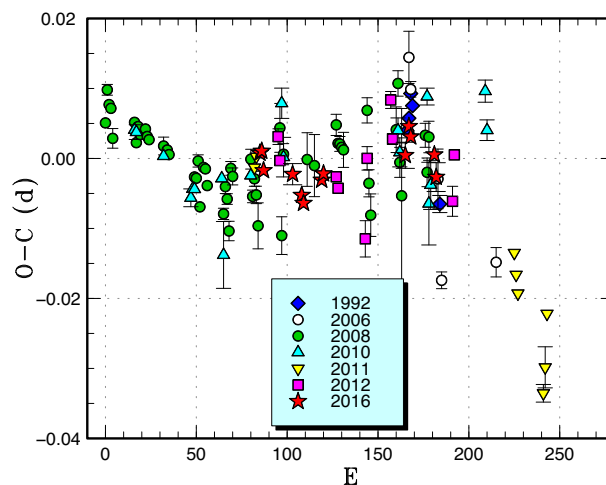


Fig. 14. Comparison of $O-C$ diagrams of AQ Eri between different superoutbursts. A period of 0.06238 d was used to draw this figure. Approximate cycle counts (E) after the start of the superoutburst were used. Since the starts of the 2012 and 2016 superoutbursts were not well constrained, we shifted the $O-C$ diagram to best fit the best-recorded 2008 one. (Color online)

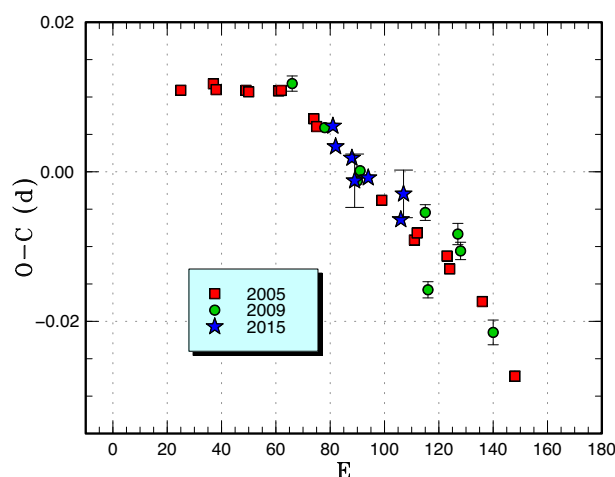


Fig. 15. Comparison of $O-C$ diagrams of AX For between different superoutbursts. A period of 0.08140 d was used to draw this figure. Approximate cycle counts (E) after the start of the superoutburst were used. (Color online)

are listed in e-table 13. A comparison of $O-C$ diagrams between different superoutbursts (figure 15) indicates that we only observed stage C superhumps in 2015. Although individual superhumps were not measured, a PDM analysis of the post-superoutburst data (BJD 2457346–2457350) yielded a strong signal of 0.08109(6) d, indicating that stage C superhumps persisted after the rapid fading from the outburst plateau.

3.15 V844 Herculis

This object was discovered as a dwarf nova (Antipin Var 43) by Antipin (1996b). The long outbursts were already

suggestive of an SUUMa-type dwarf nova. The first superhump detection was made by T. Vanmunster during an outburst in 1996 October (vsnet-obs 4061, 4075). The superhump period was first determined during the 1997 superoutburst by T. Vanmunster and L. Jensen (Cataclysmic Variables Circular, No. 141, also in vsnet-alert 935; vsnet-obs 5854). Patterson (1998) cited a superhump period of 0.05597(2) d determined from their observations. Kato and Uemura (2000) provided the first solid publication of superhumps in this system and reported a period of 0.05592(2) d. Thorstensen et al. (2002) obtained a spectroscopic orbital period of 0.054643(7) d. Oizumi et al. (2007) reported observations of the 2002, 2003, and 2006 superoutbursts. Positive P_{dot} was detected for the 2002 and 2006 superoutbursts. Oizumi et al. (2007) also summarized the known outbursts of this object. Most of the outbursts of this object were superoutbursts and only two out of 13 known outbursts were normal outbursts at the time of Oizumi et al. (2007). The 2008 superoutburst was reported in Kato et al. (2009). The 2009 and 2010 superoutbursts were reported in Kato et al. (2010). The second superoutburst in 2010 (hereafter 2010b) was reported in Kato et al. (2012). Another superoutburst in 2012 was reported in Kato et al. (2013a).

The 2015 superoutburst was detected by the ASAS-SN team (cf. vsnet-alert 18617). This detection was early enough and stage A superhumps were partly observed (vsnet-alert 18625, 18645). The times of superhump maxima are listed in e-table 14. The maxima for $E \leq 4$ correspond to the growing stage of superhumps and are stage A superhumps. Stage B–C transition probably fell in the observational gap between $E = 119$ and $E = 173$, and the late phase of stage B (with a long superhump period) was not properly observed.

A comparison of $O - C$ diagrams between different superoutbursts is shown in figure 16. Note that a different base period was used to draw the figure compared to the earlier ones. The 2010b superoutburst was artificially shifted by 40 cycles to match the others. This superoutburst was either unusual (there was a normal outburst ~ 60 d preceding the superoutburst, and superhumps may have started to develop before the superoutburst) or the initial part of the superoutburst was missed (there was only one negative observation with a meaningful upper limit immediately before this superoutburst).

3.16 MM Hydrae

MM Hya was originally selected as a CV by the Palomar–Green survey (Green et al. 1982). The SUUMa-type nature was confirmed by Patterson et al. (2003). See Kato et al. (2015a) for more history. The 2015 superoutburst was detected by R. Stubbings on March 9 (vsnet-alert 18395).

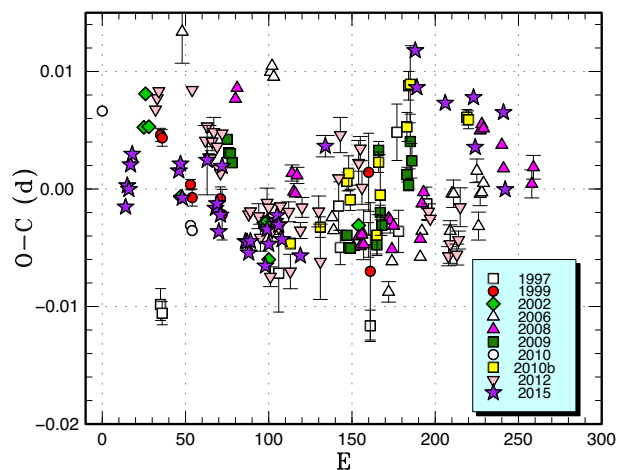


Fig. 16. Comparison of $O - C$ diagrams of V844 Her between different superoutbursts. A period of 0.05595 d was used to draw this figure. Approximate cycle counts (E) after the start of the superoutburst were used. The 2010b superoutburst were artificially shifted by 40 cycles to match the others. (Color online)

Two superhumps were recorded on March 19, when the object apparently entered the rapid fading phase: BJD 2457096.9366(12) ($N = 36$) and 2457096.9936(17) ($N = 43$).

3.17 RZ Leonis

RZ Leo (= AN 30.1919) was discovered as a variable star or a nova by Wolf (1919). The object was detected at a photographic magnitude of 10–11 on 1918 March 13. This magnitude scale was probably 1–2 mag too bright compared to the modern scale [this tendency is common to other *Astronomische Nachrichten* papers in the 1910s, see e.g., GR Ori in Kato et al. (2014a)]. Bertaud (1951) listed the object as a probable nova. Herbig (1958) provided an identification chart. The identification by Khatsov (1971) was incorrect. Brun and Petit (1957) and Petit (1960) listed this object as a dwarf nova. Vogt and Bateson (1982) listed this object as a possible WZ Sge-type object (probably based on the large outburst amplitude).

Since the object had been suspected to be a dwarf nova with rare outbursts, it has been sporadically monitored by amateur observers since the 1970s. Since 1982, it had been monitored more systematically and the second historical outburst was detected by R. Ducoty on 1984 December 29 at a visual magnitude of 12.9 (Cristiani et al. 1985; McNaught 1985; Mattei et al. 1985). Richter (1985) studied past photographic plates and detected several (some of them were questionable) outbursts only reaching 13 mag. Richter (1985) suggested that the cycle length might be as short as 6 yr. Although spectroscopic observation in outburst confirmed the dwarf nova-type nature (Cristiani et al.

1985), the object was listed as a recurrent nova in Kholopov et al. (1985). Szkody (1987) reported *JHK* photometry on 1985 January 21, 23 d after the outburst detection. Szkody (1987) ascribed the magnitude $J=14.0$ to the intermediate (“Mid”) state. In modern knowledge, this observation probably reflected the “red phase” following a superoutburst (e.g., see subsection 4.6 in Kato 2015).

On 1987 November 28, there was another outburst reaching a visual magnitude of 12.3–12.5 detected by S. Lubbock (Hurst et al. 1987; Mattei et al. 1987). This outburst lasted for at least 12 d. In the meantime, Howell and Szkody (1988) performed time-resolved CCD photometry in quiescence and detected 0.4 mag modulations with a period of 104 min and suggested the SUUMa-type classification. Since the object had been suspected to be a WZ Sge-type dwarf nova (Vogt & Bateson 1982), it has been discussed assuming this classification (Downes 1990; O’Donoghue et al. 1991). In O’Donoghue et al. (1991), the presence of a short (normal) outburst in 1989 (Narumi et al. 1989) was in particular discussed since various authors had claimed the absence of short outbursts in WZ Sge.

Despite these outburst detections, no secure outburst had been detected before 2000 (there was a possible outburst in 1990 October–November in the AAVSO data, only detected by a single observer). The 2000 outburst was detected by R. Stubbings on December 20 at a visual magnitude of 12.1 (vsnet-alert 5437; Mattei et al. 2000). The detection of superhumps finally led to the identification of an SUUMa-type dwarf nova (vsnet-alert 5446, 5448, Ishioka et al. 2000, 2001). Since the orbital period had already been measured to be 0.07651(26) d (Mennickent & Tappert 2001; Mennickent et al. 1999), Ishioka et al. (2001) identified the modulations with a period of 0.07616(21) d detected during the early stage of the outburst to be early superhumps. The orbital period has been updated to be 0.0760383(4) d by photometric observations in quiescence (Patterson et al. 2003). Dai et al. (2016) further determined the orbital period to be 0.07602997(4) d using the Kepler K2 mission data. More analyses of superhumps during the 2000 superoutburst were reported in Patterson et al. (2003) and Kato et al. (2009).

There was another superoutburst in 2006 detected by S. Kerr on May 27 at a visual magnitude of 12.5 (vsnet-outburst 6885). This outburst was not very well observed due to the limited visibility in the evening sky. An analysis of superhumps was reported in Kato et al. (2009). There have been no confirmed normal outbursts other than the 1989 one.

Howell et al. (2010) and Hamilton et al. (2011) reported the spectral type of the secondary to be M3–M4V and $M4 \pm 1$, respectively, by infrared observations. These results were consistent with the analysis of spectral energy

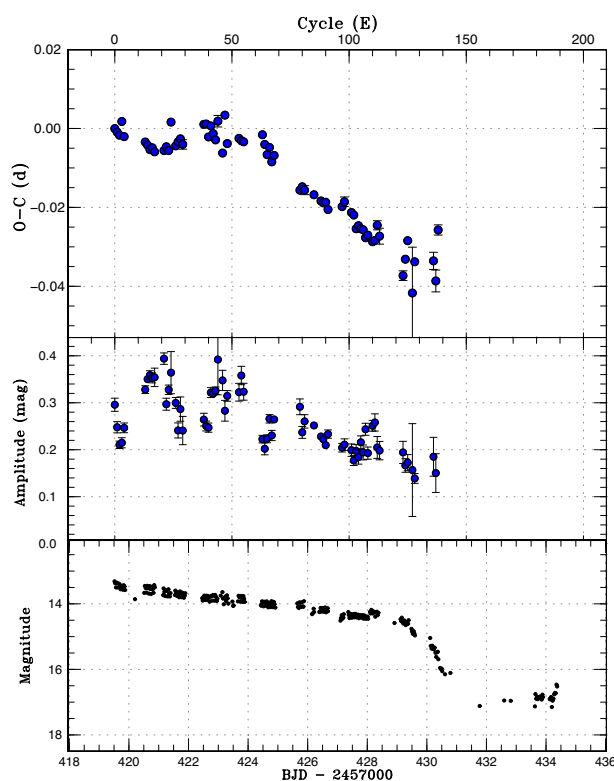


Fig. 17. $O-C$ diagram of superhumps in RZ Leo (2016). Upper: $O-C$ diagram. We used a period of 0.07865 d for calculating the $O-C$ residuals. Middle: Amplitudes of superhumps. The modulations of the amplitudes with a period of ~ 30 cycles in the initial part are the beat phenomenon between superhump period and the orbital period. Lower: Light curve. The data were binned to 0.026 d. (Color online)

distribution by Mennickent and Diaz (2002), who suggested the spectral type M5 for the secondary.

The 2016 outburst was detected by R. Stubbings at a visual magnitude of 13.0 on January 31 (vsnet-alert 19448). Subsequent observations already recorded fully developed superhumps (vsnet-alert 19452, 19458, 19466). The object rapidly faded on February 11–12 (vsnet-alert 19499). There was also a post-superoutburst rebrightening at a visual magnitude of 14.1 on February 15 (vsobs-share 12235). The times of superhump maxima are listed in e-table 15. There were clear stages B and C (figure 17). In this figure, the amplitudes of superhumps cyclically varied with a period of ~ 30 cycles, particularly in the early stage of the superoutburst. This variation most likely reflects the beat phenomenon between the superhump period and orbital period (the estimated beat period is 2.3 d or 29 superhump cycles).

A comparison of the $O-C$ diagrams (figure 18) suggests that superhumps started ~ 3 d before the initial time-resolved observation in 2016. It means that superhumps already started to develop at the time of Stubbings’s initial outburst detection. The true start of the outburst was unknown due to a 6-d gap in the observation. The $O-C$

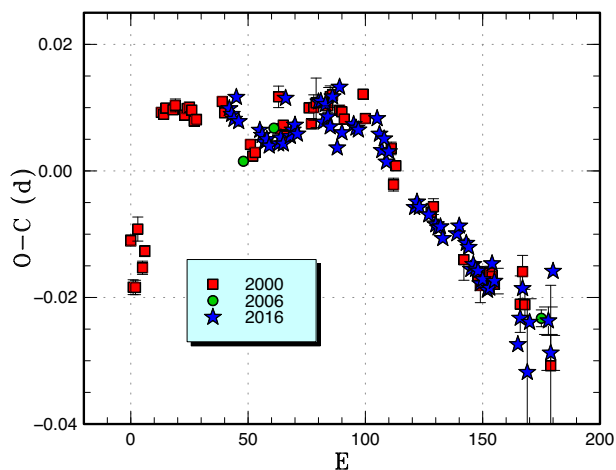


Fig. 18. Comparison of $O-C$ diagrams of RZ Leo between different superoutbursts. A period of 0.07865 d was used to draw this figure. Approximate cycle counts (E) after the start of the appearance of ordinary superhumps. Since the starts of the 2006 and 2016 outbursts were not constrained, we shifted the $O-C$ diagram of these outbursts to best fit the better-recorded 2000 one. We had to shift 48 and 42 cycles for the 2006 and 2016 outbursts, respectively. (Color online)

diagrams have stages B and C and a large positive P_{dot} typical for short- P_{orb} systems. It would be worth noting that stage C superhumps persisted long after the main superoutburst and there was no phase shift at the time of the rapid fading.

Although the existence of early superhumps was reported (Ishioaka et al. 2001), these reported early superhumps may have been different from those of typical WZ Sge-type objects since the phase of early superhumps was apparently short. The period of these modulations was not sufficiently determined to make a secure comparison with the orbital period. Although Kato et al. (2009) concluded that these modulations could not be considered as an extension of stage A superhumps, the exact identification of modulations in the earliest stage in RZ Leo still awaits confirmation. It was a pity that both the 2006 and 2016 superoutbursts were not detected sufficiently early to confirm these modulations. Future intensive observations on the next occasion are still strongly desired since RZ Leo is supposed to be an atypical (long- P_{orb}) WZ Sge-type system (cf. Kato 2015) and confirmation of early superhumps is very important to verify this classification.

Since RZ Leo apparently has a high orbital inclination (doubly peaked emission lines, ellipsoidal variations in quiescence and beat phenomenon during superoutburst), we attempted to detect the orbital variations during the three superoutbursts (2000, 2006, and 2016). All the combinations of these superoutbursts yielded a consistent period (the alias was selected within the range considering the error in Dai et al. 2016) within respective errors, and we

identified 0.07603005(2) d to be the updated orbital period (e-figure 1).¹³

3.18 V585 Lyrae

V585 Lyr was discovered as a dwarf nova (TK 4) by Kryachko (2001). Kryachko (2001) already suggested the SUUMa-type classification based on the presence of long and short outbursts. The 2003 superoutburst was well observed and analyzed in detail (Kato et al. 2009). The 2012 superoutburst was also observed in Kato et al. (2013a).

The object is located in the Kepler field and two superoutbursts (2010 January–February and 2012 April–May) and one normal outburst (2013 January) were recorded during the Kepler mission. Although this target was also observed in short-cadence mode in limited epochs, all outbursts observed by Kepler were recorded in long-cadence mode, making detailed analysis of the superhump evolution difficult. Kato and Osaki (2013a) analyzed the Kepler long-cadence observations in 2010 using Markov-Chain Monte Carlo (MCMC)-based modeling of long-exposure (~ 29 min) sampling and derived an $O-C$ diagram. This analysis confirmed the results of ground-based photometry with higher time resolutions but frequent gaps (Kato et al. 2009). The particularly important point was that Kepler observation confirmed the superhump stages (A–C) and the lack of phase jump around the termination of the superoutburst. V585 Lyr was also unique among Kepler observations of dwarf novae: this object showed a rebrightening both in the 2000 and 2012 superoutbursts, though such rebrightenings are relatively common among other SUUMa/WZ Sge-type dwarf novae (cf. Kato et al. 2009; Kato 2015). There were “mini-rebrightenings” between the main superoutburst and the rebrightening (Kato & Osaki 2013a). Meyer and Meyer-Hoffmeister (2015) interpreted these “mini-rebrightenings” as a result of reflection of cooling waves between the lower branch and the intermediate branch in the S-curve of the thermal equilibrium of the accretion disk. V585 Lyr was also the only object in the Kepler data in which no precursor outburst was associated with the superoutburst and a delay of development of superhumps was recorded. This was interpreted as a result of highly accumulated mass in the disk before the outbursts started (Kato & Osaki 2013a), corresponding to “case B” superoutburst (the mass stored in the disk before the superoutburst is large enough and the disk can remain at radius of the 3 : 1 resonance or beyond for some time before superhumps start to develop) discussed by Osaki and Meyer (2003).

¹³ E-figures are available only on online edition as Supporting Information.

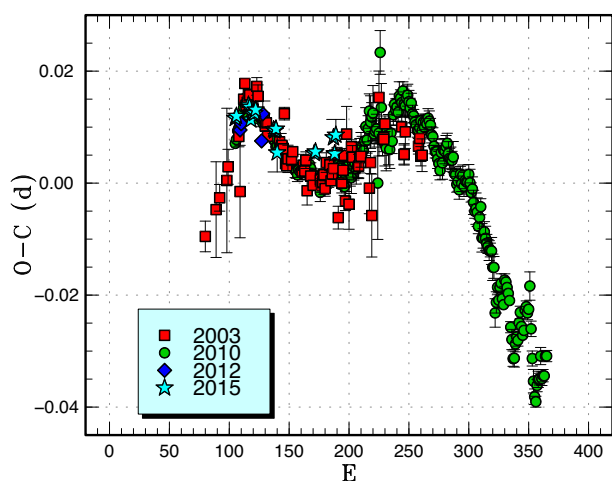


Fig. 19. Comparison of $O-C$ diagrams of V585 Lyr between different superoutbursts. The 2010 data refer to Kepler observations analyzed in Kato and Osaki (2013a). A period of 0.06045 d was used to draw this figure. Approximate cycle counts (E) after the start of the superoutburst were used. The starts of the 2010 and 2012 superoutbursts were well determined by the Kepler data. We had to shift 49 and 80 cycles for the 2003 and 2015 data, respectively, to obtain the best match with the 2010 data. These values suggest that the outbursts were missed for 3 d and 5 d for the 2003 and 2015 superoutbursts, respectively, or these superoutbursts had exceptionally smaller scales. Considering the limited visual monitoring, the first possibility looks more likely. (Color online)

The 2015 superoutburst was detected by the ASAS-SN team (vsnet-alert 18688). Subsequent observations detected superhumps (vsnet-alert 18698, 18722). The times of superhump maxima are listed in e-table 16. The final part of stage A and early part of stage B were observed (figure 19).

3.19 V2051 Ophiuchi

V2051 Oph was discovered as an emission-line object in outburst (Sanduleak 1972). Sanduleak (1972) suggested that this object is a dwarf nova rather than a nova. Bond, Wagner, and Tapia (1977) listed this object as a candidate polar, although this list included various objects (EM Cyg: dwarf nova; V Sge: novalike variable; CL Sco, HK Sco: symbiotic stars) which are not currently considered to be related to polars. Angel, Liebert, and Stockman (1977) reported that this object is an eclipsing system with a period of 96 min. Angel, Liebert, and Stockman (1977) also reported strong Balmer, He I and He II emission lines. Bond (2004) confirmed this spectroscopic finding. After a suggestion of similarity with HT Cas (Patterson 1980), this object started to be monitored by amateur astronomers in 1980. Secure outburst detections were not made in the 1980s. F. Bateson, Royal Astronomical Society of New Zealand, reported only a limited number of outbursts up to 1997 (only reaching 13.0–13.5 mag and without evidence for superoutbursts: vsnet-chat 546; see also Warner & Cropper 1983). This

object was considered to be too faint for amateur telescopes (cf. citation in Warner & O’Donoghue 1987).

The history of classification of this object has long been confusing. Warner and Cropper (1983) obtained high-speed photometry and found eclipse profiles were highly variable. Warner and Cropper (1983) suggested that this object is similar to other SU UMa-type eclipsing dwarf novae Z Cha, OY Car, and HT Cas. The analysis of flickering suggested a possibility that the inner region of the disk may be truncated as in polars (Warner & Cropper 1983). A spectroscopic study by Cook and Brunt (1983) suggested that the white dwarf is eclipsed. Wenzel (1984) surveyed about 400 Sonneberg plates with limiting magnitudes of 11.5–13 mag and found no major outburst. Wenzel (1984) considered this finding to be compatible with a polar rather than a high-amplitude dwarf nova. Watts et al. (1986) reported detailed spectrophotometric analysis and suggested the similarity of the disk structure to that of OY Car. Warner and O’Donoghue (1987) reported high-speed photometry and the reconstructed eclipse map did not show evidence of a well-established accretion disk. Warner and O’Donoghue (1987) suggested that this object is a low-field polar based on these observations.

In 1997, several faint outbursts were recorded by R. Stubbings: 13.9 mag on June 27 (vsnet-alert 1019), 13.6 mag on August 7 (vsnet-obs 6643, vsnet-alert 1129) and 14.2 mag on September 24 (vsnet-obs 7540, vsnet-alert 1239). There was another outburst on 1998 March 27 at 13.6 mag (vsnet-alert 1600). On 1998 March 18, there was a bright outburst reaching 11.9 mag (the outburst started 1 d earlier) (vsnet-alert 1796). CCD observations by L. T. Jensen revealed humps and eclipses (vsnet-alert 1814). Observations by S. Kiyota identified these humps as superhumps (vsnet-alert 1819). Upon detection announcement of this superoutburst, B. Warner wrote (vsnet-alert 1833): “The eclipse centered on a ‘superhump’ shown on your Web page is just the enhanced orbital hump that appears during outburst.” T. Kato reported that superhump signatures were present in observations by S. Kiyota and Osaka Kyoiku U. team and pointed out that B. Warner actually recorded the fading part of a superoutburst in Warner and O’Donoghue (1987), during which an apparent superhump was recorded only one night (vsnet-alert 1835). J. Patterson’s team also reported the identification of the observed humps as superhumps (vsnet-alert 1859). The result by S. Kiyota was published in Kiyota and Kato (1998).

Another superoutburst was recorded in 1999 July–August. (vsnet-alert 3284, 3308, 3315, 3330, 3347). There was also a rebrightening (vsnet-alert 3354). After this outburst, there was no doubt about the SU UMa-type classification of this object [see also Vriellmann and Offutt

(2000, 2003) and Papadaki et al. (2008)]. Kato et al. (2001) reported a supercycle of 227 d and the recurrence time of normal outbursts of 45 d. In our series of papers, the 1999, 2003, and 2009 superoutbursts were analyzed in Kato et al. (2009), the 2010 one was reported in Kato et al. (2010). Despite that the recent observations suggest that this object is an ordinary SUUMa-type dwarf nova, there has been an argument, using eclipse maps, that outbursts in this system have properties that are different from what the disk instability model suggests (Baptista et al. 2007; Andrade & Baptista 2014; Wojcikiewicz & Baptista 2014). Baptista (2012) suggested that dwarf novae have two groups; the one which can be understood in the framework of the disk instability model and the other which can only be explained in terms of the mass-transfer instability model. Baptista (2012) claimed that V2051 Oph belongs to the latter group.

In addition to the above references, this object has been thoroughly investigated since it is fairly close and has received much attention from early times: eclipse analysis (Baptista et al. 1998; Vrielmann et al. 2002; Papadaki et al. 2008), flickering (Bruch 2000; Baptista & Bortoletto 2004), spectroscopy (Steghs et al. 2001; Saito & Baptista 2006; Longa-Peña et al. 2015), and secular variation of the orbital period (Echevarria & Alvarez 1993; Baptista et al. 2003).

The 2015 superoutburst was detected by R. Stubbings (vsnet-alert 18650). The outburst was detected on May 21 and reached a peak brightness of 11.9 mag on May 23. The object faded rather quickly and it was already around 14 mag when observations of superhumps were performed (vsnet-alert 18675). During the past superoutbursts, the object was mostly around 13 mag or fainter when CCD time-resolved observations were performed despite that the peak visual magnitude reached 12 or even brighter. The short duration of the brightness peak may have been the reason why past plate collections and visual monitoring failed to record relatively frequent superoutbursts. Such a short superoutburst peak may be the result of a high inclination and would deserve further study.

The times of superhump maxima in 2015 are listed in e-table 17. We possibly detected stage B and the initial part of stage C by comparison with other superoutbursts of this object (figure 20).

The object was observed after the superoutburst and the superhump signal with a period of 0.06373(2) d was detected up to the next normal outburst (BJD 2457186, June 13). If we assume a disk radius of $0.35 \pm 0.04a$, where a is the binary separation, for the post-superoutburst state of an ordinary SUUMa-type dwarf nova (Kato & Osaki 2013b), the mass ratio is estimated to be $q = 0.11(3)$. Although this value is smaller than $q = 0.19(3)$ (Baptista et al. 1998), who obtained the value from eclipse observations, and $q = 0.18(5)$ (Longa-Peña et al. 2015)

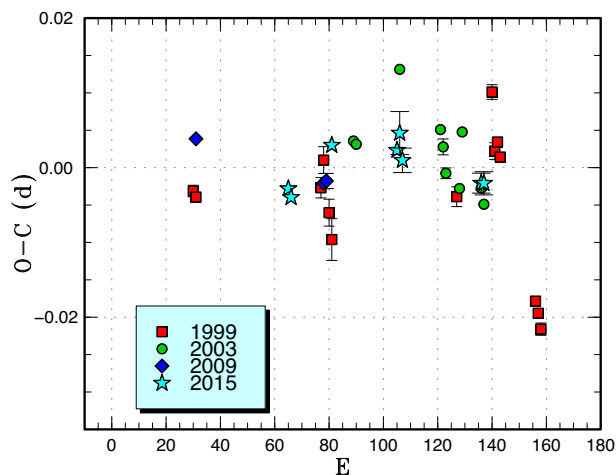


Fig. 20. Comparison of $O - C$ diagrams of V2051 Oph between different superoutbursts. A period of 0.06430 d was used to draw this figure. Approximate cycle counts (E) after the start of the superoutburst were used. (Color online)

by Doppler tomography, our smaller value for a short- P_{orb} object appears to fit more comfortably on the evolutionary diagram (e.g., figure 5 in Kato & Osaki 2013b, see also figure 68 in this paper). Since eclipse light curves in this system were very variable (Warner & O'Donoghue 1987) and ingress/egress features of the hot spot are difficult to define (Baptista et al. 1998), determination of q from eclipse observations would suffer intrinsic uncertainties. Our new value using post-superoutburst superhumps would be treated as a new measurement of q with comparable significance.

We have also updated the eclipse ephemeris by using MCMC analysis (Kato et al. 2013a) of the eclipse observations of our 1999–2015 data:

$$\text{Min(BJD)} = 2453189.48679(1) + 0.0624278552(2)E. \quad (1)$$

The epoch refers to the center of the entire observation.

3.20 V368 Pegasi

V368 Peg is a dwarf nova (Antipin Var 63) discovered by Antipin (1999). The SUUMa-type nature was identified by J. Pietz during the 1999 superoutburst (vsnet-alert 3317). The 2000, 2005, and 2006 superoutbursts were studied in Kato et al. (2009) and the 2009 superoutburst was reported in Kato et al. (2010).

The 2015 superoutburst was visually detected by P. Schmeer on September 14 (vsnet-alert 19063). This superoutburst was also detected by C. Chiselbrook (AAVSO) on the same night. Single-night observations on September 17

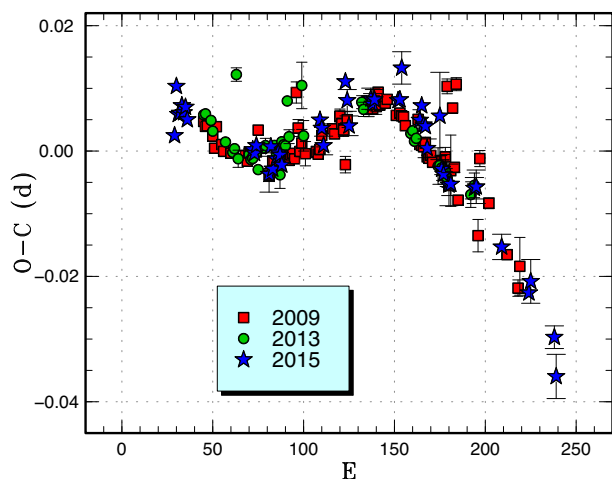


Fig. 21. Comparison of $O-C$ diagrams of V650 Peg between different superoutbursts. A period of 0.06975 d was used to draw this figure. Approximate cycle counts (E) after the start of the superoutburst were used. In Kato et al. (2014b), cycles were counted since the detection of the outbursts, contrary to the description in Kato et al. (2014b). The starts of the outbursts were not known at the time of Kato et al. (2014b). The start of the 2015 outburst is much better defined and we shifted the other outbursts to fit the 2015 one. (Color online)

recorded two superhump maxima: BJD 2457283.3273(3) ($N = 76$) and 2457283.3969(4) ($N = 64$).

3.21 V650 Pegasi

This dwarf nova is an SUUMa-type dwarf nova selected by P. Wils (cf. Shears et al. 2011). The object was formerly referred to as ASAS J224349+0809.5. For more history, see Kato et al. (2014b).

The 2015 outburst was detected by the ASAS-SN team on September 5 (cf. vsnet-alert 19032). Superhumps were soon detected (vsnet-alert 19034, 19059, 19066, 19069). The times of superhump maxima are listed in e-table 18. Although stage A was not recorded, stages B and C were clearly detected (figure 21).

3.22 PU Persei

PUPer was discovered as a dwarf nova (= S9727) by Hoffmeister (1967), who detected two outbursts. Romano and Minello (1976) also detected two outbursts. Both Hoffmeister (1967) and Romano and Minello (1976) recorded short and long outbursts. Busch, Häussler, and Splittergerber (1979) recorded a further two long outbursts. Bruch, Fischer, and Wilmsen (1987) detected another outburst. The presence of two types of outbursts and the large outburst amplitude made PUPer an excellent candidate for an SUUMa-type dwarf nova. Kato and Nagami (1995) observed a normal outburst in 1995 October, and Kato and Matsumoto (1999a) finally detected superhumps

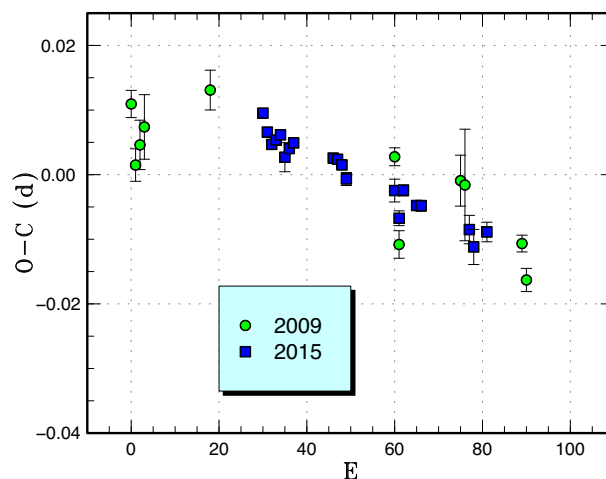


Fig. 22. Comparison of $O-C$ diagrams of PU Per between different superoutbursts. A period of 0.06831 d was used to draw this figure. Approximate cycle counts (E) after the start of the observation were used. Since the starts of neither outburst were constrained, we shifted the $O-C$ diagram of the 2015 outburst to best fit the better-recorded 2009 one. (Color online)

during the 1998 September outburst. The 2009 superoutburst was reported in Kato et al. (2009).

The 2015 outburst was detected by E. Muylaert via CCD observations on October 3 (cf. vsnet-alert 19114). Superhumps were detected (vsnet-alert 19124, 19130, 19144). The times of superhump maxima are listed in e-table 19. A comparison with the 2009 data suggests that we only recorded stage C superhumps (figure 22).

3.23 QY Persei

QYPer was discovered as a dwarf nova (= S9178) by Hoffmeister (1966). Pinto and Romano (1976) reported another outburst at a photographic magnitude of 13.7 on 1971 September 21. The object has been renowned for its low frequency of outbursts and the 1989 October outburst was reported by Rosino and Candeo (1989). Although there was an outburst in 1994 October, it faded rather quickly. The next confirmed outburst occurred in 1999 December and superhumps were detected (Kato et al. 2009). Contrary to the expectations related to a WZ Sge-type dwarf nova, the superhump period was long (~ 0.0786 d). The object was considered to be a long-period system resembling WZ Sge-type dwarf novae, although no early superhumps have been detected (Kato 2015). The next confirmed outburst (superoutburst) occurred in 2005 September, which was not well observed (Kato et al. 2009).

The 2015 outburst was detected by M. Hiraga at an unfiltered CCD magnitude of 14.7 on November 14 (vsnet-alert 19263). The object was fainter than 16.2

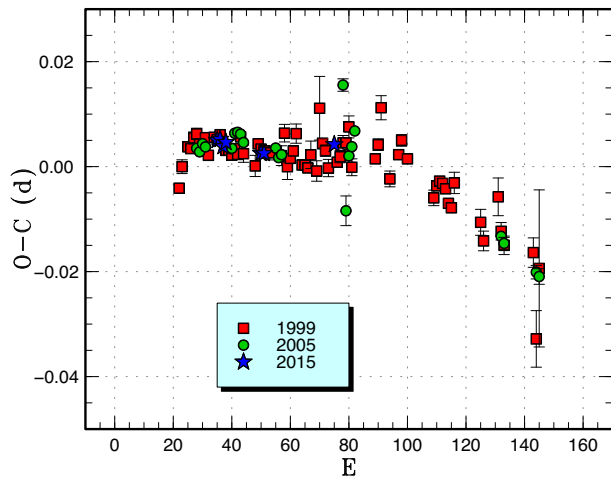


Fig. 23. Comparison of $O-C$ diagrams of QYPer between different superoutbursts. A period of 0.07862 d was used to draw this figure. Approximate cycle counts (E) after the start of the superoutburst were used. Since the start of the 2015 superoutburst was not well constrained, we shifted the $O-C$ diagram to best fit the others. (Color online)

two days before. Subsequent observations detected superhumps (vsnet-alert 19267, 19281). The times of superhump maxima are listed in e-table 20. The early appearance of superhumps after the start of the outbursts (figure 23) suggest that the object is less likely a WZ Sge-type dwarf nova. Since the 2015 outburst was much fainter than the 1999 outburst, there remains a possibility that the object shows superoutbursts of different extent as in the WZ Sge-type object AL Com (Kimura et al. 2016a).

3.24 TY Piscium

For the history of this well-known SUUMa-type object, see Kato et al. (2014b). The 2015 superoutburst was visually detected by E. Muylaert at a magnitude of 12.2 on October 29. Our observations covered the later part of the outburst and recorded superhumps in e-table 21. A comparison of $O-C$ diagrams of TY Psc between different superoutbursts is given in figure 24.

3.25 V493 Serpentis

This object (= SDSS J155644.24-000950.2) was selected as a dwarf nova by SDSS (Szkody et al. 2002). The SUUMa-type nature was confirmed during the 2006 and 2007 superoutbursts (Kato et al. 2009). See Kato et al. (2014a) for more history. The 2015 superoutburst was detected by the ASAS-SN team in its early phase (vsnet-alert 18666). Subsequent observations indeed recorded stage A superhumps (vsnet-alert 18673, 18683) and later development (vsnet-alert 18721). The times of superhump maxima are listed in e-table 22. Although transitions between stages were rather

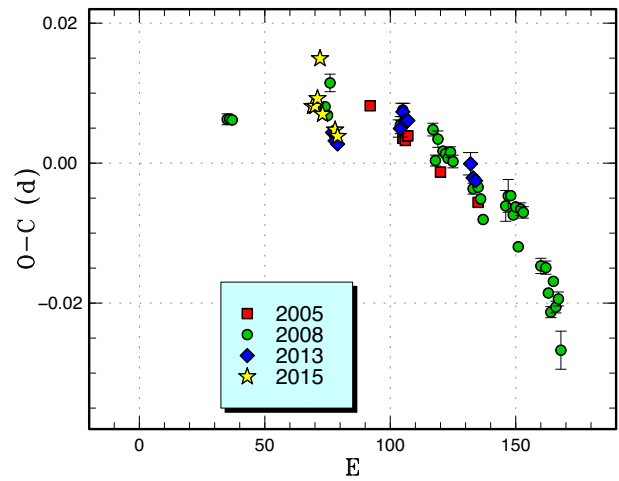


Fig. 24. Comparison of $O-C$ diagrams of TY Psc between different superoutbursts. A period of 0.07066 d was used to draw this figure. Approximate cycle counts (E) after the start of the superoutburst were used. Since the start of the 2013 superoutburst was not well constrained, we shifted the $O-C$ diagram to best fit the others. (Color online)

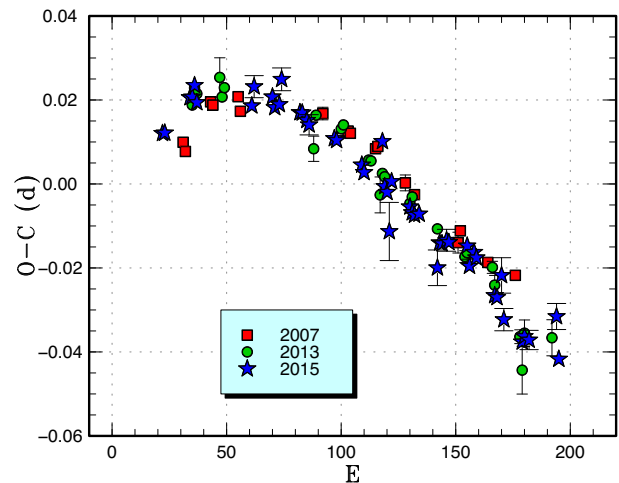


Fig. 25. Comparison of $O-C$ diagrams of V493 Ser between different superoutbursts. A period of 0.08300 d was used to draw this figure. Approximate cycle counts (E) after the start of the superoutburst were used. Since the start of the 2013 superoutburst was not well constrained, we shifted the $O-C$ diagram to best fit the better-recorded 2007 one. (Color online)

smooth, we adopt stage classifications listed in table 3 which refer to the well-recorded observation in Kato et al. (2009) (figure 25). The resultant $\epsilon^* = 0.0449(13)$ for stage A superhumps corresponds to $q = 0.129(5)$, which is in good agreement with $q = 0.136(6)$ using the 2007 observation (Kato & Osaki 2013b).

3.26 V1212 Tauri

V1212 Tau was discovered as an eruptive object near M 45 (Parsamyan et al. 1983). See Kato et al. (2012, 2014a) for more history. The 2016 superoutburst was detected on

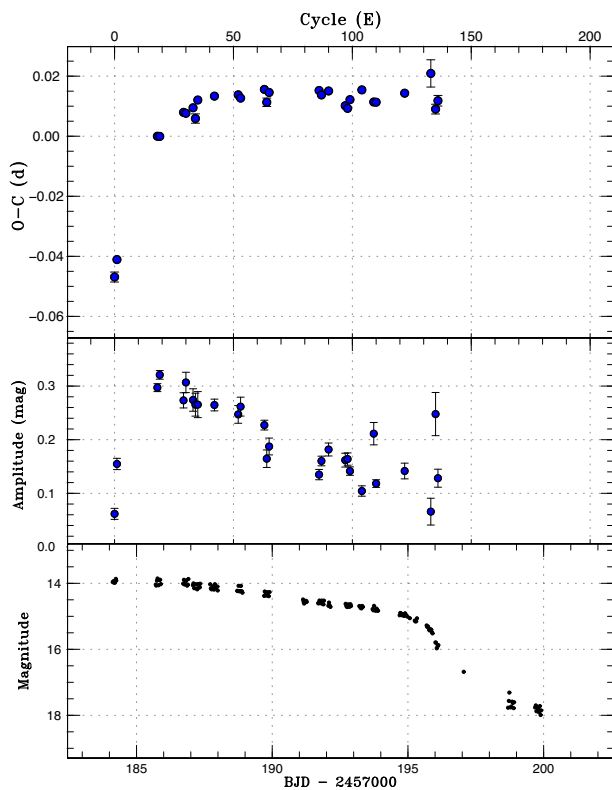


Fig. 26. $O-C$ diagram of superhumps in KK Tel (2015). Upper: $O-C$ diagram. We used a period of 0.08761 d for calculating the $O-C$ residuals. The superhump maxima up to $E=19$ are stage A superhumps. Middle: Amplitudes of superhumps. The amplitudes were small around $E=0$. It is worth noting that the epoch of the peak amplitude was earlier than the flattening of the $O-C$ diagram (pure stage B superhumps). Lower: Light curve. The data were binned to 0.029 d. The initial outburst detection was on BJD 2457182.7, 3 d before the start of our observation. It took 4 d for this object to fully develop stage B superhumps. (Color online)

February 2 at $V=15.91$ by the ASAS-SN team. The superoutburst was also detected by M. Moriyama on February 7 at an unfiltered CCD magnitude of 15.6 (vsnet-alert 19462, 19465). Only single-night observations on February 8 were obtained and two superhumps were recorded: BJD 2457427.0376(10) ($N=103$) and 2457427.1028(28) ($N=52$).

3.27 KK Telescopii

KK Tel was discovered as a dwarf nova by Hoffmeister (1963b). Howell et al. (1991) performed time-resolved photometry in quiescence and recorded a period of 0.084 d. The SUUMa-type nature was clarified during the 2002 superoutburst (Kato et al. 2003b). Kato et al. (2003b) noticed an exceptionally large period decrease of superhumps; KK Tel was considered to be a prototypical SUUMa-type dwarf nova with a large period decrease and this result was often referred to for comparison [cf. MNDra

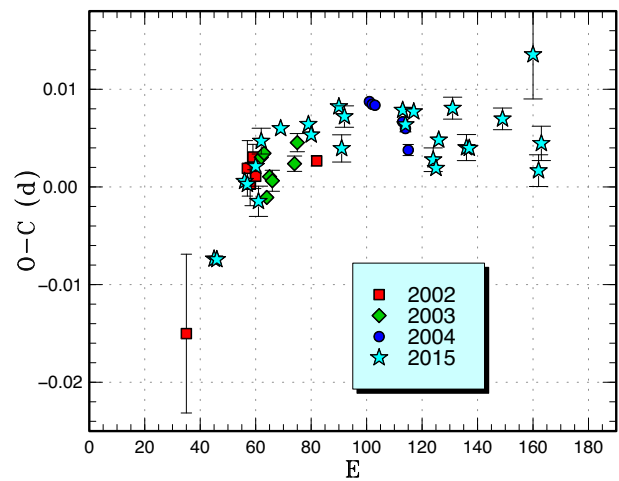


Fig. 27. Comparison of $O-C$ diagrams of KK Tel between different superoutbursts. A period of 0.08761 d was used to draw this figure. Approximate cycle counts (E) after the start of the superoutburst were used. In contrast to the diagram in Kato et al. (2009), the epochs were shifted by 24, 30, and 20 cycles for the 2002, 2003, and 2004 superoutbursts, respectively, to best match the 2015 result. These values suggests that either the true starts of the 2002–2004 superoutbursts were missed by 2–3 d, or the 2015 superoutburst started earlier than the others (such as a form of a precursor outburst). (Color online)

(Nogami et al. 2003); KSUMa (Olech et al. 2003); V419 Lyr (Rutkowski et al. 2007)]. This detection of a large period decrease was before the establishment of the common pattern of period variations (stages A–C; Kato et al. 2009), and it has been clarified that the large period decrease in KK Tel was likely a result of stage A–B transition.

The 2015 superoutburst was detected by the ASAS-SN team on June 9 (cf. vsnet-alert 18713). Subsequent observations detected superhumps (vsnet-alert 18719, 18732, 18801). The times of superhump maxima are listed in e-table 23. The maxima up to $E=19$ were stage A superhumps (figure 26). Since the 2015 observation started 2 d later than the initial outburst detection, it took ~ 60 cycles for this object to develop stage B superhumps. It was probably not by chance that stage A superhumps in this system were well recorded both in 2002 and 2015, but it was likely a result of the relatively long-lasting stage A in this system (figure 28). In Kato et al. (2014b, 2016a), we proposed that systems having q close to the stability border of the 3 : 1 resonance show slow evolution of superhumps (see also subsection 4.4). This is also probably the case for KK Tel and V419 Lyr. It is also worth noting that the epoch of the peak amplitude was earlier than the flattening of the $O-C$ diagram (pure stage B superhumps; figure 26). This tendency was also seen in the long-period system V1006 Cyg with a long duration of stage A (Kato et al. 2016a).

Since the period of stage A superhumps is well determined for KK Tel, precise determination of the orbital period will lead to a measurement of q , providing a test for this hypothesis.

3.28 CI Ursae Majoris

This object was discovered by Goranskij (1972) and was confirmed to be an SUUMa-type dwarf nova by Nogami and Kato (1997). See Kato et al. (2014a) for more history. The 2016 outburst was detected at an unfiltered CCD magnitude of 14.4 on March 14 by M. Hiraga (vsnet-alert 19626). The outburst did not receive special attention since

it faded rather quickly. The outburst, however, turned out to be a precursor based on the ASAS-SN observations (vsnet-alert 19626). Only single-night observations were obtained, yielding the superhump maxima in table 4.

Table 4. Superhump maxima of CI UMa (2016).

E	Max*	Error	$O - C^\dagger$	N^\ddagger
0	57470.6381	0.0042	-0.0017	44
1	57470.7042	0.0017	0.0012	27
2	57470.7665	0.0019	0.0001	17
3	57470.8314	0.0021	0.0018	23
4	57470.8925	0.0037	-0.0004	26
5	57470.9551	0.0105	-0.0011	19

*BJD-2400000.

† Against max = 2457470.6398 + 0.063283E.

‡ Number of points used to determine the maximum.

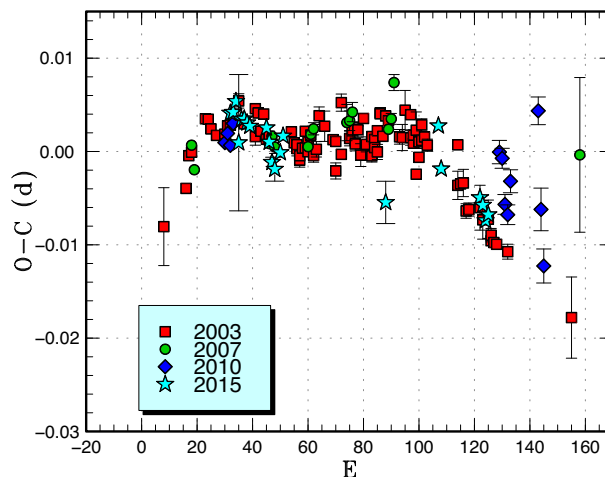


Fig. 28. Comparison of $O - C$ diagrams of KS UMa between different superoutbursts. A period of 0.07019 d was used to draw this figure. Approximate cycle counts (E) after the start of the superoutburst were used. Since the 2003 superoutburst was very well recorded, we shifted the others to fit the 2003 one. We had to shift 18, 30, and 32 cycles for the 2007, 2010, and 2015 data, respectively. Note that this treatment is different from the corresponding figure in Kato et al. (2009). (Color online)

Table 5. List of recent outbursts of MR UMa.

Year	Month	Max*	Magnitude	Type	Source
2002	3	52341	12.7	Super	VSNET, AAVSO, Kato et al. (2009)
2003	3	52711	12.8	Super	VSNET, AAVSO, Kato et al. (2009)
2004	3	53084	13.2	Super	VSNET, AAVSO
2005	3	53440	12.9	Super	VSNET, AAVSO
2005	4	53474	15.3	Normal	AAVSO
2006	5	53870	12.8	Super	VSNET, AAVSO
2006	11	54058	13.1 †	?	VSNET
2007	4	54205	12.5	Super	VSNET, AAVSO, Kato et al. (2009)
2008	2	54503	12.7	Super	VSNET, AAVSO
2008	6	54627	12.9	Normal	VSNET, AAVSO
2009	4	54948	13.2	Normal	VSNET, AAVSO
2010	4	55303	12.7	Super	VSNET, AAVSO, Kato et al. (2010)
2011	5	55684	12.9	Normal	VSNET, AAVSO
2012	6	56090	13.2	Super	VSNET, AAVSO, Kato et al. (2013a)
2013	3	56354	13.2	Super	VSNET, AAVSO, Kato et al. (2014a)
2013	11	56610	12.8	Super?	AAVSO
2014	2	56708	13.3 ‡	Normal	AAVSO
2014	4	56770	13.5	Normal	VSNET, AAVSO
2015	3	57094	12.8 §	Super	VSNET, AAVSO, this paper

*JD-2400000.

† Single visual observation.

‡ Single CCD observation.

§ Refers to the main superoutburst.

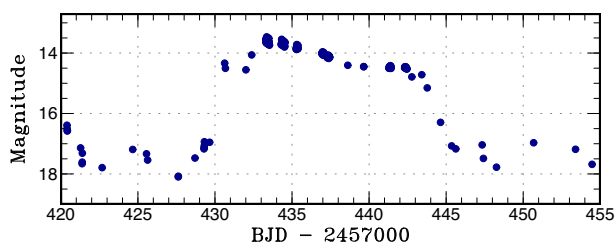


Fig. 29. Light curve of the superoutburst of NSV 2026 (2016). The data were binned to 0.01 d. The initial precursor part of the outburst and subsequent rise to the superoutburst maximum are clearly depicted. The widths of the light curve mainly reflect the amplitudes of superhumps. (Color online)

3.29 KS Ursae Majoris

KSUMa was originally discovered as an emission-line object (= SBS1017+533) (Balayan 1997). The SUUMa-type nature was confirmed during the 1998 outburst. Olech et al. (2003) studied the 2003 superoutburst in detail. For more history, see Kato et al. (2009).

The 2015 superoutburst was detected by K. Hirose at $V = 13.0$ on December 6. Subsequent observations detected superhumps (vsnet-alert 19330). The times of superhump maxima are listed in e-table 24. A comparison of $O - C$ diagrams suggests that we observed stage B (initial part) and stage C, with a long gap in the observations between them (figure 28).

3.30 MR Ursae Majoris

This object is a well-known SUUMa-type dwarf nova. See Kato et al. (2014a) for the history. The 2015 March superoutburst had a precursor outburst on March 7 (visually detected by E. Muylaert, vsnet-alert 18426). We observed on one night during the fading part of the precursor outburst and obtained two superhump maxima: BJD 2457091.4918(3) ($N=72$) and 2457091.5573(5) ($N=72$). Although these superhumps most likely correspond to stage A superhumps, the period was not meaningfully determined.

Recent outbursts of this object are listed in table 5. Although observations up to 2005 inferred a supercycle of approximately a year, recent observations suggest that the supercycles varied considerably and they can be as short as ~ 260 d.

3.31 NSV 2026

3.31.1 Introduction

This object was discovered as a variable star (= HV 6907) by Hoffleit (1935). The exact coordinates were given by Webbink et al. (2002). The object was identified to be a dwarf nova by a detection of an outburst by CRTS

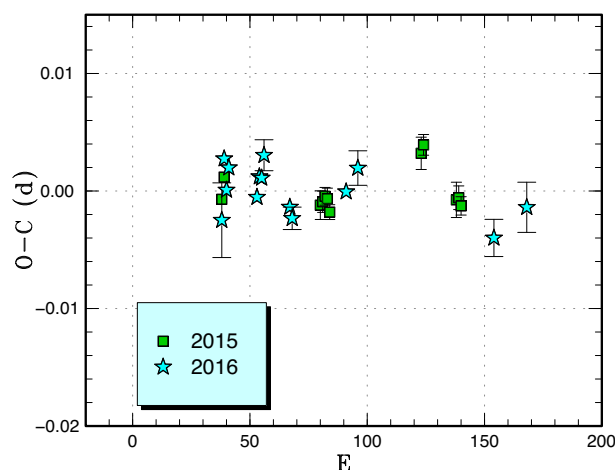


Fig. 30. Comparison of $O - C$ diagrams of NSV 2026 between different superoutbursts. A period of 0.06982 d was used to draw this figure. Approximate cycle counts (E) after the starts of the outbursts were used. The start of the 2016 outburst refers to the precursor outburst. Since the start of the 2015 outburst was not well constrained, the $O - C$ curve was shifted as in the 2016 one. (Color online)

Mount Lemmon survey (= MLS101214:052959+184810) in 2010 (vsnet-alert 12503). It has been monitored for outbursts since then. Several outbursts were recorded by BAAVSS/AAVSO observers (since 2012) and by the MISAO project (two outbursts in 2011 and one in 2012). There is an X-ray counterpart 1RXS J052954.9+184817. There were two relatively long outbursts in 2012 February–March and 2014 February. Although time-resolved photometry was undertaken, no convincing superhumps were detected.¹⁴

3.31.2 2015 superoutburst

The 2015 November bright outburst was detected by J. Shears on November 8 at an unfiltered CCD magnitude of 13.6 (vsnet-outburst 18873).¹⁵ This outburst turned out to be a superoutburst, as superhumps were detected (vsnet-alert 19258; e-figure 2). The times of superhump maxima are listed in e-table 25. Although there was an apparent stage transition (vsnet-alert 19282), we gave a globally averaged period due to insufficient observations.

3.31.3 2016 superoutburst

The 2016 superoutburst was detected by J. Shears on February 12 at an unfiltered CCD magnitude of 14.4 (BAAVSS alert 4308). Subsequent observations detected superhumps (vsnet-alert 19485, 19498, 19509). The outburst started with a precursor (figure 29). The times of superhump maxima are listed in e-table 26. Although the initial part of the data ($E \leq 58$) most likely refers to stage B, we gave a globally averaged period since the observations

¹⁴ (<http://www.britastro.org/vss/NSV2026.pdf>).

¹⁵ See also (<http://www.britastro.org/vss/NSV2026.pdf>) for the BAAVSS campaign.

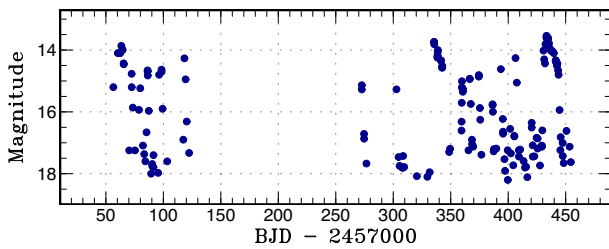


Fig. 31. Long-term curve of NSV 2026 from AAVSO observations. The data were binned to 0.1 d. (Color online)

were not sufficient to determine P_{dot} for stage B. A comparison of the $O - C$ diagrams (figure 30) suggests that the later parts of the 2015 and 2016 observations were likely stage C.

3.31.4 Interpretation

Although the 2012 and 2014 outbursts were not very well observed, the lack of prominent superhumps would suggest that these outbursts may have been long, normal outbursts as seen in TU Men (Warner 1995b; Bateson et al. 2000), V1006 Cyg (Kato et al. 2016a) and potentially NY Ser (Pavlenko et al. 2014). The big difference between NSV 2026 and these objects is the orbital period – TU Men, V1006 Cyg, and NY Ser have long orbital periods in or above the period gap, while NSV 2026 is not. If the presence of long normal outbursts is due to the difficulty in attaining the 3 : 1 resonance, it would be easy to understand why most objects showing this behavior have long P_{orb} , and the case of NSV 2026 might require another explanation. Since superhump amplitudes became significantly smaller in the 2016 superoutburst in the late phase, it may just have been that the 2012 and 2014 observations did not record the phases with large-amplitude superhumps. Confirmation of superhumps in every long outburst of NSV 2026 would check these possibilities.

AAVSO observations of this object show a relatively regular supercycle pattern: normal outbursts with a recurrence time of 6–14 d and the supercycle length of ~ 95 d (figure 31). As judged from this light curve, NSV 2026 looks like a fairly normal SUUMa-type dwarf nova with frequent outbursts.

3.32 ASASSN-13ah

This object was detected as a transient on 2013 April 23 by the ASAS-SN team (Shappee et al. 2013). The object was confirmed as a dwarf nova in outburst by spectroscopy (Shappee et al. 2013). Although there were observations during the 2015 outburst (cf. vsnet-alert 18619) by KU team, the observations were insufficient to confirm superhumps.

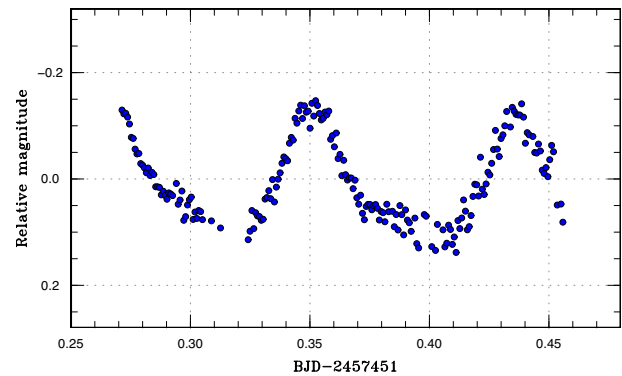


Fig. 32. Superhumps in ASASSN-13az (2016). (Color online)

The 2016 outburst was detected by the ASAS-SN team on February 11 at $V=16.4$. Subsequent observations detected superhumps (vsnet-alert 19480, 19497; e-figure 3). The times of superhump maxima are listed in e-table 27.

3.33 ASASSN-13ak

This object was detected as a transient at $V=15.4$ on 2013 May 23 by the ASAS-SN team (Stanek et al. 2013). The MASTER network also detected this outburst (Shurpakov et al. 2013). There is an X-ray counterpart (1RXS J174827.1+505053). There have been five outbursts (including the 2015 one) in the CRTS data. The SDSS colors suggested a short orbital period (vsnet-alert 15742).

The 2015 outburst was detected by E. Muylaert on May 8 at an unfiltered CCD magnitude of 15.1 (vsnet-alert 18607). This object was confirmed as an SUUMa-type dwarf nova by the detection of superhumps (vsnet-alert 18612, 18613, 18615, 18624; e-figure 4). The times of superhump maxima are listed in e-table 28. The superhump stage is unknown.

3.34 ASASSN-13az

This object was detected as a transient at $V=14.4$ on 2013 July 1 by the ASAS-SN team (vsnet-alert 15892). Although the object was identified with a 20.8 mag (B_i) star in the USNO-B1.0 catalog, this object was later found to be unrelated by spectroscopy (cf. vsnet-alert 19555). Although there was a 14.858-mag detection close to the ASAS-SN position in URAT1 catalog (Zacharias et al. 2015), the identification is unclear. The object may have been recorded in outburst. If this identification is confirmed, the coordinates are RA $18^{\text{h}}42^{\text{m}}58^{\text{s}}.21$, Dec $+73^{\circ}42'28''.4$.

The 2016 outburst was detected by the ASAS-SN team on March 1 at $V=14.42$. Subsequent observations detected superhumps (vsnet-alert 19554; figure 32). Two superhump maxima were recorded: BJD 2457451.3514(3)

($N=77$) and 2457451.4374(5) ($N=61$). The best superhump period with the PDM method is 0.0843(3) d.

3.35 ASASSN-14ca

This object was detected as a transient at $V=15.5$ on 2014 June 7 by the ASAS-SN team (Davis et al. 2014). The object was initially reported as an unusual long-lived transient from a red source. Davis et al. (2014) also reported an outburst in 2005 July in the CRTS data, which lasted for at least 6 d. Upon this report, Cao and Kulkarni (2014) examined the PTF/iPTF archival data and found another brightening in 2009 November, which lasted at least for 15 d. Cao and Kulkarni (2014) reported that the color temperature is consistent with a Mira star. Prieto et al. (2014) reported a spectrum taken on June 9 and it had a strong blue continuum, Balmer lines in absorption, $H\alpha$ line in double-peaked emission and $\text{He II } 468.6 \text{ nm}$ in emission. The object was confirmed to be a dwarf nova in outburst. The object was independently suggested to be a dwarf nova (vsnet-alert 17369) and D. Denisenko detected an outburst in 2009 November in the MASTER network observations, the same one reported in Cao and Kulkarni (2014). The $g=20.6$ SDSS counterpart may be an unrelated unresolved red star.

The 2015 outburst was detected by the ASAS-SN team on July 7 at $V=15.53$ (cf. vsnet-alert 18833). Subsequent observations detected superhumps (vsnet-alert 18852; e-figure 5). The times of superhump maxima are listed in e-table 29. The alias selection was based on the $O-C$ analysis of the second night.

3.36 ASASSN-14dh

This object was detected as a transient at $V=15.93$ on 2014 June 27 by the ASAS-SN team. There were past known outbursts in the CRTS data and ASAS-3 data (see also vsnet-alert 17424, 18823).

The 2015 outburst was detected by ASAS-SN on July 2 at $V=13.3$. Subsequent observations detected superhumps (vsnet-alert 18840, 18842; e-figure 6). The times of superhump maxima are listed in e-table 30. The maxima for $E \leq 89$ corresponds to superhumps after the rapid fading. This outburst was observed only during the late phase and we probably observed only stage C superhumps.

3.37 ASASSN-14fz

This object was detected as a transient at $V=15.18$ on 2014 August 20 by the ASAS-SN team. The light curve of the 2014 outburst was suggestive of an SUUMa-type precursor outburst (vsnet-alert 17647).

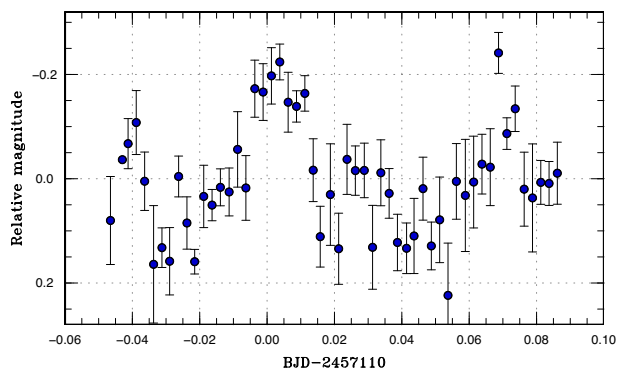


Fig. 33. Superhumps in ASASSN-14le (2014). The data were binned to 0.0025 d. (Color online)

The 2015 outburst was detected by the ASAS-SN team on May 27 at $V=14.21$. Subsequent observations detected superhumps (vsnet-alert 18672, 18685; e-figure 7). The times of superhump maxima are listed in e-table 31. The epochs $E \leq 1$ correspond to stage A superhumps. It was not clear whether there was a stage transition in the later part of the outburst, and we list a global P_{dot} in table 3.

3.38 ASASSN-14le

This object was detected as a transient at $V=16.4$ on 2014 November 29 by the ASAS-SN team. Observations on December 5 detected superhumps (figure 33). The times of maxima are BJD 2456997.0031(12) ($N=135$) and 2456997.0719(20) ($N=113$). The superhump period was estimated to be 0.068(1) d using these times of maxima and with the PDM method.

3.39 ASASSN-15cl

This object was detected as a transient at $V=13.9$ on 2015 February 1 by the ASAS-SN team. The object was found to be already in outburst at $V=14.8$ on January 31. There were three past outbursts reaching $V=13.3$ in the ASAS-3 data (cf. vsnet-alert 18256). Although the 2015 outburst was observed on two nights by S. Kiyota, no definite superhump signal was detected.

The 2016 outburst was detected by the ASAS-SN team at $V=13.8$ on January 17 (vsnet-alert 19421). Subsequent observations detected long-period superhumps (vsnet-alert 19427, 19431). The superhumps were still growing (see also figure 34) and the period then dramatically shortened (vsnet-alert 19431, 19436, 19442). The times of superhump maxima are listed in e-table 32. The behavior was very similar to another long- P_{orb} system V1006 Cyg (Kato et al. 2016a) and we identified $E \leq 22$ to be stage A superhumps (figure 35). The sharp decrease in the period was likely due to stage B to C transition around $E=33$. The

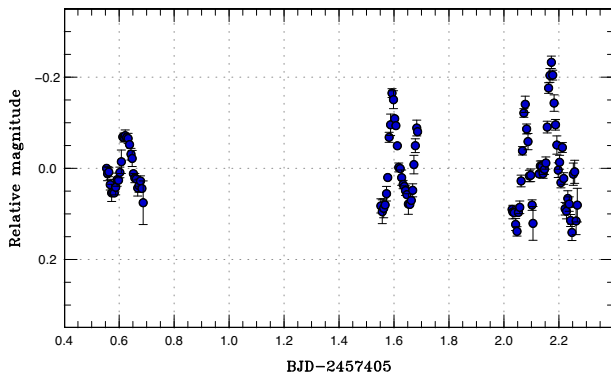


Fig. 34. Growing superhumps in ASASSN-15cl (2016). The data were binned to 0.005 d. (Color online)

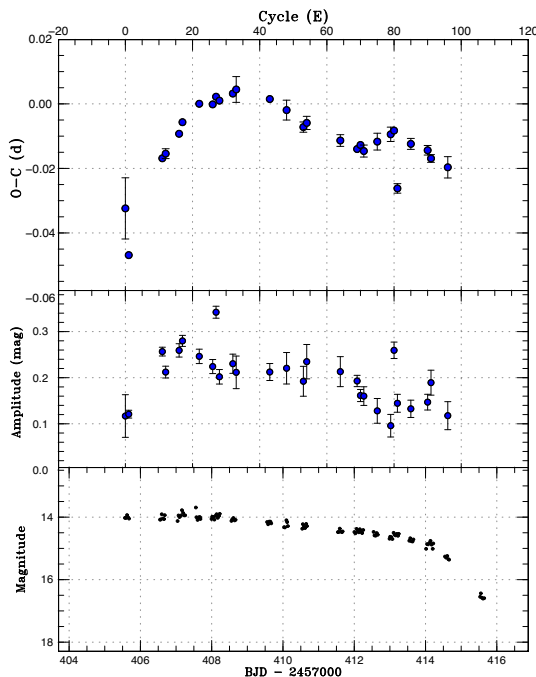


Fig. 35. $O - C$ diagram of superhumps in ASASSN-15cl (2016). Upper: $O - C$ diagram. We used a period of 0.09423 d for calculating the $O - C$ residuals. The superhump maxima up to $E = 22$ are stage A superhumps, maxima between $E = 22$ and $E = 33$ are identified as stage B superhumps. After this, the period decreased to a constant one (stage C superhumps). Middle: Amplitudes of superhumps. The amplitudes were small around $E = 0$. Lower: Light curve. The data were binned to 0.031 d. (Color online)

periods given in table 3 refers to these period identifications. The mean profile excluding stage A superhumps is shown in e-figure 8.

Kato et al. (2016a) discussed whether the long duration of the growing stage of superhumps in a long- P_{orb} system reflects the slow growth rate of the 3:1 resonance when the mass ratio is close to the stability limit of the 3:1 resonance (see also subsection 4.4). Yet another example, ASASSN-15cl, also supports the idea that

this mechanism is likely working in many long- P_{orb} systems. Future determination of the orbital period in this system will allow the measurement of q using the period of stage A superhumps in this study. Such a measurement will test the hypothesis of whether the system has a borderline q .

3.40 ASASSN-15cy

This object was detected as a transient at $V = 14.6$ on 2015 February 16 by the ASAS-SN team. The coordinates are $08^{\text{h}}11^{\text{m}}50^{\text{s}}.53$, $-12^{\circ}27'51''.5$ (based on S. Kiyota's image on February 20, UCAC4 reference stars). There is no quiescent counterpart in the available catalogs.

Up until February 20, the object showed only little variations. On February 22 (6 d after the initial detection), it showed prominent superhumps with a very short (~ 0.050 d) period (vsnet-alert 18326, 18327). There were long gaps in the observation and the next continuous run was on February 28. There was only one superhump detection on February 26. Using the period determined from the continuous run on February 22 and the single epoch on February 26, we have tried several possible periods and obtained the smallest $O - C$ scatter using a period of 0.04996 d up to February 28. The cycle counts and $O - C$ values assuming this period are shown in e-table 33. The mean superhump profile is shown in e-figure 9. We should note, however, this choice may not be correct, particularly if there was strong period variation when there were gaps in the observation. The times for $E \geq 161$ were uncertain since the amplitudes of superhumps were already small (~ 0.07 mag) and the object already faded close to 16 mag. The phase jump between $E = 122$ and $E = 161$ was too large to be identified as a stage B-C transition. Although there may have been a true phase jump, the conclusion is unclear due to the poor quality of the data around these epochs.

The resultant superhump period suggests that this object belongs to EI Psc-type objects with compact secondaries having an evolved core (cf. T. Ohshima et al. in preparation). Since the quiescent brightness is below the limit of photographic surveys, the outburst amplitude is likely larger than 6 mag. This object shares properties with CSS J174033.5+414756 ($P_{\text{orb}} = 0.04505$ d, outburst amplitude ~ 6.7 mag; Kato et al. 2014a, 2015a; Prieto et al. 2013; Nesci et al. 2013; T. Ohshima et al. in preparation), which is classified as a WZ Sge-type object in Kato (2015). Although a period of 0.0494(2) d was inferred from the observations on the first two nights (cf. vsnet-alert 18327), this period is uncertain due to the low amplitude (less than 0.02 mag) and limited coverage.

3.41 ASASSN-15dh

This object was detected as a transient at $V = 15.2$ on 2015 February 12 by the ASAS-SN team. There was another outburst on October 29 at $V = 15.03$ detected by the ASAS-SN team (see also vsnet-alert 19228). Subsequent observations detected superhumps (vsnet-alert 19218, 19228; e-figure 10). The times of superhump maxima are listed in e-table 34. There was probably a stage transition at around $E = 11$. We were not able to determine the type of transition. In table 3, we list a global value.

3.42 ASASSN-15dp

This object was detected as a transient at $V = 14.1$ on 2015 February 22 by the ASAS-SN team. The object was recorded in outburst in 1989 at a red magnitude of 15.2 in GSC 2.3 (GSC2.3 NCCX024953). The quiescent magnitude was 19.4(4) (green magnitude, Initial Gaia Source List).

Early observations soon detected superhumps (vsnet-alert 18350). It soon became apparent that early observations recorded the final part of the precursor outburst with a relatively rapid fading, and stage A superhumps were observed on the first two nights (vsnet-alert 18363, 18417). E-figure 11 shows the profile of stage B superhumps. The times of superhump maxima are listed in e-table 35. The maxima for $E \leq 24$ correspond to stage A superhumps. There was no observed transition to stage C superhumps.

The object entered the rapid fading stage on March 11, 17 d after the initial outburst detection. It took ~ 8 d to develop stage B superhumps, which is relatively long. It was also somewhat unusual that the fading part of the precursor outburst was observed even 5 d after the initial detection. The lack of stage C superhumps and small P_{dot} are usual characteristics of WZ Sge-type dwarf novae (Kato 2015). Since the system has a relatively long superhump period, there could even be a chance of a candidate period bouncer, if our measurement of P_{dot} is correct. Since the present observations lack the earliest data and post-outburst data, this object should require further observation on the next outburst occasion.

3.43 ASASSN-15dr

This object was detected as a transient at $V = 14.9$ on 2015 February 22 by the ASAS-SN team. On February 28, the object started to show growing superhumps (vsnet-alert 18366). Stable superhumps were observed later (vsnet-alert 18384; e-figure 12). The times of superhump maxima are listed in e-table 36. Although the times for $E \leq 2$ apparently correspond to stage A superhumps, the stage A superhump period could not be determined due to the lack of

the data. The photometric quality for this object was not good enough due to its faintness (16.3 mag on February 26, which was much fainter than the ASAS-SN report).

3.44 ASASSN-15ea

This object was detected as a transient at $V = 16.1$ on 2015 February 25 by the ASAS-SN team. There was one previous outburst reaching 14.15 mag on 2006 October 4 in the CRTS data. Although T. Vanmunster reported the detection of superhumps (vsnet-alert 18357), this period was later rejected (vsnet-alert 18373).

Although individual superhumps maxima were difficult to determine due to the poor coverage (we do not give a table of superhump maxima), a PDM analysis yielded a strong signal of superhumps (e-figure 13). Although the best period is 0.09522(8) d, 1-d aliases are still possible. If this period is confirmed, the object is located on the lower edge of the period gap.

3.45 ASASSN-15ee

This object was detected as a transient at $V = 12.6$ on 2015 March 2 by the ASAS-SN team. The outburst amplitude exceeded 7 mag, and was considered to be a good candidate for a WZ Sge-type dwarf nova (vsnet-alert 18364). The object initially faded rather rapidly without strong modulations (vsnet-alert 18381). Ordinary superhumps started to appear on March 8, 6 d after the initial detection, and reached a peak amplitude of 0.17 mag within 1 d. The superhumps started to decay slowly (vsnet-alert 18392, 18394, 18415, 18423, 18428, 18437; e-figure 14). The times of superhump maxima are listed in e-table 37. The epochs $E \leq 14$ likely correspond to stage A superhumps since the amplitudes grew up to $E = 14$ (figure 36). The epoch for $E \geq 200$ probably correspond to stage C superhumps. There was no strong indication of early superhumps before the development of ordinary superhumps.

Although the outburst amplitude is large, the object is probably not an extreme WZ Sge-type dwarf nova since the growth of superhumps is quick and the P_{dot} for stage B superhumps is large [$+8.1(1.2) \times 10^{-5}$]. The inclination of this object is probably low, as suggested from the lack of early superhumps, which would have made the outburst amplitude larger.

3.46 ASASSN-15eh

This object was detected as a transient at $V = 15.6$ on 2015 March 3 by the ASAS-SN team. The object was apparent during a precursor outburst, and the SUUMa-type nature was suspected (vsnet-alert 18380). Superhumps

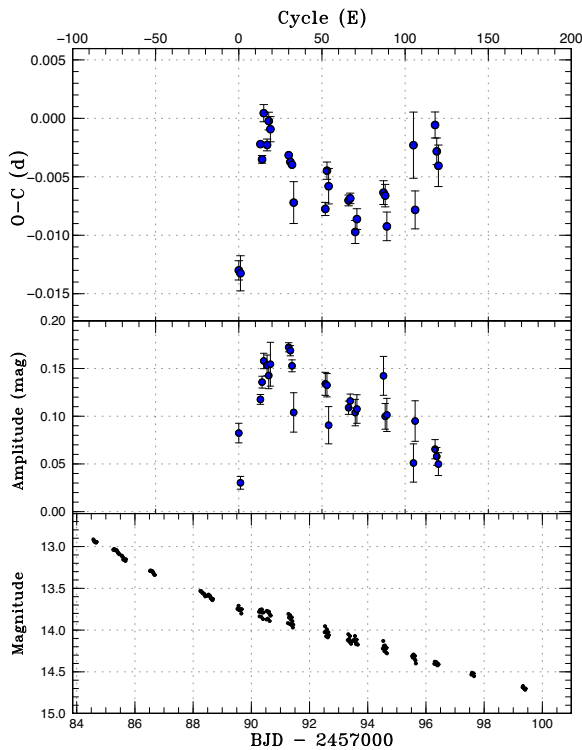


Fig. 36. $O - C$ diagram of superhumps in ASASSN-15ee (2015). Upper: $O - C$ diagram. We used a period of 0.05716 d for calculating the $O - C$ residuals. Middle: Amplitudes of superhumps. Lower: Light curve. The data were binned to 0.019 d. (Color online)

were subsequently detected (vsnet-alert 18391, 18393; e-figure 15). The times of superhump maxima are listed in e-table 38. Although there may have been a stage transition between the second and the final night, we list the mean value in table 3 due to the lack of data.

3.47 ASASSN-15ev

This object was detected as a transient at $V = 15.1$ on 2015 March 16 by the ASAS-SN team. The object has an X-ray counterpart 1SXPS J073819.6–825039. Subsequent observations detected superhumps (vsnet-alert 18465, 18482; e-figure 16). The times of superhump maxima are listed in e-table 39. The superhump period in table 3 was determined with the PDM method. The object started fading rapidly on March 26–27, ~ 10 d after the outburst detection. The upper limit of the duration of the plateau phase was 13 d, which is relatively short for an SUUMa-type dwarf nova with this superhump period.

3.48 ASASSN-15fo

This object was detected as a transient at $V = 15.4$ on 2015 March 19 by the ASAS-SN team. It further brightened to $V = 14.7$ on March 20. Subsequent observations

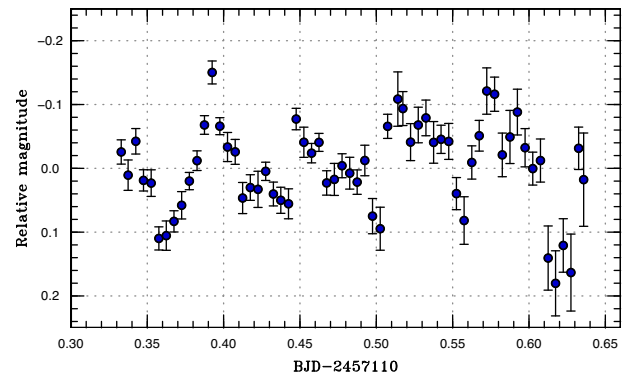


Fig. 37. Superhumps in ASASSN-15fo (2015). The data were binned to 0.005 d. (Color online)

detected superhumps (vsnet-alert 18498). The superhumps were clearly seen only on the first night of our observations (figure 37). Although there were observations on later nights, they did not yield a meaningful superhump signal due to the faintness of the object (fainter than 16 mag after March 31). We restricted our analysis to the first-night observation. The times of superhump maxima are listed in e-table 40. The period given in table 3 is by the PDM analysis. The object started fading rapidly on April 4, giving 16 d for the duration of the superoutburst.

3.49 ASASSN-15fu

This object was detected as a transient at $V = 15.6$ on 2015 March 27 by the ASAS-SN team. Superhumps were immediately detected (vsnet-alert 18503, 18506, 18522; e-figure 17). The times of superhump maxima are listed in e-table 41. Although there was a stage B–C transition in the later part of the observation, the period of stage C superhumps (table 3) was uncertain due to the limited quality of the observation.

3.50 ASASSN-15gf

This object was detected as a transient at $V = 15.2$ on 2015 April 2 by the ASAS-SN team. There is an $r = 21.5$ mag counterpart in IPHAS DR2. Subsequent observations detected superhumps (vsnet-alert 18520, 18525). Due to the shortness of the runs, there were many equally acceptable 1-d aliases found by the PDM analysis (e-figure 18). We have chosen the one which gives the smallest $O - C$ scatter (e-table 42). We should note that other 1-d aliases are still possible. In table 3, we give the period selected by the $O - C$ method and refined by the PDM analysis.

3.51 ASASSN-15gh

This object was detected as a transient at $V = 14.6$ on 2015 April 1 by the ASAS-SN team. No quiescent counterpart was recorded. Before April 9, there was little indication of hump-like variations. On April 10, superhumps became apparent. Since the object had a very low signal-to-noise ratio due to the faintness (the object was already at 16.2 mag on April 10; it was only 15.5 mag on April 4 and the ASAS-SN detection magnitude may have been too bright), only the data between April 10 and 14 (BJD 2457122–2457127) were used to determine superhumps. Among the potential aliases, we selected the one which minimizes the scatter in the $O - C$ diagram (e-figure 19). Other possibilities still remain. The times of superhump maxima are listed in e-table 43. In table 3, we give the period selected by the $O - C$ method and refined by the PDM analysis.

3.52 ASASSN-15gi

This object was detected as a transient at $V = 15.4$ on 2015 April 1 by the ASAS-SN team. Subsequent observations detected superhumps (vsnet-alert 18521, 18529; e-figure 20). The times of superhump maxima are listed in e-table 44. The $O - C$ data indicate the presence of stage B–C transition around $E = 65$. At the time of observation on April 4, the object was at 15.8 mag. The magnitude in the initial report on the ASAS-SN transients page ($V = 14.6$) was probably erroneous.

3.53 ASASSN-15gn

This object was detected as a transient at $V = 14.2$ on 2015 April 3 by the ASAS-SN team (vsnet-alert 18518). The likely quiescent counterpart was recorded very faint (22.4 mag on J plate). The object did not initially show strong short-term variations. On April 14 (11 d after the outburst detection), it started to show superhumps (vsnet-alert 18546, 18548, 18550, 18556, 18559; e-figure 21). On April 25, it started to fade rapidly (figure 38). The times of superhump maxima are listed in e-table 45. Although it was initially suggested that superhumps in this system grew slowly (vsnet-alert 18550), the $O - C$ data would indicate that stage A superhumps were likely only recorded for the initial night when superhumps started to appear. In table 3, we list a period of stage A superhumps with an assumption that $E = 18$ corresponds to the end of stage A. There was some indication of stage C after $E = 112$.

This object has a large outburst amplitude, a long superhump period, a long waiting time before the appearance of superhumps, and a small P_{dur} . These features are suggestive of a period bouncer (cf. Kato 2015). The small

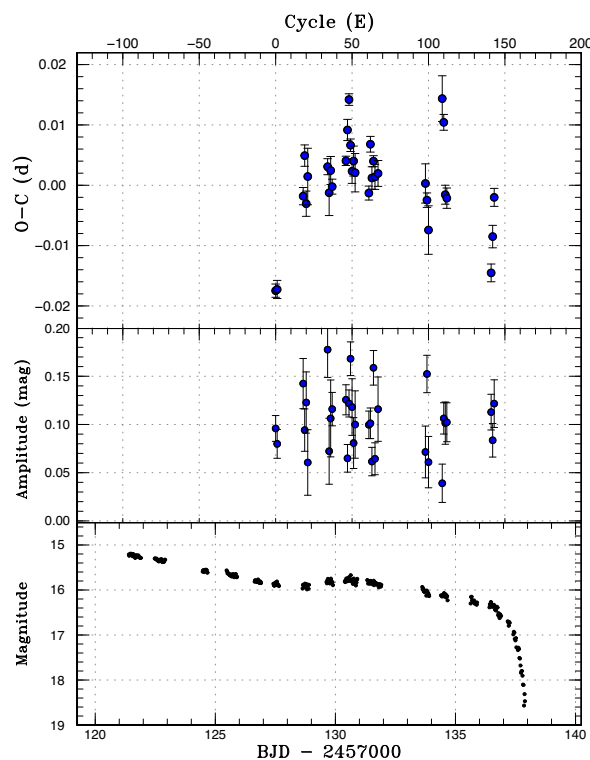


Fig. 38. $O - C$ diagram of superhumps in ASASSN-15gn (2015). Upper: $O - C$ diagram. We used a period of 0.06364 d for calculating the $O - C$ residuals. Middle: Amplitudes of superhumps. Lower: Light curve. The data were binned to 0.021 d. (Color online)

amplitude of superhumps is also suggestive of a small tidal effect and the superhump profile is more symmetric than in other SUUMa-type dwarf novae (e-figure 21). The growth time of superhumps, however, is short, which is not compatible with a small q if this object is a period bouncer. It may be possible either that the growing stage of superhumps was not well recorded due to the faintness of the object (15.5 mag at the time of emergence of superhumps) and low sampling rates on some nights, or that the stage identification is not correct and all the superhumps are stage A superhumps. Neither possibility is ruled out because the superhumps were close to the detection limit and the data were not so densely obtained. The small amplitude and relatively symmetric profile of the superhumps may suggest that the outburst terminated before the superhump developed fully. Since the behavior of superhumps is known to be complex in period bouncers (cf. Kato 2015; C. Nakata et al. in preparation), this possibility may deserve consideration.

3.54 ASASSN-15gq

This object was detected as a transient at $V = 15.4$ on 2015 April 10 by the ASAS-SN team. There is a $g = 21.6$ mag SDSS object (SDSS J101510.86+812418.7) 1'5 distant

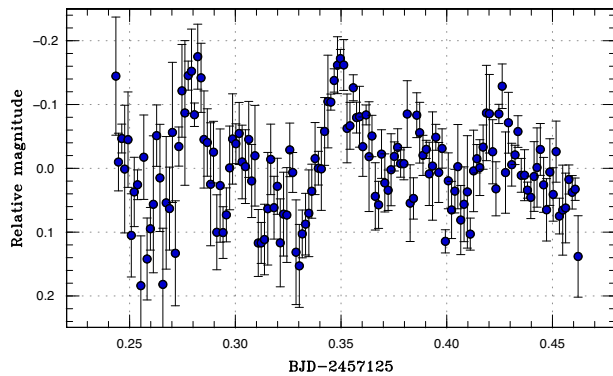


Fig. 39. Superhumps in ASASSN-15gs (2015). The data were binned to 0.0015 d. (Color online)

from this position. This SDSS object is less likely the quiescent counterpart since it has colors (e.g., $u - g = 0.76$) unlike a CV.

The object initially showed double-wave modulations (vsnet-alert 18526, 18528, 18531, 18539), which we identify to be early superhumps (e-figure 22). The object is thus identified as a WZ Sge-type dwarf nova. Later the object showed fully developed ordinary superhumps (vsnet-alert 18549, 18558, 18593; e-figure 23). The times of maxima of ordinary superhumps are listed in e-table 46. The times for $E \leq 1$ are clearly of stage A superhumps. There is a suggestion for stage B–C transition after $E = 120$. In table 3, we list a period of stage A superhumps with an assumption that $E = 15$ corresponds to the end of stage A. This fractional superhump excess [$\epsilon^* = 0.038(2)$] corresponds to $q = 0.107(8)$. Although we could not observe the termination of stage A superhumps, the above value is likely close to the actual value since if stage A terminated much earlier than $E = 15$, the value of ϵ^* should be larger, which will give an unacceptably large q for a WZ Sge-type object.

Considering the large positive P_{dot} for stage B superhumps, the presence of stage C superhumps, the relatively long orbital period, and the short duration of stage A, this object is probably a borderline WZ Sge/SUUMa-type object rather than an extreme WZ Sge-type object (cf. Kato 2015).

3.55 ASASSN-15gs

This object was detected as a transient at $V = 15.7$ on 2015 April 8 by the ASAS-SN team. There is an X-ray counterpart (1SXPS J135917.3–375242). The object was observed on one night and superhumps were detected (vsnet-alert 18541, figure 39). The times of superhump maxima are listed in e-table 47. The best period found with the PDM method was 0.0719(8) d.

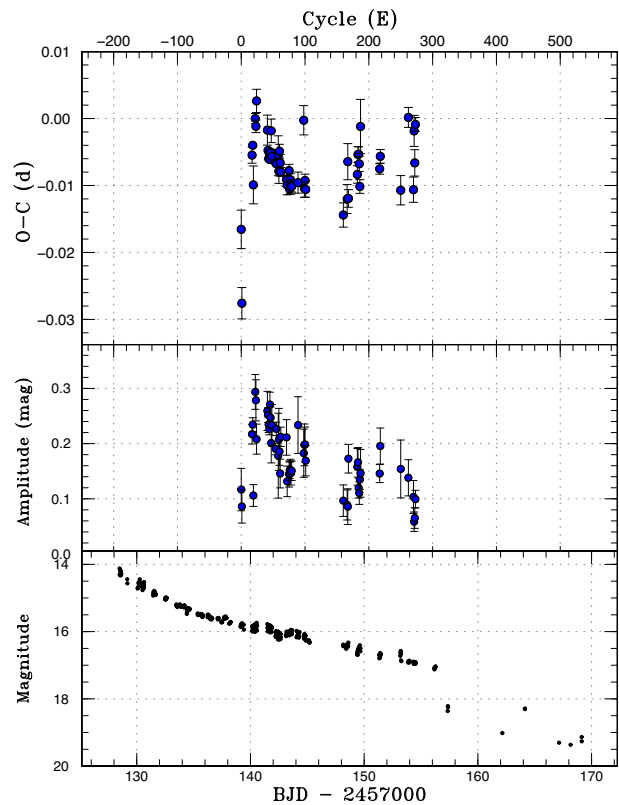


Fig. 40. $O - C$ diagram of superhumps in ASASSN-15hd (2015). Upper: $O - C$ diagram. We used a period of 0.05611 d for calculating the $O - C$ residuals. Middle: Amplitudes of superhumps. Lower: Light curve. The data were binned to 0.019 d. (Color online)

3.56 ASASSN-15hd

This object was detected as a transient at $V = 14.0$ on 2015 April 15 by the ASAS-SN team (vsnet-alert 18547). The large outburst amplitude inferred from the faint ($g = 21.4$ – 21.9 mag) SDSS counterpart already suggested a WZ Sge-type object.

The object initially showed large-amplitude (0.3 mag) variations which resembled ordinary superhumps, but they gradually became double-wave modulations characteristic to early superhumps (vsnet-alert 18552, 18555, 18557, 18573; e-figure 24). The object then showed ordinary superhumps (vsnet-alert 18582, 18585, 18594, 18604, 18609; e-figure 25). The times of superhump maxima are listed in e-table 48. There was a clear transition from stage A to B around $E = 22$. There was no strong indication of transition to stage C (figure 40).

The ϵ^* of 0.028(4) for stage A superhumps corresponds to $q = 0.076(12)$. This relatively low q value appears to be consistent with the small P_{dot} of stage B superhumps (cf. Kato 2015). There was one post-superoutburst rebrightening (figure 40). We cannot, however, exclude the possibility of more rebrightenings since the object was not well observed after the superoutburst.

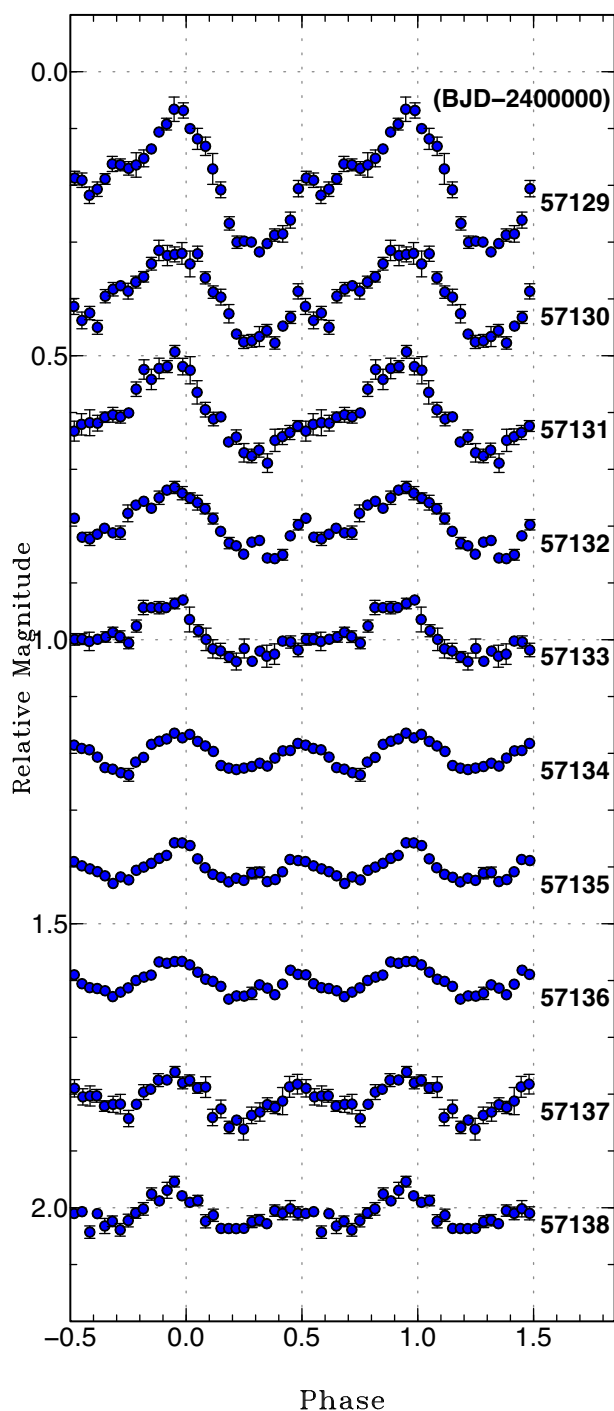


Fig. 41. Evolution of profile of early superhumps in ASASSN-15hd (2015). A period of 0.055410 d was used to draw this figure. (Color online)

The object is notable for its initially large amplitude of early superhumps and the single-peaked “saw-tooth” profile at the beginning (figure 41). The mean amplitude of early superhumps of 0.09 mag implies that ASASSN-15hd belongs to a group of WZ Sge-type objects with largest amplitudes of early superhumps (Kato 2015). The initial “saw-tooth”-like profile was also recorded in V455 And (cf. Kato 2015). Since the large amplitude of early superhumps

strongly suggests a high orbital inclination, the common presence of the “saw-tooth”-like profile in this system and an eclipsing system V455 And suggests that this feature is seen only in high-inclination systems.

3.57 ASASSN-15hl

This object was detected as a transient at $V=16.2$ on 2015 April 19 by the ASAS-SN team. Superhumps (e-figure 26) were soon detected (vsnet-alert 18568). The times of superhump maxima are listed in e-table 49. The superhump stage is unknown.

3.58 ASASSN-15hm

This object was detected as a transient at $V=13.6$ on 2015 April 18 by the ASAS-SN team (vsnet-alert 18563). On April 26 (8 d after the outburst detection), this object started to show superhumps (vsnet-alert 18578, 18587; e-figure 27). The times of superhump maxima are listed in e-table 50. The $O-C$ values clearly indicate that stage B started relatively late (around $E=34$). The slow evolution of superhumps suggests a relatively low q , although it was impossible to determine the q value from stage A superhumps due to the lack of information about the orbital period. Although the large outburst amplitude suggests a WZ Sge-type object, we do not have evidence for it.

3.59 ASASSN-15hn

This object was detected as a transient at $V=12.9$ on 2015 April 17 by the ASAS-SN team (vsnet-alert 18564). The quiescent counterpart was very faint (21.9 mag in GSC 2.3.2 on J plate) and the large outburst amplitude suggested a WZ Sge-type dwarf nova. Ordinary superhumps started to appear on April 30–May 1 (13–14 d after the outburst detection; vsnet-alert 18592, 18599, 18605, 18610; e-figure 28). The object started to fade rapidly on May 11, 24 d after the outburst detection. The times of superhump maxima are listed in e-table 51. Stage A lasted nearly 30 cycles (figure 42), which implies a small q (Kato 2015).

There was no indication of early superhumps before the appearance of ordinary superhumps. The upper limit for the amplitude of early superhumps was 0.005 mag, probably suggesting a low orbital inclination. Although this object did not show early superhumps, all the observed features suggest the WZ Sge-type classification: long duration (13–14 d) before the appearance of ordinary superhumps, long duration of stage A (~ 30 cycles), small P_{dot} for stage B superhumps, low amplitude of superhumps, and the lack of stage C superhumps. The empirical relation between P_{dot} for stage B superhumps and q [equation (6) in

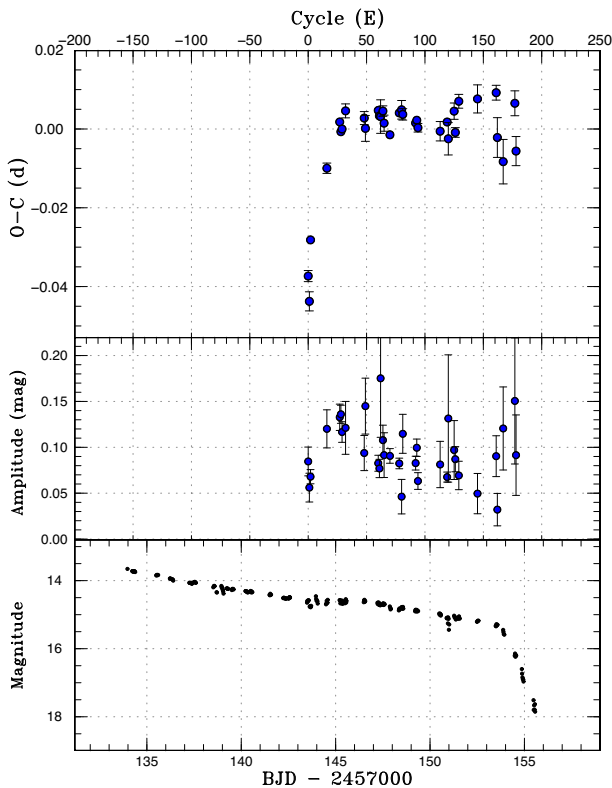


Fig. 42. $O - C$ diagram of superhumps in ASASSN-15hn (2015). Upper: $O - C$ diagram. We used a period of 0.06185 d for calculating the $O - C$ residuals. Middle: Amplitudes of superhumps. Lower: Light curve. The data were binned to 0.021 d. (Color online)

Kato 2015] gives a q of 0.058(9). Since the object has a relatively long superhump period, this estimated q would place it in a region of period bouncers. The apparent large outburst amplitude would favor this interpretation. Ordinary superhumps started to appear at 14.7 mag. Although quiescent magnitude is highly uncertain, the “amplitude” when ordinary superhumps appear (7.2 mag) is also in the region of period bouncers (see figure 23 of Kato 2015).

3.60 ASASSN-15ia

This object was detected as a transient at $V=15.3$ on 2015 April 25 by the ASAS-SN team. The object faded to $V=15.6$ on April 26 and brightened to $V=15.3$ on April 27, suggesting a precursor outburst. Superhumps were detected in observations starting 4 d after the outburst detection (e-figure 29). The times of superhump maxima are listed in e-table 52. Both stages B and C were recorded. The early part of stage B was not observed. The rapid fading from the superoutburst plateau apparently took place on May 7. The total duration of the superoutburst was 11 d.

3.61 ASASSN-15ie

This object was detected as a transient at $V=14.0$ on 2015 May 4 by the ASAS-SN team. On May 9 (5 d after the outburst detection), superhumps started to appear (vsnet-alert 18606, 18611, 18616, 18634; e-figure 30). The times of superhump maxima are listed in e-table 53. The maxima for $E \leq 2$ recorded stage A superhumps. Although there were observations, the times of maxima between $E=138$ and $E=222$ could not be determined due to the low amplitudes of superhumps and the faintness (16.2 mag) of the object. The maxima around $E=223$ correspond to the stage B–C transition, when superhumps again became apparent and the object brightened slightly. The object started fading rapidly on May 25 and the total duration of the superoutburst was 20 d.

Despite the apparent large outburst amplitude, the short delay before the appearance of superhumps and the presence of stage C make this object less likely an extreme WZ Sge-type object.

3.62 ASASSN-15iv

This object was detected as a transient at $V=15.8$ on 2015 May 11 by the ASAS-SN team. Superhumps were present 2 d after the outburst detection (vsnet-alert 18614, 18643; e-figure 31). The times of superhump maxima are listed in e-table 54. There was a clear stage B–C transition around $E=88$. The object started fading rapidly between May 23 and 25. The total duration of the superoutburst was about 13 d.

3.63 ASASSN-15iz

This object was detected as a transient at $V=16.7$ on 2015 May 11 by the ASAS-SN team. It was initially suspected that this object could be identified with a cataloged high proper motion object (cf. vsnet-alert 18620). This high proper motion, however, was found to be spurious by examination of archival plates (B. Skiff, vsnet-alert 18623). The object showed large-amplitude superhumps (vsnet-alert 18626, 18644; e-figure 32). The times of superhump maxima are listed in e-table 55. In this table, we adopted a period [0.08140(6) d] which appears to give the smallest scatter in the $O - C$ diagram. Other longer 1-d aliases [particularly 0.08863(7) d] are still possible, and the cycle numbers in this table may be subject to correction.

3.64 ASASSN-15jj

This object was detected as a transient at $V=14.5$ on 2015 May 16 by the ASAS-SN team. Superhumps were already

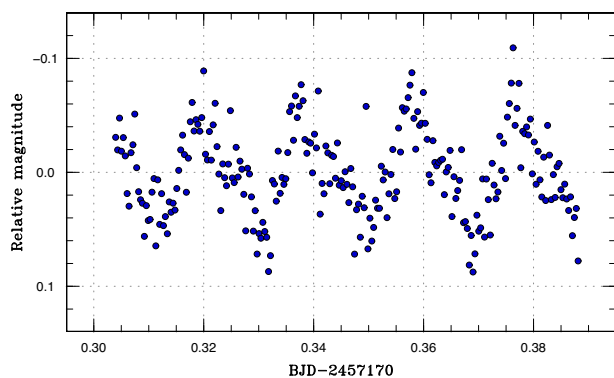


Fig. 43. Superhumps in ASASSN-15kf (2015). This object is likely an AM CVn-type system. (Color online)

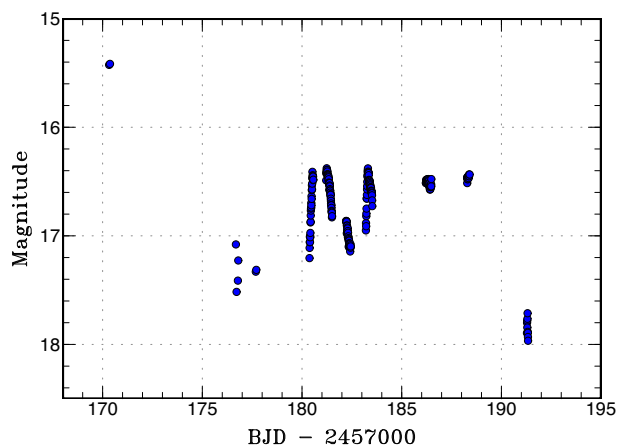


Fig. 44. Outburst light curve of ASASSN-15kf (2015). The data for BJD 2457176–2457178 were binned to 0.05 d. The other data were binned to 0.0064 d. (Color online)

present on May 19 and were continuously observed (vsnet-alert 18637, 18642, 18655; e-figure 33). The times of superhump maxima are listed in e-table 56. The $O - C$ diagram shows a clear pattern of stages B and C. The large positive P_{dot} [$+8.1(0.6) \times 10^{-5}$] is typical for this superhump period.

3.65 ASASSN-15kf

This object was detected as a transient at $V = 15.0$ on 2015 May 27 by the ASAS-SN team. Subsequent observations detected very short period superhumps [period 0.0192(1) d, figure 43], making this object a likely AM CVn-type object (vsnet-alert 18669). The superhumps were clearly detected only on this night, and the object faded after a 6-d gap in observation. The times of superhump maxima are listed in e-table 57. The period given in table 3 refers to the one determined with the PDM method.

The object then showed (probably damping) oscillations (vsnet-alert 18712, 18724; figure 44), which are characteristic to AM CVn-type superoutbursts (cf. Kato et al. 2004a,

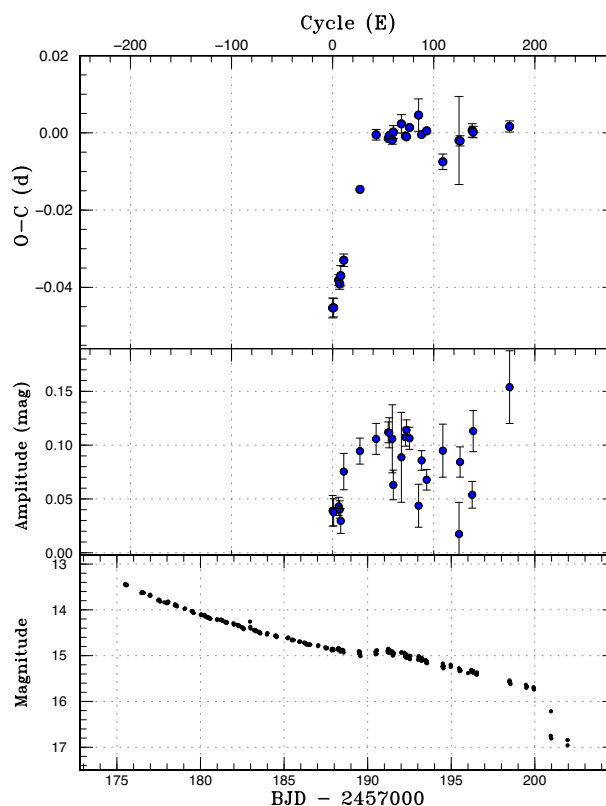


Fig. 45. $O - C$ diagram of superhumps in ASASSN-15kh (2015). Upper: $O - C$ diagram. We used a period of 0.06048 d for calculating the $O - C$ residuals. Middle: Amplitudes of superhumps. Lower: Light curve. The data were binned to 0.020 d. (Color online)

2013a, 2014a; Nogami et al. 2004; Levitan et al. 2015; Isogai et al. 2016). During this phase, there were weak variations with a period of 0.01906(1) d, which may be late stage superhumps or the orbital variation (e-figure 34).

3.66 ASASSN-15kh

This object was detected as a transient at $V = 13.2$ on 2015 June 1 by the ASAS-SN team. No quiescent counterpart is known. Emerging (ordinary) superhumps were observed on June 14 (13 d after the outburst detection, vsnet-alert 18734, 18758, 18799; e-figure 35). The times of superhump maxima are listed in e-table 58. The $O - C$ diagram shows clear stages A and B. Stage A lasted for 43 cycles and there was no indication of stage C (figure 45). The object started fading rapidly on June 27, 26 d after the outburst detection.

The amplitude of early superhumps was below the limit (0.01 mag) of our detection although the long duration before the appearance of stage A superhumps (figure 45) strongly suggests that the 2 : 1 resonance was working.

The small P_{dot} [$+1.2(1.6) \times 10^{-5}$] suggests that the object has a small q . The empirical relation between P_{dot} for stage B superhumps and q [equation (6) in Kato 2015] gives a q of 0.065(9). Combined with the long duration of

stage A superhumps, low amplitude of superhumps (probably reflecting the small tidal torque) and the long superhump period, this object is a good candidate for the period bouncer. The brightness when the superhump appeared was 14.9 mag. Kato (2015) has shown that the quiescent brightness is 6.4 and 7.2 mag (in average) fainter in WZ Sge-type objects and period bouncers, respectively. The expected quiescent brightness is 21.3 and 22.1 mag, respectively, and it is not a surprise that there was no previous detection of the quiescent counterpart.

3.67 ASASSN-15le

This object was detected as a transient at $V = 14.9$ on 2015 June 12 by the ASAS-SN team. There is a $V = 14.9$ mag star $5''$ from this position. There is a GALEX counterpart with an NUV magnitude of 19.5(1). There was at least one long outburst reaching $V = 13.6$ in 2007 October in the ASAS-3 data. Superhumps were soon detected (vsnet-alert 18736, 18746; e-figure 36). Although there were observations after BJD 2457193, we could not detect a confident superhump signal on later nights, probably due to the contamination by the nearby star. We only listed superhump maxima for the initial three nights in e-table 59.

3.68 ASASSN-15lt

This object was detected as a transient at $V = 13.8$ on 2015 June 21 by the ASAS-SN team. The object soon developed superhumps (vsnet-alert 18797; e-figure 37). The early evolution (3 d after the outburst detection, less than 7 d after the outburst maximum even considering the observational gap in the ASAS-SN data) of superhumps apparently excludes the possibility of a WZ Sge-type object. The times of superhump maxima are listed in e-table 60. There was an apparent stage A–B transition around $E = 50$. The maxima after $E = 188$ were likely stage C superhumps, which were associated with the small brightening of the object. Due to the observational gap, the P_{dot} for stage B superhumps could not be determined. We adopted the period of stage A superhumps determined from the maxima $E \leq 17$.

3.69 ASASSN-15mb

This object was detected as a transient at $V = 13.0$ on 2015 June 30 by the ASAS-SN team. There is a likely X-ray counterpart, 1RXS J025246.3–395853. There was a past outburst in 2009, which was initially detected at $V = 12.74$ by ASAS-3 on October 31, and was observed at 14.2 mag (unfiltered CCD) by CRTS on November 18 (vsnet-alert 18818, 18821).

During the 2015 outburst, superhumps were detected (vsnet-alert 18838, 18843). Due to the short nightly observations, we could not detect many superhumps. The data, however, showed periodic signals in different segments via PDM analysis (e-figures 38, 39). Since the $O - C$ analysis is not helpful in identifying the alias, we selected the strongest signal in the PDM analysis and assigned the cycle counts (e-table 61). The maxima for $E \leq 173$ were recorded in the post-superoutburst phase. Since there was significant brightening during the superoutburst plateau around BJD 2457217, the maxima after this can be attributed to stage C superhumps. We include $E = 43$ to stage C in table 3 based on the continuity of the $O - C$ curve. There remain possibilities of other 1-d aliases.

The superoutburst lasted at least 19 d (but less than 23 d). The object showed a post-superoutburst rebrightening on July 29, 11 d after the rapid fading from the superoutburst plateau. The second observation during the 2009 outburst likely detected the rapidly fading part or a rebrightening.

3.70 ASASSN-15mt

This object was detected as a transient at $V = 13.7$ on 2015 July 18 by the ASAS-SN team (Simonian et al. 2015). The object has a strong UV excess in quiescence. ($U - g = -0.74$, Greiss et al. 2012).

Subsequent observations immediately detected superhumps (vsnet-alert 18878, 18882, 18890; e-figure 40). The times of superhump maxima are listed in e-table 62. After $E = 42$, there was significant reduction of the superhump amplitudes and we identified this epoch to be stage B–C transition. As is usual for a system with a long superhump period, the transition is not as sharp as in short-period systems. The object started fading rapidly on July 28–29, and the duration of the superoutburst was at least 11 d (but shorter than 16 d).

3.71 ASASSN-15na

This object was detected as a transient at $V = 14.8$ on 2015 July 20 by the ASAS-SN team. Double-wave modulations were immediately detected (vsnet-alert 18884). The object was initially suspected as an AM CVn-type dwarf nova (cf. vsnet-alert 18910), which was incorrect due to the mistaken identity of a non-existent rapid fading (cf. vsnet-alert 18923). The object showed growth of superhumps associated with the brightening of the system (vsnet-alert 18923, 18933; e-figure 41).

The times of superhump maxima after the development of superhumps are listed in e-table 63. Although there were modulations before these epochs, we have not been

able to determine the individual maxima due to the poor statistics (due to the faintness of the object). The epoch, $E=174$, probably corresponds to a stage C superhump. The cycle count between $E=111$ and $E=174$ is somewhat ambiguous. Using the data between BJD 2457231.6 and 2457233.8, a period of 0.06491(12) d was obtained, which we identified to be the period of stage A superhumps. The data before BJD 2457231.5 were well expressed by a shorter period of 0.06297(2) d, which we identified to be the period of early superhumps (e-figure 42). By using these periods, we have obtained $q=0.081(5)$.

Although the orbital period (approximated by the period of early superhumps) is much longer than the period minimum, the object does not have a very low q , which is expected for a period bouncer. The short duration of stage A and large amplitude of superhumps (e-figure 41) are also consistent with a high q (Kato 2015). The system may be similar to WZ Sge-type dwarf novae with multiple rebrightenings (MASTER OT J211258.65+242145.4, MASTER OT J203749.39+552210.3; Nakata et al. 2013).

3.72 ASASSN-15ni

This object was detected as a transient at $V=12.9$ on 2015 July 28 by the ASAS-SN team (Dong et al. 2015). The dwarf nova-type nature was spectroscopically confirmed (Berardi 2015).

Although no clear superhumps were visible before August 7 (10 d after the outburst detection), ordinary superhumps appeared (vsnet-alert 18945, 18950, 18959, 18968, 18976; e-figure 43). The times of superhump maxima are listed in e-table 64. Clear stages A and B can be recognized. Stage A lasted at least 26 cycles. A retrospective analysis of the early data detected low-amplitude double-wave early superhumps (e-figure 44) confirming the WZ Sge-type classification. The period of an early superhump with the PDM method is 0.05517(4) d. The fractional superhump excess $\epsilon^* = 0.027(2)$ of stage A corresponds to $q = 0.074(2)$. The low value of q is consistent with the long duration of stage A, relatively small P_{dot} , and low amplitude of ordinary superhumps.

3.73 ASASSN-15nl

This object was detected as a transient at $V=14.1$ on 2015 August 1 by the ASAS-SN team. The object was found to be already bright ($V=13.3$) on July 29. Although no superhump-like modulations were recorded in our early observations, the object showed superhumps on August 9 (vsnet-alert 18958, 18966; e-figure 45). Since there was a gap in the observation between August 5 and 9, we could not determine when superhumps started to appear but it

took more than 7 d to develop superhumps. The times of superhump maxima are listed in e-table 65.

3.74 ASASSN-15ob

This object was detected as a transient at $V=15.2$ on 2015 August 9 by the ASAS-SN team. There were previous outbursts in the CRTS data. Subsequent observations detected superhumps (vsnet-alert 18975, 18982, 18991; e-figure 46). The times of superhump maxima are listed in e-table 66.

3.75 ASASSN-15oj

This object was detected as a transient at $V=13.8$ on 2015 August 15 by the ASAS-SN team. There were four previous outbursts in the CRTS data. Subsequent observations detected superhumps (vsnet-alert 19007; e-figure 47). The times of superhump maxima are listed in e-table 67. This table is based on a candidate period. Other aliases [0.07203(1) d, 0.07764(1) d] are also viable.

3.76 ASASSN-15ok

This object was detected as a transient at $V=13.7$ on 2015 August 15 by the ASAS-SN team. There was at least one well-recorded outburst (2008 February) in ASAS-3 data (vsnet-alert 18980). Although the object was initially suspected to be an SS Cyg-type due to the relatively bright counterpart in 2MASS (vsnet-alert 18980), the 2MASS colors are consistent (such as $J - K \sim 0$) with those of an outbursting dwarf nova. The object was accidentally detected in outburst in 2MASS scans. Subsequent observations detected superhumps (vsnet-alert 18987, 18994, 19008; e-figure 48). The times of superhump maxima are listed in e-table 68. The observations apparently covered the later phase of the superoutburst (the object faded rapidly 9 d after the initial observation) and the maxima for $E \geq 25$ likely represent stage C superhumps. The maxima $E < 25$ were likely the final phase of stage B superhumps.

3.77 ASASSN-15pi

This object was detected as a transient at $V=16.4$ on 2015 September 8 by the ASAS-SN team. The object was already $V=16.1$ on September 5 (ASAS-SN data). There is no known quiescent counterpart. Superhumps were detected on single-night observation on September 10 (vsnet-alert 19046; e-figure 49). The best period determined by the PDM method is 0.0785(2) d. The times of superhump maxima are listed in e-table 69.

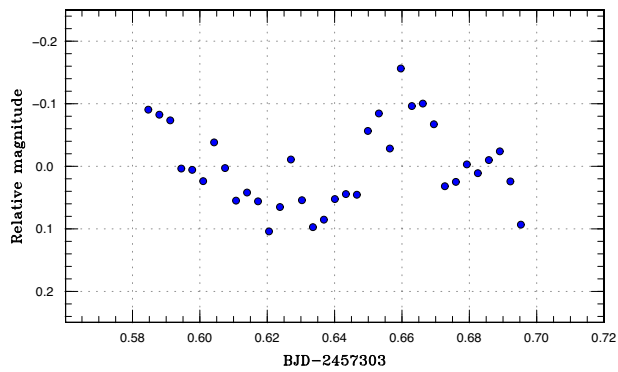


Fig. 46. Likely superhumps in ASASSN-15ql (2015). (Color online)

3.78 ASASSN-15pu

This object was detected as a transient at $V=13.7$ on 2015 September 18 by the ASAS-SN team (Stanek et al. 2015). There is a $B_j=22.1$ mag counterpart in GSC 2.3.2. The large outburst amplitude already suggested a WZ Sge-type dwarf nova (Stanek et al. 2015). Early superhumps were immediately recorded (vsnet-alert 19074; the period was corrected in vsnet-alert 19095; e-figure 50), Ordinary superhumps started to grow on September 28 (vsnet-alert 19095, 19125; e-figure 51). The times of superhump maxima are listed in e-table 70. The maxima for $E \leq 18$ correspond to stage A superhumps. The ϵ^* for stage A superhumps [0.028(5)] corresponds to $q=0.074(16)$.

3.79 ASASSN-15qe

This object was detected as a transient at $V=15.0$ on 2015 October 2 by the ASAS-SN team. The object was found to be rising at $V=16.3$ on October 1. There is a $B_j=21.2$ mag counterpart in GSC 2.3.2. Subsequent observations detected superhumps (vsnet-alert 19112, 19131; e-figure 52). The times of superhump maxima are listed in e-table 71. Due to the gap in the observation between $E=62$ and $E=175$, the cycle count between them is uncertain. We used maxima for $E \leq 62$ for determining the period in table 3.

3.80 ASASSN-15ql

This object was detected as a transient at $V=15.4$ on 2015 October 4 by the ASAS-SN team. The object was found to be already bright at $V=14.8$ on September 30. Although the observation on October 8 suggested the presence of superhumps (vsnet-alert 19141; figure 46), the object was already rapidly fading 4 d later, and no confirmatory observations were obtained.

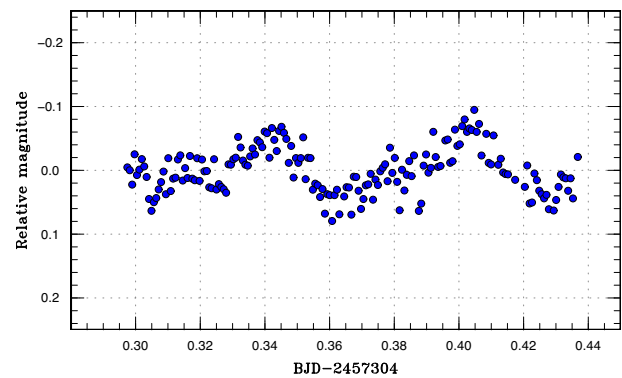


Fig. 47. Likely early superhumps in ASASSN-15qo (2015). (Color online)

3.81 ASASSN-15qo

This object was detected as a transient at $V=15.2$ on 2015 October 7 by the ASAS-SN team. Observations on October 8 detected modulations (vsnet-alert 19142; figure 47). The data, however, on later nights were fragmentary and not conclusive. As judged from the large outburst amplitude and the profile of the humps (slower rise), we consider that these modulations were early superhumps and the object is likely a WZ Sge-type dwarf nova. The period determined from the single-night observations is 0.062(1) d, which is long for a WZ Sge-type dwarf nova.

3.82 ASASSN-15qq

This object was detected as a transient at $V=16.2$ on 2015 October 7 by the ASAS-SN team. The object was found to be already bright at $V=15.7$ on October 4. Superhumps were immediately detected (vsnet-alert 19152, 19163, 19171; e-figure 53). The times of superhump maxima are listed in e-table 72. The stage of superhumps was not clear. It is possible that the data are a combination of stages B and C, since the outburst detection was not made early enough. In table 3, we give a globally averaged value.

3.83 ASASSN-15rf

This object was detected as a transient at $V=15.7$ on 2015 October 13 by the ASAS-SN team. Although observations on the initial night (October 16; figure 48) detected likely superhumps, we could not detect a significant signal on four nights since October 22, probably due to the low signal-to-noise ratio.

3.84 ASASSN-15rj

This object was detected as a transient at $V=16.0$ on 2015 October 14 by the ASAS-SN team. Subsequent observations detected superhumps (vsnet-alert 19168, 19174; e-figure 54). The times of superhump maxima are listed

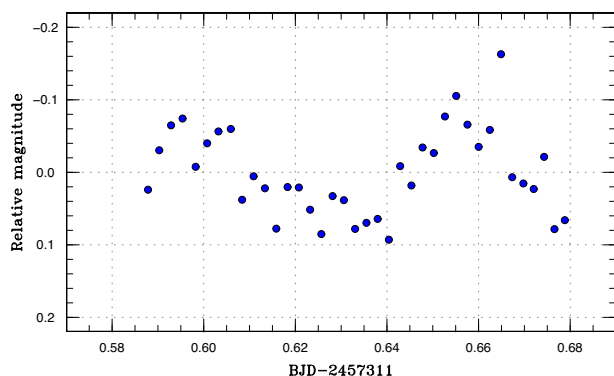


Fig. 48. Likely superhumps in ASASSN-15rf (2015). (Color online)

in e-table 73. The mean superhump period found with the PDM method is 0.09255(4) d.

3.85 ASASSN-15ro

This object was detected as a transient at $V=15.5$ on 2015 October 18 by the ASAS-SN team. Subsequent observations detected superhumps (vsnet-alert 19181, 19185). The times of superhump maxima are listed in e-table 74. The large superhump amplitudes suggest that we observed stage B superhumps.

3.86 ASASSN-15rr

This object was detected as a transient at $V=14.6$ on 2015 October 17 by the ASAS-SN team (the detection announcement was after the observation on October 21 at $V=15.3$). The quiescent counterpart is very faint ($B_j=22.0$) and the large outburst amplitude received attention. Subsequent observations detected superhumps (vsnet-alert 19196; e-figure 56). Due to the shortness of the observing runs and the gap in the observation, there remained possibilities of aliases. The times of superhump maxima are listed in e-table 75 with the assumption of the alias which gives the smallest absolute $O-C$ values.

3.87 ASASSN-15rs

This object was detected as a transient at $V=14.5$ on 2015 October 21 by the ASAS-SN team. The object was also cataloged as an $H\alpha$ emission-line object IPHASJ044633.68+485755.6 (Drew et al. 2005). Subsequent observations detected long-period superhumps (vsnet-alert 19195; e-figure 57). The times of superhump maxima are listed in e-table 76. Due to the gap in the observation, the cycle count between $E=22$ and $E=92$ is somewhat uncertain. Since the superhump period of this system is long, the superhump period may have strongly

decreased during the observation (Kato et al. 2009, 2016a; see also subsection 4.4). We restrict the period analysis for $E \leq 22$ in table 3 and e-figure 57.

3.88 ASASSN-15ry

This object was detected as a transient at $V=15.9$ on 2015 October 22 by the ASAS-SN team (the detection announcement was after the observation on October 24 at $V=15.3$). The object was also independently detected by S. Ueda (TCP J05285567+3618388) on October 24 at an unfiltered CCD magnitude of 14.2.¹⁶ (Our observations suggest that this estimate was too bright by ~ 1 mag.) The object was also cataloged as an $H\alpha$ emission-line object, IPHAS2 J052855.67+361839.0 (Barentsen et al. 2014). Subsequent observations detected superhumps (vsnet-alert 19193; e-figure 58). Only single-night observations are available and the times of superhump maxima are listed in e-table 77. The superhump period given in table 3 is based on the PDM analysis.

3.89 ASASSN-15sc

This object was detected as a transient at $V=14.6$ on 2015 October 24 by the ASAS-SN team. The object was still rising at $V=16.2$ on October 22. Although there is a 19.9-mag star $5''$ distant in the Initial Gaia Source List, this object appears too bright and too red for the quiescent counterpart. Time-resolved photometry started on October 28. There were no periodic modulations on the first two nights. Growing likely superhumps were detected on October 30 and further observations confirmed superhumps (vsnet-alert 19215, 19217, 19219, 19226, 19236, 19238, 19249, 19277; e-figure 59). The times of superhump maxima are listed in e-table 78. The $O-C$ data clearly indicate the stages A–B–C with a strongly positive P_{dot} typical for this short superhump period. Although stage C was present, the short duration of stage C (typical for a short-period system) made it difficult to determine the period of stage C superhumps.

3.90 ASASSN-15sd

This object was detected as a transient at $V=14.8$ on 2015 October 27 by the ASAS-SN team. Subsequent observations detected superhumps (vsnet-alert 19210; e-figure 60). The object rapidly faded on November 5. The times of superhump maxima are listed in e-table 79. The lack of a significantly positive P_{dot} expected for this superhump period suggests that we only observed stage C superhumps.

¹⁶ (<http://www.cbat.eps.harvard.edu/unconf/followups/J05285567+3618388.html>).

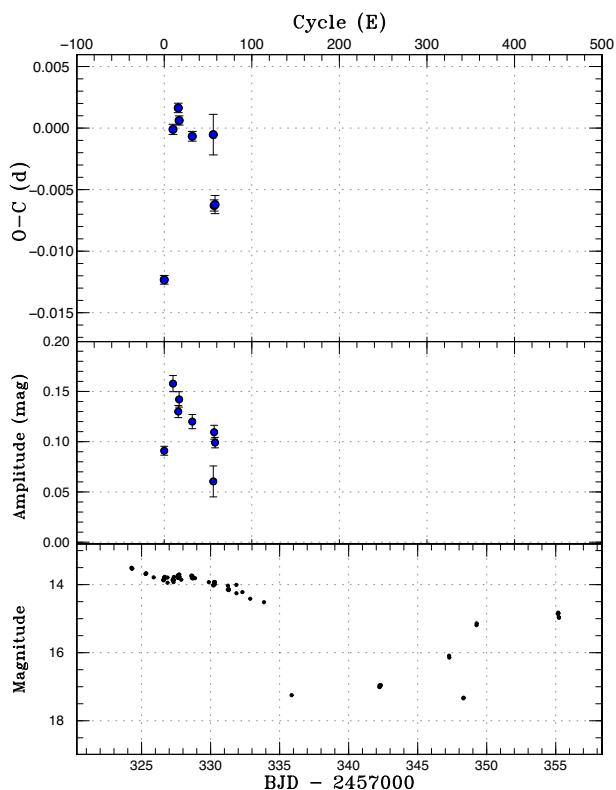


Fig. 49. $O-C$ diagram of superhumps in ASASSN-15se (2015). Upper: $O-C$ diagram. We used a period of 0.06343 d for calculating the $O-C$ residuals. Middle: Amplitudes of superhumps. Lower: Light curve. The data were binned to 0.021 d. (Color online)

The duration of the superoutburst plateau was shorter than 11 d, considering the negative observation in the ASAS-SN data on October 24. The development of superhumps and the duration of the superoutburst may be somewhat atypical for this superhump period and further observations are needed to understand the object better.

3.91 ASASSN-15se

This object was detected as a transient at $V=13.04$ on 2015 October 25 by the ASAS-SN team. The outburst announcement was after the $V=13.46$ observation on October 28 (vsnet-alert 19208). No superhumps were detected on October 28 and 29. Growing superhumps were detected on October 31 (vsnet-alert 19216). Further data confirmed the superhumps (vsnet-alert 19220, 19227; the period given in vsnet-alert 19227 was in error due to the confusion with ASASSN-15sc; e-figure 61). The times of superhump maxima are listed in e-table 80. Although $E=0$ corresponded to a stage A superhump, we could not determine the period of stage A superhumps. The object showed at least two rebrightenings on November 15 (vsnet-alert 19286) and November 20–22 (vsnet-alert

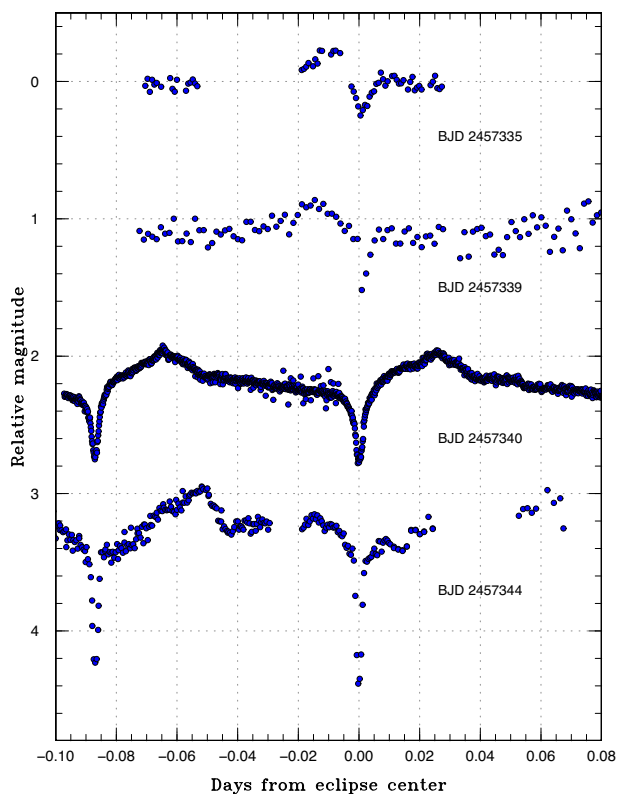


Fig. 50. Light curve of ASASSN-15sl. Superposition of superhumps and eclipses is well visible. (Color online)

19294) (figure 49). It is not clear whether the rebrightenings are type-A/B (multiple rebrightenings with small amplitudes) or type-B (discrete multiple rebrightenings) in Kato (2015). Since the superhump period is relatively long, this object may belong to WZ Sge-type dwarf novae with multiple rebrightenings as described by Nakata et al. (2014).

3.92 ASASSN-15sl

This object was detected as a transient at $V=15.0$ on 2015 November 3 by the ASAS-SN team. The object soon turned out to be a deeply eclipsing SUUMa-type dwarf nova (vsnet-alert 19254, 19259, 19264, 19278, 19279; figure 50). The eclipse ephemeris was determined by using MCMC analysis (Kato et al. 2013a) of the observations:

$$\text{Min}(\text{BJD}) = 2457341.23671(7) + 0.0870484(7)E. \quad (2)$$

This ephemeris is not intended for long-term prediction of eclipses. The epoch refers to the center of the observation. The times of superhump maxima outside the eclipses are listed in e-table 81. Although the superhump stage is unknown, we should note that most of our observations were in the later phase of the superoutburst. These superhumps may be mostly stage C superhumps.

3.93 ASASSN-15sn

This object was detected as a transient at $V=15.4$ on 2015 November 4 by the ASAS-SN team. The object was in outburst at $g=15.57$ in the Kepler Input Catalog. The object was recorded at $g=20.85$ and $U=19.94$ in quiescence in the Extended Kepler-INT Survey (Greiss et al. 2012). Subsequent observations detected superhumps (vsnet-alert 19247, 19257; e-figure 62). The times of superhump maxima are listed in e-table 82. Since we observed the relatively late stage of the superoutburst, the break in the $O-C$ diagram around $E=27$ probably reflects stage B–C transition. We gave a global value in table 3.

3.94 ASASSN-15sp

This object was detected as a transient at $V=13.9$ on 2015 November 8 by the ASAS-SN team. There is an X-ray counterpart 1RXS J075806.5–572239. There was an outburst on 2008 January 26–28 reaching $V=14.02$ detected by ASAS-3 (vsnet-alert 19246). There were double-humped variations on November 9 (vsnet-alert 19252), which developed into full superhumps on November 12 (vsnet-alert 19256, 19260, 19280; e-figure 63). The initial variation probably reflected growing phase superhumps (part of stage A). The times of superhump maxima are listed in e-table 83. The maxima for $E \leq 1$ correspond to stage A superhumps. Due to the gap in the observation before $E=33$, we could not determine the period of stage A superhumps. The P_{dot} was positive, as is expected for this superhump period. Although there were observations after $E=138$, we could not determine individual times of maxima. A PDM analysis of the data between BJD 2457345 and 2457352 (late part of the plateau phase with slight brightening) yielded a strong signal of 0.05829(4) d. This period is adopted as that of stage C superhumps in table 3.

3.95 ASASSN-15su

This object was detected as a transient at $V=15.0$ on 2015 November 15 by the ASAS-SN team. Previous outbursts were recorded in the CRTS data. Superhumps were immediately detected (vsnet-alert 19285). Although only one superhump maximum was measured at BJD 2457345.5947(6) ($N=57$), the period has been reasonably determined as 0.0670(3) d (figure 51, e-figure 64).

3.96 ASASSN-15sv

This object was detected as a transient at $V=15.8$ on 2015 November 16 by the ASAS-SN team. Superhumps were immediately detected (vsnet-alert 19284; figure 52).

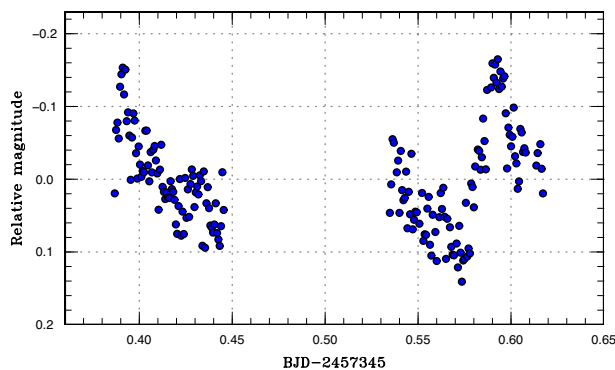


Fig. 51. Superhumps in ASASSN-15su (2015). (Color online)

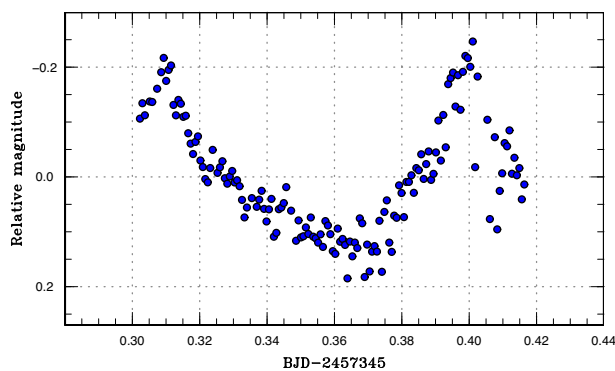


Fig. 52. Superhumps in ASASSN-15sv (2015). (Color online)

The long superhump period placed the object in the period gap. Two superhump maxima were recorded: BJD 2457345.3086(9) ($N=52$) and 2457345.3998(9) ($N=72$). The superhump period is 0.091(1) d.

3.97 ASASSN-15ud

This object was detected as a large-amplitude transient at $V=15.3$ on 2015 December 14 by the ASAS-SN team. There is a $B_i=22.1$ mag counterpart in GSC 2.3.2. Single-night observations detected superhumps (vsnet-alert 19353; e-figure 65). The times of superhump maxima are listed in e-table 84. Although the outburst amplitude is large, the object is likely an ordinary SUUMa-type dwarf nova as judged from the early appearance of superhumps. The period given in table 3 is based on the PDM analysis.

3.98 ASASSN-15uj

This object was detected as a large-amplitude transient at $V=14.3$ on 2015 December 20 by the ASAS-SN team (cf. vsnet-alert 19352). Subsequent observations detected double-wave early superhumps (vsnet-alert 19359, 19361, 19368; e-figure 66) confirming the WZ Sge-type classification. The best period of early superhumps with the PDM method is 0.055266(7) d. The object then showed growing

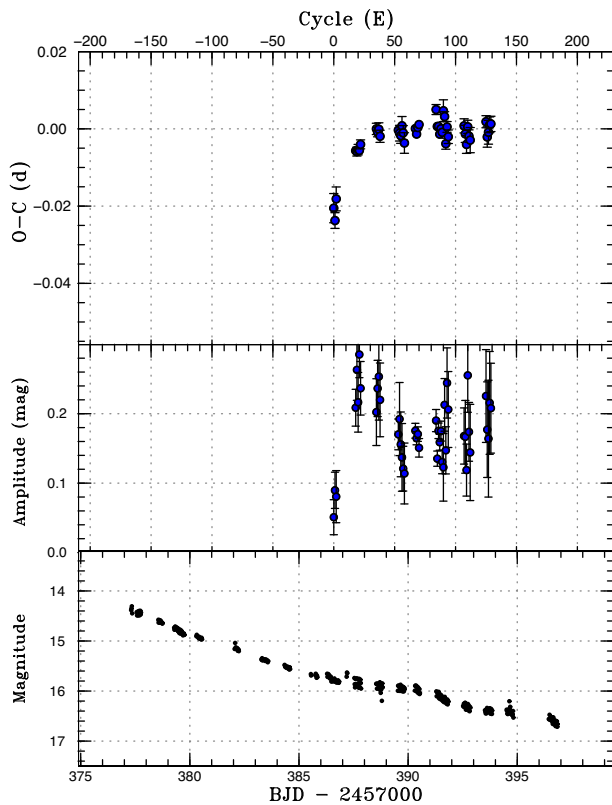


Fig. 53. $O-C$ diagram of superhumps in ASASSN-15uj (2015). Upper: $O-C$ diagram. We used a period of 0.05580 d for calculating the $O-C$ residuals. Middle: Amplitudes of superhumps. Lower: Light curve. The data were binned to 0.018 d. (Color online)

ordinary superhumps (vsnet-alert 19392; e-figure 67). The outburst lasted at least up to 2016 January 17 ($V = 16.43$, part of the rebrightening phase?, ASAS-SN data). The times of superhump maxima are listed in e-table 85. The maxima for $E \leq 22$ correspond to stage A superhumps (figure 53). The measured $\epsilon^* = 0.0243(13)$ for stage A superhumps corresponds to $q = 0.064(4)$. The almost constant period of stage B superhumps is also consistent with this small q (cf. Kato 2015). The object is a WZ Sge-type dwarf nova likely in a relatively evolved state.

3.99 ASASSN-15ux

This object was detected as a large-amplitude transient at $V = 14.4$ on 2015 December 29 by the ASAS-SN team. No quiescent counterpart is known. Subsequent observations detected early superhumps (these modulations were initially reported as superhumps) (vsnet-alert 19390, 19391, 19396; e-figure 68). The object started to show ordinary superhumps on 2016 January 12 (vsnet-alert 19409, 19411; e-figure 69). The large amplitude of early superhumps and the complex profile of individual superhumps suggested the presence of eclipses (vsnet-alert 19391, 19409). The

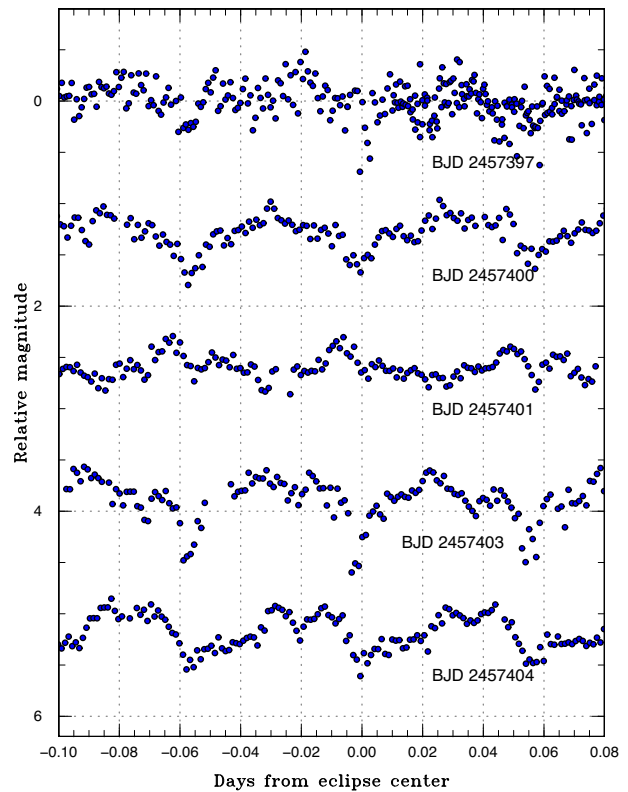


Fig. 54. Light curve of ASASSN-15ux after the appearance of the eclipses. Shallow eclipses with variable profiles were recorded. (Color online)

eclipsing nature was confirmed by further observations (vsnet-alert 19423; figure 54).

The eclipse ephemeris was determined by using MCMC analysis (Kato et al. 2013a) of the observations after BJD 2457396.5 (when eclipses became apparent):

$$\text{Min(BJD)} = 2457400.82908(10) + 0.056109(2)E. \quad (3)$$

This ephemeris is not intended for long-term prediction of eclipses. The epoch refers to the center of the observations used. The period of early superhumps was 0.056091(4) d, 0.03% shorter than the orbital period. This value is in very good agreement with the other eclipsing WZ Sge-type dwarf novae (Kato 2015).

The times of superhump maxima determined from observations outside the eclipses are listed in e-table 86. Although hump maxima for $E \leq 3$ looked like stage A superhumps, they may have been a transition phase from early superhumps to ordinary superhumps (e.g., WZ Sge, figure 126 in Kato et al. 2009), we have disregarded these maxima in determining the period of stage A superhumps. There also remains ambiguity in cycle counts between $E = 3$ and $E = 55$. The maxima for $E \geq 73$ are clearly stage B superhumps.

Although the object is very faint, the object is a rare WZ Sge-type dwarf nova with high-amplitude early superhumps (the mean amplitude of 0.38 mag is one of the largest, cf. Kato 2015) and eclipses. The object deserves further detailed observations.

3.100 ASASSN-16af

This object was detected as a transient at $V=15.5$ on 2016 January 10 by the ASAS-SN team. Subsequent observations detected superhumps (vsnet-alert 19417, 19419, 19424; e-figure 70). The times of superhump maxima are listed in e-table 87. A positive P_{dot} typical for this superhump period was recorded.

3.101 ASASSN-16ag

This object was detected as a transient at $V=16.2$ on 2016 January 11 by the ASAS-SN team. Although the observations on January 12.4–12.6 UT did not detect superhumps, superhumps were detected immediately after these observations (vsnet-alert 19407). Although these superhumps were possibly stage A superhumps, we could not determine the stage due to the lack of observations and the low signal-to-noise ratios caused by faintness of the object. In e-table 88, we list times of maxima using a period which reasonably expresses all the observations (see also e-figure 71). The object apparently has a low outburst amplitude (3.5 mag) for an SUUMa-type dwarf nova.

3.102 ASASSN-16ao

This object was detected as a transient at $V=16.1$ on 2016 January 13 by the ASAS-SN team. The outburst faded below $V=18.0$ on January 16 (ASAS-SN data). The object was observed by B. Monard on January 19 when it was at about 18.7 mag. These observations detected modulations attributable to superhumps (vsnet-alert 19433; figure 55). The identification, however, is not secure since the object was not in a very bright state (the identification of a precursor in vsnet-alert 19433 was probably incorrect). The best period from these observations was 0.0639(5) d. Further observations are needed to firmly characterize the nature of this object.

3.103 ASASSN-16aq

This object was detected as a transient at $V=15.1$ on 2016 January 17 by the ASAS-SN team. The large outburst amplitude suggested a possible WZ Sge-type dwarf nova (cf. vsnet-alert 19428). Superhump-type modulations were immediately recorded (vsnet-alert 19432; figure 56). Two

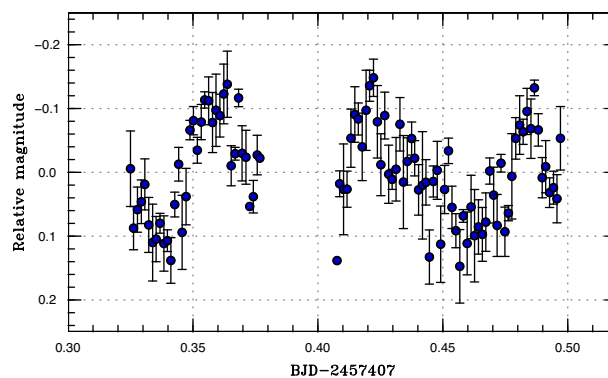


Fig. 55. Possible superhumps in ASASSN-16ao (2016). The data were binned to 0.0015 d. (Color online)

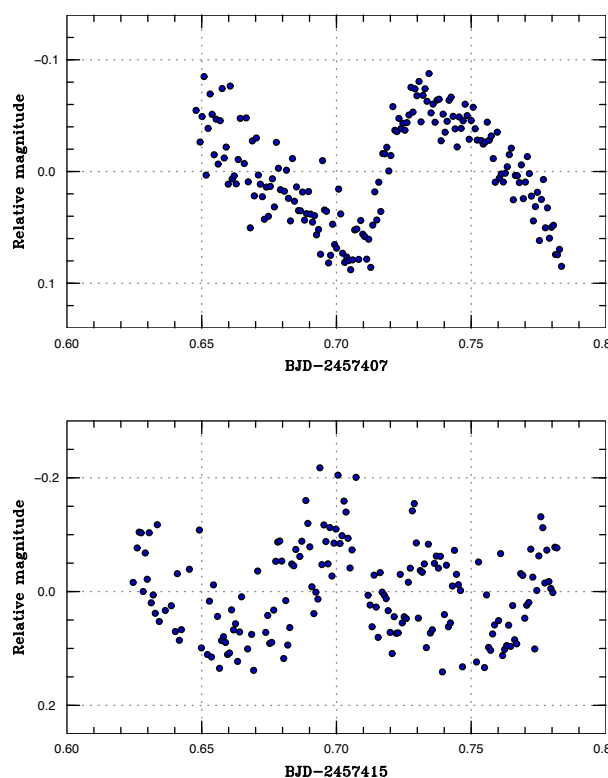


Fig. 56. Superhumps in ASASSN-16aq (2016). (Color online)

superhump maxima were detected: BJD 2457407.7398(6) ($N=97$) and 2457415.7009(20) ($N=83$). Since there was a long gap of observations between these two maxima, we could not choose an unambiguous period. The light curve suggests that the period is relatively longer (longer than 0.08 d). This period is, however, too long for a WZ Sge-type dwarf nova and the object may be a kind of large-amplitude, long- P_{orb} SUUMa-type dwarf novae such as V1251 Cyg or RZ Leo (see Kato 2015).

3.104 ASASSN-16bh

This object was detected as a transient at $V = 12.7$ on 2016 February 6 by the ASAS-SN team (Simonian et al. 2016). The object was suspected to be a WZ Sge-type dwarf nova based on the large (~ 8 mag) outburst amplitude. Early observations detected low-amplitude modulations, which were suspected to be early superhumps (vsnet-alert 19476, 19479). After the development of ordinary superhumps, the period of early superhumps was established (vsnet-alert 19513). In e-figure 72, we show the mean profile of early superhumps using the high-quality data from the southern hemisphere (B. Monard). The best period with the PDM method was $0.05346(2)$ d. It is noteworthy that the profile has three peaks in one cycle (in contrast to two peaks in many WZ Sge-type dwarf novae, cf. Kato 2015).

Ordinary superhumps then appeared (vsnet-alert 19484, 19513, 19520, 19521; e-figure 73). The times of superhump maxima are listed in e-table 89. The maxima for $E \leq 15$ were very clearly stage A superhumps. After $E = 206$ (rapid fading phase), there was probably a phase jump. Similar phenomena were recorded in other WZ Sge-type dwarf novae (e.g., GW Lib: figur 33 in Kato et al. 2009; FL Psc = ASASJ002511+1217.2: figure 34 in Kato et al. 2009; V355 UMa: figure 43 in Kato et al. 2012).

The object rapidly faded from the superoutburst plateau on February 25. This fading was actually a “dip” seen in many WZ Sge-type dwarf novae (Kato 2015) (see figure 57). The object brightened again on February 28 (vsnet-alert 19536) and this rebrightening was a plateau-type one without major fluctuations (vsnet-alert 19567). On March 9, the object rapidly faded from the rebrightening phase (vsnet-alert 19569). During the rebrightening phase, superhumps were present and grew in amplitudes (figure 57). The times of superhump maxima during the rebrightening phase are listed in e-table 90, although the data were rather noisy due to the faintness. The superhumps, however, were very apparent on March 6 (BJD 2457454), the final night before the rapid fading. The mean period of the superhumps during the rebrightening phase was determined to be $0.05389(3)$ d with the PDM method (e-figure 74).

The resultant ϵ^* for stage A superhumps was $0.0283(3)$, corresponding to $q = 0.076(1)$. Using the relation between P_{dot} and q in equation (6) in Kato (2015), we can obtain $q = 0.076(6)$, consistent with that from stage A superhumps.

It took 7 d from the outburst detection to the emergence of ordinary superhumps for this object. This value is relatively short among WZ Sge-type dwarf novae, particularly among objects with type-A rebrightenings (see figure 18 in Kato 2015). Since the gap in the ASAS-SN data before the outburst detection was very short, this delay in the appearance of superhumps should not exceed 9 d.

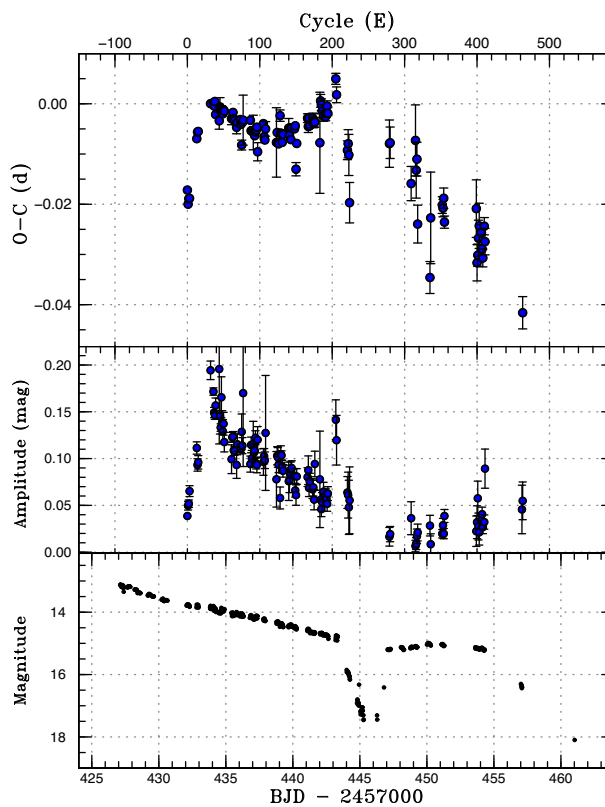


Fig. 57. $O - C$ diagram of superhumps in ASASSN-16bh (2016). Upper: $O - C$ diagram. We used a period of 0.05403 d for calculating the $O - C$ residuals. Middle: Amplitudes of superhumps. Lower: Light curve. The data were binned to 0.017 d. (Color online)

We can estimate the disk radius during the rebrightening using the superhump period as shown in subsection 4.3 in Kato and Osaki (2013b). The mean superhump period during the rebrightening phase gives ϵ^* of $0.0080(7)$. This value corresponds to a radius of $0.26(2)a$, where a is the binary separation, if we can ignore the pressure effect. This value is small compared to the values ($0.30a - 0.38a$) in the post-outburst state of WZ Sge-type dwarf novae (Kato & Osaki 2013b). Although a pressure effect may have reduced ϵ^* and give a systematically small disk radius, it is likely that the disk radius during the plateau-type rebrightening was indeed small.

The object resembles AL Com (cf. Howell et al. 1996; Kato et al. 1996a; Patterson et al. 1996; Nogami et al. 1997; Ishioka et al. 2002) in many respects. The apparent brightness may even qualify this object to be the southern counterpart of AL Com. Since the superoutbursts in AL Com appear to have some degree of diversity (cf. Uemura et al. 2008; Kimura et al. 2016a), further monitoring for outbursts and time-resolved photometry during each superoutburst will be rewarding. Photometry and spectroscopy in quiescence to determine the exact orbital period are also desired.

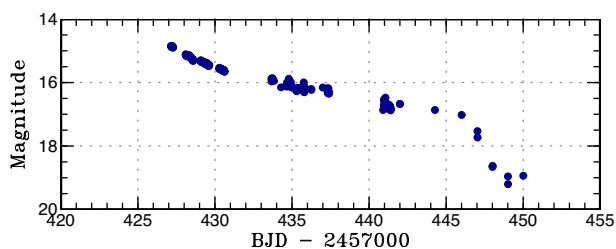


Fig. 58. Light curve of the superoutburst of ASASSN-16bi (2016). The data were binned to 0.01 d. The ASAS-SN detection corresponds to BJD 2457424.53. (Color online)

3.105 ASASSN-16bi

This object was detected as a transient on the rise from $V = 15.2$ to $V = 14.3$ on 2016 February 6 by the ASAS-SN team. The object was also detected by Gaia as Gaia16ads on February 13.¹⁷ Although an $R = 20.6$ star was initially suggested to be the quiescent counterpart, it is $6''$ from the Gaia position and is unlikely the counterpart. The large outburst amplitude suggested a possible WZ Sge-type dwarf nova. Early observations detected double-wave early superhumps (vsnet-alert 19514; e-figure 75). The best period found with the PDM method is 0.05814(5) d. Although emerging ordinary superhumps were detected (vsnet-alert 19519), the period was not well determined due to the faintness of the object. The only available superhump maxima are BJD 2457437.2963(33) $N = 39$ and 2457437.3571(8) $N = 61$. The outburst light curve is shown in figure 58. The phase of early superhumps lasted at least for 6 d, if it started immediately after the outburst detection. The entire duration of the superoutburst was 23 d.

3.106 ASASSN-16bu

This object was detected as a transient at $V = 14.5$ on 2016 February 15 by the ASAS-SN team (vsnet-alert 19491). The large outburst amplitude suggested a possible WZ Sge-type dwarf nova (cf. vsnet-alert 19500). After nine nights, ordinary superhumps emerged (vsnet-alert 19525; e-figure 76). The times of superhump maxima are listed in e-table 91. The maxima for $E \leq 30$ are clearly stage A superhumps with growing amplitudes. An analysis of the earlier part of the observation yielded a weak signal of possible early superhumps (e-figure 77). The period with the PDM method was 0.05934(13) d. By using this period and the period of stage A superhumps, the value of $\epsilon^* = 0.037(4)$. This value corresponds to $q = 0.10(1)$. Since the periods of early superhumps and stage A superhumps were not very well determined, this q value needs to be treated with caution. The other features of the behavior, including the slow growth

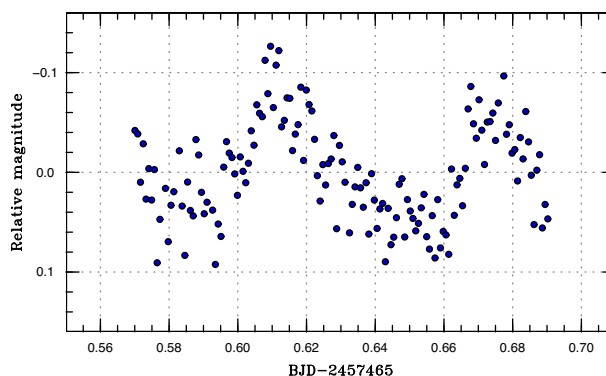


Fig. 59. Superhumps in ASASSN-16de (2016). (Color online)

of ordinary superhumps and small amplitudes of superhumps, likely suggest a low q comparable to that of a period bouncer (Kato 2015).

3.107 ASASSN-16de

This object was detected as a transient at $V = 14.5$ on 2016 March 17 by the ASAS-SN team (vsnet-alert 19491). The object was probably in outburst in USNO-A2.0 at $B = 16.1$. A blue object is present in SDSS images, but it is not listed in Abazajian et al. (2009). Subsequent observations detected superhumps (vsnet-alert 19610; figure 59). This observation on the first night gave a period of 0.063(1) d (PDM method). The times of superhump maxima were BJD 2457465.6155(8) ($N = 60$) and 2457465.6774(7) ($N = 46$). Although the object was observed on five nights in the late stage of the superoutburst (6 d after the initial observation of superhumps), the superhump signal was too weak to determine the period. The object faded rapidly on March 28, 11 d after the outburst detection.

3.108 CRTS J081936.1+191540

This object (hereafter CRTS J081936) was confirmed to be an SUUMa-type dwarf nova on its outburst in 2013 (Kato et al. 2015a). Another superoutburst was detected on 2015 March 10 by the ASAS-SN team (vsnet-alert 18411). Two superhump maxima were measured: BJD 2457093.4786(13) ($N = 85$) and 2457093.5492(18) ($N = 79$).

3.109 CRTS J095926.4-160147

This object (= CSS110226:095926-160147, hereafter CRTS J095926) was detected as a transient by CRTS on 2011 February 26. Five outbursts were recorded in the CRTS data up to 2013 July.

¹⁷ (<http://gsaweb.ast.cam.ac.uk/alerts/alert/Gaia16ads/>).

The 2015 outburst was detected on May 14 by the ASAS-SN team (vsnet-alert 18622). Our observations, starting two nights later, detected superhumps (vsnet-alert 18628, 18633, 18648; e-figure 78). The times of superhump maxima are listed in e-table 92. Although it was initially difficult to distinguish 1-d aliases due to the short observing time, observations at two different longitudes established the alias selection (vsnet-alert 18648). It is possible that maxima for $E \leq 12$ correspond to stage A superhumps since there was a large decrease in the period (by 1.5%) around $E = 11$. If it is the case, stage A in this system likely lasted more than 3 d.

3.110 CRTS J120052.9–152620

This object (= CSS110205:120053–152620, hereafter CRTS J120052) was discovered by the CRTS on 2011 February 5. The 2011 superoutburst was observed only on two nights and the analysis was reported in Kato et al. (2012). Due to the lack of observations, there remained ambiguity in selecting the superhump period (Kato et al. 2012).

The 2016 superoutburst was detected by the ASAS-SN team at $V = 13.78$ on March 14 (cf. vsnet-alert 19590). Subsequent observations detected superhumps (vsnet-alert 19609, 19618; e-figure 79). The times of superhump maxima are listed in e-table 93. These observations recorded the relatively late phase of the superoutburst and these superhumps may be of stage C. In table 3, we give a mean period.

Thanks to the new observation, it has become evident that an alias different from that reported in Kato et al. (2012) was the correct superhump period during the 2011 superoutburst (vsnet-alert 19618). The corrected period for the 2011 superoutburst based on this identification is 0.08882(3) d.

3.111 CRTS J163120.9+103134

This object (= CSS080505:163121+103134, hereafter CRTS J163120) was detected as a transient by CRTS on 2008 May 5. Refer to Kato et al. (2009) for the history. The 2008 and 2010 superoutbursts were reported in Kato et al. (2009) and Kato et al. (2010), respectively.

The 2015 superoutburst was detected by the ASAS-SN team (cf. vsnet-alert 18603) and superhumps were observed on single night (e-table 94). The period found via the PDM method is listed in table 3.

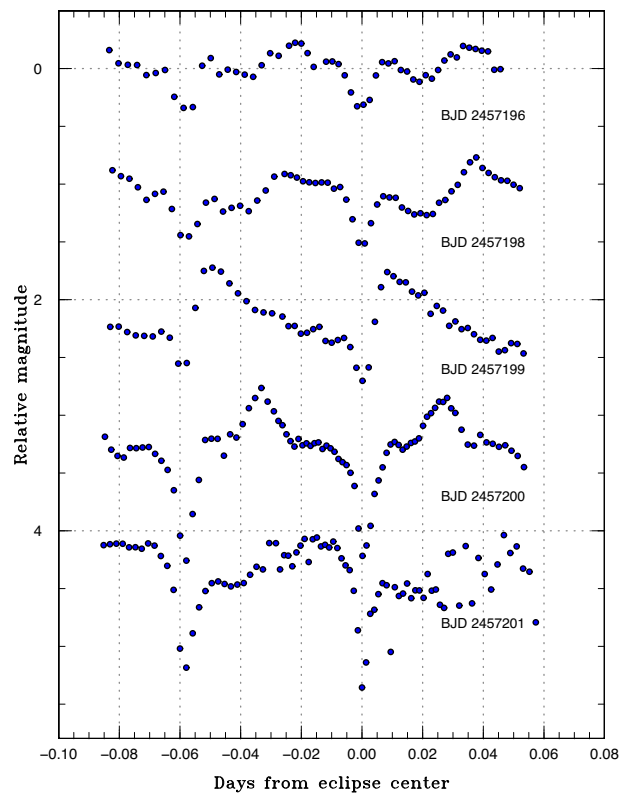


Fig. 60. Light curve of CRTS J200331 on the first five nights. Superposition of growing superhumps and eclipses are well visible. (Color online)

3.112 CRTS J200331.3–284941

This object (= SSS100615:200331–284941, hereafter CRTS J200331) was discovered by the CRTS Siding Spring Survey (SSS) on 2010 June 15. Since the 2010 outburst had a fading tail resembling those of WZ Sge-type dwarf novae (cf. vsnet-alert 18763), the object received special attention.

The 2015 outburst, the second known outburst of this object, was detected by the ASAS-SN team on June 20 at $V = 14.84$. The initial observation revealed that this object is an eclipsing SUUMa-type (or WZ Sge-type) dwarf nova (vsnet-alert 18788). The eclipses became clearer as the outburst proceeded and we have obtained the eclipse ephemeris by using MCMC analysis (Kato et al. 2013a) of the present observations:

$$\text{Min(BJD)} = 2457200.79900(6) + 0.0587048(3)E. \quad (4)$$

This ephemeris is not intended for long-term prediction of eclipses.

The object showed growing superhumps up to June 26 (figure 60) and the object significantly brightened after this epoch. Before June 26 superhumps with a long period of 0.06058(2) d were observed (note that the period reported in vsnet-alert 18798 referred to this period). We identified them to be stage A superhumps. On the three subsequent

nights, stable superhumps were recorded, which we identified to be stage B superhumps. The times of superhump maxima are listed in e-table 95. The cycle count between $E=84$ and $E=250$ was ambiguous. The period of stage A superhumps corresponds to $q=0.084(1)$, which is close to those of WZ Sge-type dwarf novae (Kato 2015). The duration of stage A superhumps (more than 50 cycles) is also long, consistent with the small q . All the pieces of evidence suggest that this object is located near the borderline of SUUMa-type and WZ Sge-type objects. Since our initial observation started 3 d after the ASAS-SN detection, it was not clear whether there were early superhumps before this observation. We can, however, probably rule out the long-lasting (more than 10 d) phase of early superhumps seen in typical WZ Sge-type dwarf novae.

This object is probably the first one in which the period of stage A superhumps were sufficiently measured in a deeply eclipsing system. Determination of system parameters in quiescence using eclipse modeling in such a system would provide a direct test for our method of q determination using stage A superhumps (cf. Kato & Osaki 2013b).

3.113 CRTS J212521.8–102627

This object (= CSS080927:212522–102627, hereafter CRTS J212521) was discovered by CRTS on 2008 September 27. There were at least six outbursts (up to 2013 September) in the CRTS data.

The 2015 outburst was detected by the ASAS-SN team on August 23 at a magnitude of $V=15.0$. Since the past outbursts recorded in the ASAS-SN data resembled superoutbursts, an SUUMa-type dwarf nova was suspected (vsnet-alert 19000). Observations soon recorded superhumps (vsnet-alert 19006, 19010; e-figure 80). The times of superhump maxima are listed in e-table 96. Although the basic superhump period was determined to be $0.0791(1)$ d from the observations on the first two nights, the cycle count is ambiguous between $E=26$ and $E=100$. The maxima for $E \geq 100$ may represent stage C superhumps. We list a period in table 3 that is only based on the initial two nights.

3.114 CRTS J214738.4+244554

This object (= CSS111004:214738+244554, hereafter CRTS J214738) was discovered by CRTS on 2011 November 4 (Breedt et al. 2014). The 2011 and 2014 superoutbursts were reported in Kato et al. (2013a) and Kato et al. (2015a), respectively.

The 2015 superoutburst was visually detected by C. Chiselbrook on December 15 (cf. vsnet-alert 19351). Only one superhump maximum was recorded: BJD 2457376.8752(4) ($N=84$).

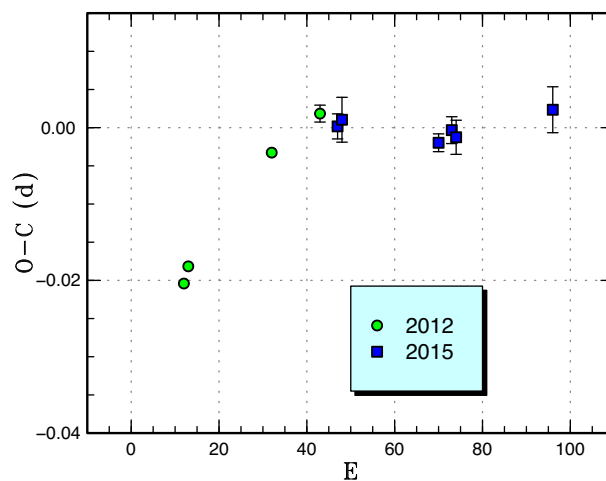


Fig. 61. Comparison of $O-C$ diagrams of DDE 26 between different superoutbursts. A period of 0.08860 d was used to draw this figure. Approximate cycle counts (E) after the outburst detections were used. The actual starts of the outbursts were unknown. (Color online)

3.115 CSS J221822.9+344511

This object (hereafter CSS J221822) was originally discovered by CRTS (CSS120812:221823+344509) as a suspected dwarf nova on 2012 August 12 at an unfiltered CCD magnitude of 15.85. There is an X-ray counterpart (1RXS J221823.7+344507).

The 2015 outburst was detected by the ASAS-SN team on October 1 at $V=15.42-15.24$ (two measurements). Subsequent observations detected superhumps (vsnet-alert 19109, 19110, 19118, 19188; e-figure 81). The times of superhump maxima are listed in e-table 97.

3.116 DDE 26

DDE 26 is a dwarf nova discovered by Denisenko (2012). See Kato et al. (2014a) for more information. The 2015 outburst was detected by the ASAS-SN team at $V=15.7$ on December 1 (cf. vsnet-alert 19311, 19320). Subsequent observations detected superhumps (vsnet-alert 19324, 19331). The times of superhump maxima are listed in e-table 98. A comparison of $O-C$ diagrams (figure 61) indicates that the superhump period was longer in 2012. It may be possible that the 2012 observations recorded stage A superhumps, since some long- P_{orb} systems are known to show long-lasting stage A (e.g., Kato et al. 2016a; subsection 4.4). This interpretation, however, does not agree with the large amplitudes of superhumps during the 2012 observation. More observations are needed to clarify the superhump variation in this system.

3.117 IPHAS J230538.39+652158.7

This object (hereafter IPHAS J230538) was detected as an H α emission line object in the INT/WFC Photometric H α Survey (IPHAS: Witham et al. 2008). The first known outburst was detected on 2015 June 4 by the ASAS-SN team (cf. vsnet-alert 18690). The object was still rising (vsnet-alert 18695) and growing superhumps were detected (vsnet-alert 18702, 18709). Further evolution of superhumps was observed (vsnet-alert 18715, 18730, 18789; e-figure 82). The times of superhump maxima are listed in e-table 99. Although observations were rather sparse, we could identify stages A–C.

3.118 MASTER OT J003831.10–640313.7

This object (hereafter MASTER J003831) was detected as a transient at an unfiltered CCD magnitude of 12.7 on 2016 January 26 by the MASTER network (Gress et al. 2016a). Although Gress et al. (2016a) suggested either a CV or a BL Lac-type object, the presence of several past outbursts in the ASAS-3 data confirmed the dwarf nova-type classification (vsnet-alert 19443). There is a GALEX counterpart with an NUV magnitude of 18.9(1). Subsequent observations detected superhumps (vsnet-alert 19449, 19454, 19467; e-figure 83). The times of superhump maxima are listed in e-table 100. There are clear stages B and C, with a strongly positive P_{dot} characteristic to this P_{SH} . The object showed a post-superoutburst rebrightening on February 15 (vsnet-alert 19508).

3.119 MASTER OT J073325.52+373744.9

This object (hereafter MASTER J073325) was detected as a transient at an unfiltered CCD magnitude of 15.1 on 2016 February 24 by the MASTER network (Gress et al. 2016b). There was at least one outburst in the CRTS data (15.9 mag on 2008 January 31, vsnet-alert 19528). Subsequent observations immediately detected growing superhumps (vsnet-alert 19532, 19537; e-figure 84). The times of superhump maxima are listed in e-table 101. The maxima for $E \leq 19$ were undoubtedly stage A superhumps as judged from the $O - C$ values and growing amplitudes. The likely positive P_{dot} for stage B is typical for this P_{SH} and the early appearance of (ordinary) superhumps indicates that this object is an ordinary SU UMa-type dwarf nova rather than a WZ Sge-type dwarf nova as suspected from the large outburst amplitude (Gress et al. 2016b). The presence of a past outburst is consistent with this identification.

3.120 MASTER OT J120251.56–454116.7

This object (hereafter MASTER J120251) was detected as a transient at an unfiltered CCD magnitude of 16.0 on 2015 March 15 by the MASTER network (Gress et al. 2015a). This object was also detected at $V = 16.7$ on 2015 March 15 by the ASAS-SN team (= ASASSN-15fp; Danilet et al. 2015). The object faded to fainter than $V = 17.5$ on March 18 and then brightened to $V = 14.4$ on March 20 (Danilet et al. 2015). Superhumps were immediately detected (vsnet-alert 18483, 18486, 18499; e-figure 85). The times of superhump maxima are listed in e-table 102. Due to the 4-d gap in the observation, we were not able to identify the stage classification and give a global value in table 3. The initial part ($E \leq 27$) probably recorded stage B superhumps.

3.121 MASTER OT J131320.24+692649.1

This object (hereafter MASTER J131320) was detected as a transient at an unfiltered CCD magnitude of 14.7 on 2013 May 14 by the MASTER network (Denisenko et al. 2013a). There is a GALEX counterpart with an NUV magnitude of 20.6(2). Two more outbursts were recorded between 2014 and 2015 in the ASAS-SN data. The 2016 outburst was detected on February 15 at $V = 15.01$ by the ASAS-SN team (cf. vsnet-alert 19505). Subsequent observations detected superhumps (vsnet-alert 19511; e-figure 86). The times of superhump maxima are listed in e-table 103. Although we selected the alias period to minimize absolute $O - C$ residuals, the superhump amplitudes were significantly smaller on the first night. It was possible that the stage A superhumps were recorded on the initial night. If there was a strong variation in the period between two nights, our method may have failed to select the correct period. Although there was no indication of such a strong variation in the $O - C$ values, the period should be treated with caution.

3.122 MASTER OT J181523.78+692037.4

This object (hereafter MASTER J181523) was detected as a transient at an unfiltered CCD magnitude of 15.7 on 2015 August 28 by the MASTER network (Gress et al. 2015b). There is a GALEX counterpart with an NUV magnitude of 22.8(5). Superhumps were soon detected (vsnet-alert 19026, 19041; e-figure 87). The times of superhump maxima are listed in e-table 104.

3.123 MASTER OT J212624.16+253827.2

This object (hereafter MASTER J212624) was detected as a transient at an unfiltered CCD magnitude of 14.1 on

2013 June 26 by the MASTER network (Denisenko et al. 2013b). The 2013 superoutburst was well observed and a large positive P_{dot} despite the long P_{SH} was detected (Kato et al. 2014a). For more information, see Kato et al. (2014a).

The 2015 superoutburst was detected by the ASAS-SN team at $V = 14.24$ on August 27 (cf. vsnet-alert 19012). Our observation on September 1 recorded superhumps (vsnet-alert 19031). The times of superhump maxima are listed in e-table 105. Since the observation was 5 d after the outburst detection, our observation did not cover the early part of the superoutburst. Although the 2013 observation started 2 d after the outburst detection, it may have not been detected sufficiently early. Our present observations were insufficient to verify the large positive P_{dot} . Further observations, particularly in the early phase, are still needed.

3.124 N080829A

This object was originally reported as a transient by H. Mikuz on 2008 August 29 at $R = 15.98(4)$ (vsnet-alert 10485). The object was observed at around $R = 16.3$ on August 31.

The 2015 outburst was detected by CRTS on October 12 at an unfiltered CCD magnitude of 15.98. Subsequent observations detected superhumps (vsnet-alert 19162, 19164, 19167, 19169; e-figure 88). The times of superhump maxima are listed in e-table 106. The strongly positive P_{dot} is typical for stage B superhumps with this superhump period.

3.125 OT J191443.6+605214

This object (hereafter OTJ191443) was discovered by K. Itagaki (Yamaoka et al. 2008). The 2008 superoutburst was studied in Boyd et al. (2009) and Kato et al. (2009). See Kato et al. (2014a) for more history.

The 2015 outburst was detected by the ASAS-SN team on July 24. The outburst detection was probably early enough and initial observations detected low-amplitude stage A superhumps (vsnet-alert 18887). The times of superhump maxima are listed in e-table 107. Although the maxima for $E \leq 1$ were stage A superhumps, we could not determine the period of stage A superhumps (see also figure 62 for the comparison of $O - C$ diagrams).

3.126 SDSS J074859.55+312512.6

This object (hereafter SDSSJ074859) is a dwarf nova selected by Wils et al. (2010). The 2015 outburst was detected by CRTS on November 20 at an unfiltered CCD magnitude of 15.86 (cf. vsnet-alert 19292). There were frequent outbursts in past CRTS data. Observations on

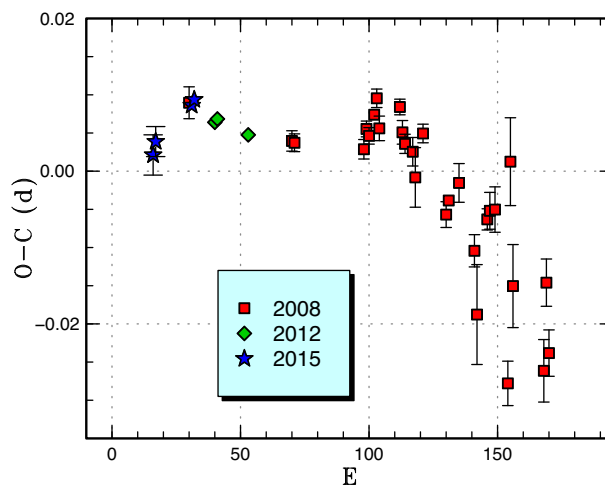


Fig. 62. Comparison of $O - C$ diagrams of OT J191443 between different superoutbursts. A period of 0.07138 d was used to draw this figure. Approximate cycle counts (E) after the start of the superoutburst were used. Since the starts of the 2008 and 2012 superoutbursts were not well constrained, we shifted the $O - C$ diagrams to fit the 2015 one, whose cycle counts are considered to be best determined. (Color online)

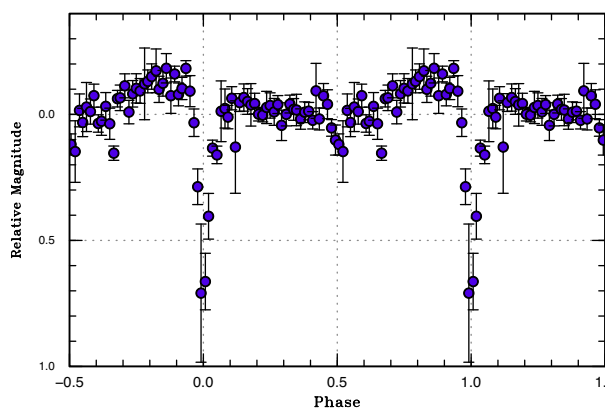


Fig. 63. Mean orbital light curve SDSS J074859. The CRTS data and our observations are used. The ephemeris of equation (5) is used. (Color online)

November 24 detected eclipses and an analysis of the CRTS data combined with the new data yielded the following ephemeris (vsnet-alert 19297):

$$\text{Min(BJD)} = 2457351.21283(2) + 0.0583110901(7)E.$$

(5)

The orbital light curve (figure 63) indicates deep eclipses and pre-eclipse orbital humps. These features, combined with the short orbital period, suggest that this object is an eclipsing SU UMa-type dwarf nova. Although we could not determine individual superhump maxima, a PDM analysis yielded a superhump period of 0.05958(3) d, 2.1% longer than the orbital period (e-figure 89). This period is listed in table 3.

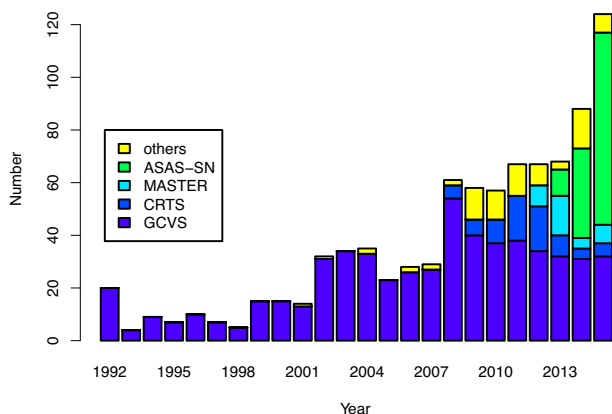


Fig. 64. Object categories in our survey. Superoutbursts with measured superhump periods are included. The year represents the year of outburst. The year 1992 represents outbursts up to 1992 and the year 2015 includes the outbursts in 2016. The category GCVS includes the objects named in the General Catalog of Variable Stars (Kholopov et al. 1985) in the latest version and objects named in New Catalog of Suspected Variable Stars (NSV; Kukarkin et al. 1982). The categories CRTS, MASTER, and ASAS-SN represent objects which were discovered in those respective surveys. A small fraction of objects discovered by these surveys are already named in GCVS and are included in the category GCVS. (Color online)

3.127 SDSS J145758.21+514807.9

This object (hereafter SDSS J145758) is a CV selected by Szkody et al. (2005). The spectrum in Szkody et al. (2005) strongly suggested a dwarf nova with a very low mass-accretion rate. The object was found to contain a pulsating white dwarf as in GW Lib (Uthas et al. 2012). The object has a photometric orbital period of 0.054087(5) d (Uthas 2011). No previous outburst was known.

J. Shears detected the first known outburst on 2015 September 29 at an unfiltered CCD magnitude of 15.3 (vsnet-outburst 18727). The object’s magnitude rose further, to 11.9 (visual magnitude) on September 30 (vsnet-alert 19097, 19098). Subsequent observations detected double-wave early superhumps (vsnet-alert 19100, 19103; e-figure 90). The period of early superhumps was shorter than the orbital period by 0.07(2)%, confirming the relation reported for other WZ Sge-type dwarf novae (Kato 2015).

Due to the short visibility in the evening sky, the development of ordinary superhumps was not well observed. Ordinary superhumps were confidently detected only during the final stage of the plateau phase (vsnet-alert 19187; e-figure 91). The object started fading rapidly 3 d after these observations of ordinary superhumps. The times of maxima of ordinary superhumps are listed in e-table 108. The maxima for $E \geq 181$ refer to superhumps during the rapid fading and they were not used in determining the superhump period in table 3. No post-superoutburst observations were available and it was not known whether this

fading was a “dip” as in other WZ Sge-type dwarf novae or not.

3.128 SDSS J164248.52+134751.4

This object (hereafter SDSS J164248) is a CV selected by Szkody et al. (2009). Szkody et al. (2009) suggested an orbital period of 1.3 hr. Southworth et al. (2008) obtained a spectroscopic orbital period of 0.07889(11) d and also reported Doppler tomography with an unusual brightness distribution in the accretion disk. Despite one well-recorded outburst detection at an unfiltered CCD magnitude of 14.7 in the CRTS data, there had not been any outbursts until 2012 September 6, when E. Muylaert recorded an outburst at an unfiltered CCD magnitude of 15.9 (cvnet-outburst 4910). This 2012 outburst quickly faded.

The 2016 outburst was detected at $V=15.46$ by the ASAS-SN team (cf. vsnet-alert 19575). Subsequent observations detected superhumps (vsnet-alert 19582, 19593; e-figure 92). The times of superhump maxima are listed in e-table 109. Since the superhump period of 0.07928(2) d is too close to the suggested orbital period, this orbital period does not seem to have been well determined. It is likely that the baseline for the spectroscopic observations was not sufficient to obtain an accurate orbital period. For this reason, we did not include this orbital period in table 3.

4 Discussion

4.1 Statistics of objects

In Kato et al. (2015a), we introduced the statistics of the sources of the objects studied in our surveys and noticed the rapid increase of the objects registered as ASAS-SN CVs. Several dwarf novae received new variable star designations in the latest updates of the General Catalog of Variable Stars (Kazarovets et al. 2015a, 2015b) since Kato et al. (2015a), and these newly named objects are included in the GCVS category. The tendency pointed out in Kato et al. (2015a) became more prominent and roughly two thirds of the objects studied in this survey are now ASAS-SN CVs (figure 64). The present GCVS names appear to be almost complete discoveries up to 2008 in the literature (dwarf novae reported in IAUCs and CBETs appear to be designated more quickly than other literature) and it is hoped that the GCVS team could give more final designations to newly discovered dwarf novae.

4.2 Period distribution

In figure 65, we give distributions of superhump and estimated orbital periods (see the caption for details) since

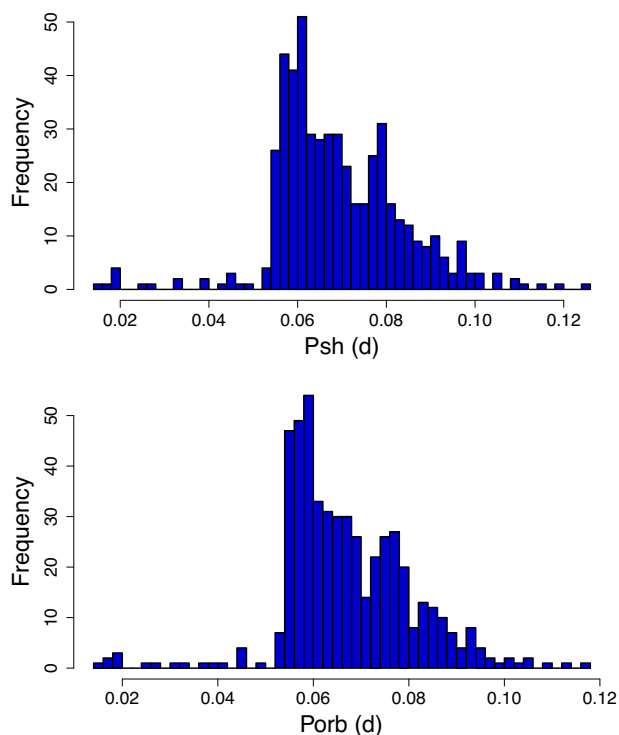


Fig. 65. Distribution of superhump periods in this survey. The data are from Kato et al. (2009, 2010, 2012, 2013a, 2014a, 2014b, 2015a), and this paper. The mean values are used when multiple superoutbursts were observed. The number of objects is 511. Upper: Distribution of superhump periods. Lower: Distribution of orbital periods. For objects with superhump periods shorter than 0.053 d, the orbital periods were assumed to be 1% shorter than superhump periods. For objects with superhump periods longer than 0.053 d, we used the calibration in Kato et al. (2012) to estimate orbital periods. (Color online)

Table 6. Ephemerides of eclipsing systems.

Object	Epoch (BJD)	Period (d)
V2051 Oph	2453189.48679(1)	0.0624278552(2)
ASASSN-15sl	2457341.23671(7)	0.0870484(7)
ASASSN-15ux	2457400.82908(10)	0.056109(2)
CRTS J200331	2457200.79900(6)	0.0587048(3)
SDSS J074859	2457351.21283(2)	0.0583110901(7)

Kato et al. (2009). For readers' convenience, we also list in table 6 new ephemerides of eclipsing systems newly determined or updated in this study. When there are multiple observations of superoutbursts of the same object, we adopted an average of the measurements. Since most non-magnetic CVs below the period gap are considered to be SUUMa-type dwarf novae, this distribution reflects the distribution of non-magnetic CVs below the period gap. As already pointed out in Kato et al. (2015a), the sharp cut-off at a period of 0.053 d (the objects below this period are either AM CVn-type systems or EI Psc-type objects) and the apparent absence of the strong signature of the lower

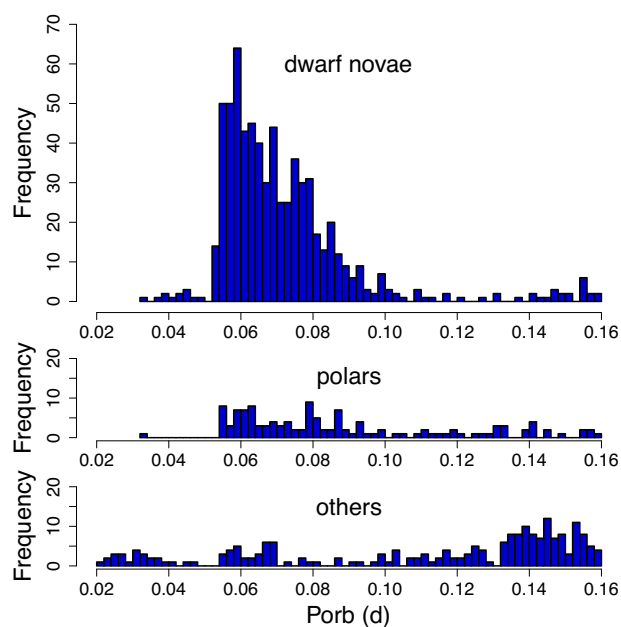


Fig. 66. Distribution of orbital periods in the latest version of RKCAt (Ritter & Kolb 2003; Edition 7.23, 2015 June 30). The three histograms represent distributions of dwarf novae (DN in RKCAt), polars (AM in RKCAt) and others. The number of dwarf novae in the region of 0.02–0.12 d (corresponding to figure 65) is 676. (Color online)

edge of the period gap are even more apparent. The updated statistics confirms the findings in Kato et al. (2015a). The same statistics using the latest version of RKCAt (Ritter & Kolb 2003; Edition 7.23, 2015 June 30) are shown in figure 66. The result confirms the general trend seen in our sample, although it is not surprising since more than half the dwarf novae in this P_{orb} region in RKCAt are from our surveys. The disrupted magnetic braking may be weaker or more CVs may be formed in the period gap than had been supposed.

4.3 Period derivatives during stage B

Figure 67 represents the updated relation between P_{dot} for stage B versus P_{orb} . Although this is essentially an updated version of the corresponding figures in the earlier papers of this series, we have omitted poor-quality observations (quality C) and simplified the symbols. The object listed in this paper with large negative P_{dot} is PM J03338, which had a separate precursor and a long stage A (Kato et al. 2016b). Other objects with large negative P_{dot} in earlier papers are UV Gem (2003), PUUMa (2012), and CYUMa (2014). UV Gem is famous for the large negative P_{dot} and it is possibly interpreted as a stage A–B transition rather than period variation during stage B (cf. Kato et al. 2016a). PUUMa is an eclipsing object and the P_{dot} determination may have suffered from the beat phenomenon. In CYUMa

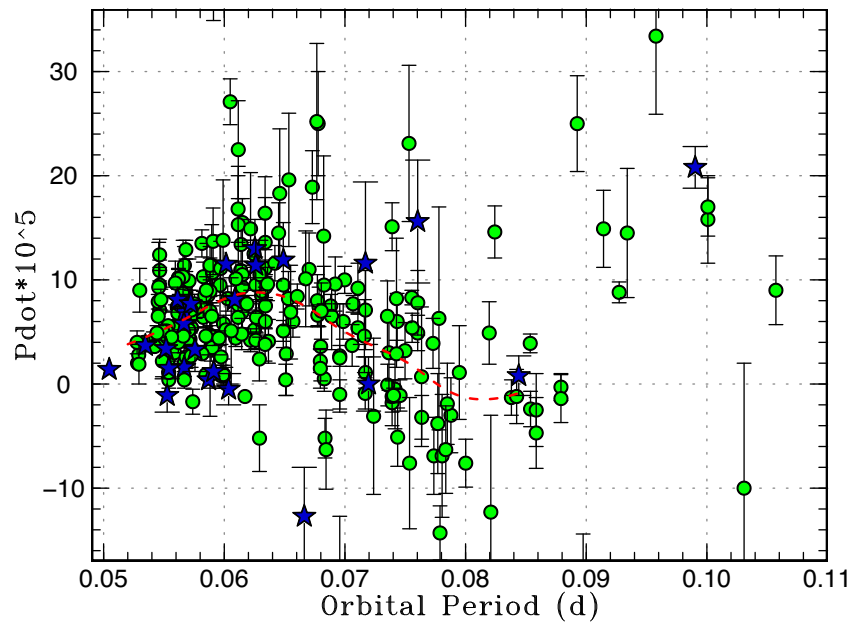


Fig. 67. P_{dot} for stage B versus P_{orb} . Filled circles and filled stars represent samples in Kato et al. (2009, 2010, 2012, 2013a, 2014a, 2014b, 2015a), and this paper, respectively. The curve represents the spline-smoothed global trend. (Color online)

Table 7. Comparison of SU UMa-type objects with long phase of stage A superhumps.

Object	P_{orb}^*	P_A^\dagger	P_B^\ddagger	P_C^\S	Duration	$q^\#$	Ref.**
V1006 Cyg (2015)	0.09903(9)	0.1093(3)	0.10541(4)	0.10444(5)	≥ 32	0.34(2)	(1)
MN Dra (2012)	0.0998(2)	0.10993(9)	0.10530(6)	–	≥ 39	0.327(5)	(2)
MN Dra (2013)	0.0998(2)	0.1082(1)	0.10504(7)	–	≥ 18	0.258(5)	(2)
CRTS J214738.4+244554 (2011)	0.09273(3)	0.0992(3)	0.09715(2)	–	≥ 21	0.204(11)	(3)
OT J064833.4+065624 (2014)	–	0.1052(4)	0.10033(3)	–	≥ 38	–	(3)
V452 Cas (2007)	–	0.08943(7)	0.08869(2)	–	20–35	–	(4)
KK Tel (2015)	–	0.09005(12)	0.08761(2)	–	≥ 25	–	(4)
ASASSN-15cl (2016)	–	0.0961(3)	0.09463(10)	0.09391(7)	≥ 22	–	(4)

*Orbital period (d).

[†]Period of stage A superhumps (d).

[‡]Period of stage B superhumps (d).

[§]Period of stage C superhumps (d).

^{||}Duration of stage A (cycles).

[‡]Determined from stage A superhumps.

**References: (1) Kato et al. (2016a); (2) Kato et al. (2014b); (3) Kato et al. (2015a); (4) This work.

(2014), the stage transition was rather smooth and it was difficult to define the border of stage B. These outliers have their own reasons for being outside the distribution of the majority of objects, and the main trends in this figure seem to apply to most ordinary superoutbursts.

4.4 Long-period objects with long-lasting stage A

It had been known that some long- P_{orb} systems show a strong decrease in the superhump periods [cf. MN Dra and UV Gem, see subsection 4.10 in Kato et al. (2009)]. Although the origin of this strong period variation had remained a mystery, Kato et al. (2014b) proposed a working

hypothesis that these strong period variations are a result of the combination of stages A and B. This interpretation requires that stage A in these systems is unusually long. In Kato et al. (2014b), the case of MN Dra was studied, which lacked the spectroscopically determined orbital period. Kato et al. (2016a) presented a more convincing example of V1006 Cyg, whose orbital period had been determined spectroscopically. It appears to have been established that at least some long- P_{orb} systems show a long-lasting stage A, which implies that the 3:1 resonance grows slowly in these systems. Kato et al. (2014b, 2016a) suggested that the mass ratios close to the borderline of the 3:1 resonance is responsible for this phenomenon.

Table 8. New estimates for the binary mass ratio from stage A superhumps.

Object	ϵ^* (stage A)	q from stage A
V1006 Cyg	0.094(3)	0.34(2)
V493 Ser	0.0449(13)	0.129(5)
ASASSN-15gq	0.038(2)	0.107(8)
ASASSN-15hd	0.028(4)	0.076(12)
ASASSN-15na	0.030(2)	0.081(5)
ASASSN-15ni	0.0027(2)	0.074(2)
ASASSN-15po	0.0251(5)	0.067(2)
ASASSN-15pu	0.028(5)	0.074(16)
ASASSN-15uj	0.0243(13)	0.064(4)
ASASSN-16bh	0.0283(3)	0.076(1)
ASASSN-16bu	0.037(4)	0.10(1)
CRTS J200331	0.0310(2)	0.084(1)
PM J03338	0.0604(13)	0.172(4)

An updated list of long- P_{orb} SUUMa-type objects with long phase of stage A superhumps is given in table 7. For V452 Cas, we used the best observed superoutburst (2007) in Shears et al. (2009) and modified the superhump stages listed in Kato et al. (2009) according to the modern interpretation (see also subsection 3.5 and figure 6). The duration of stage A in KK Tel is from the combined O – C diagram (see also subsection 3.27 and figure 27). ASASSN-15rs (subsection 3.87) and DDE 26 (subsection 3.116) may belong to this category.

4.5 Mass ratios from stage A superhumps

Since the new interpretation of stage A as representing the dynamical precession rate at the 3 : 1 resonance in Kato and Osaki (2013b), the application of this method produced a steady stream of q measurements. We list new estimates for q from stage A superhumps in table 8. This table also includes new objects that were studied in detail in other papers. The appropriate references are listed in table 3.

In table 9, we list all stage A superhumps recorded in the present study.

A updated distribution of mass ratios is shown in figure 68 [for the list of objects, see Kato and Osaki (2013b) and Kato et al. (2015a)]. We have newly added PHL 1445 with $P_{\text{orb}} = 0.052985$ d and $q = 0.087(6)$ (McAlister et al. 2015, eclipse observation). It is worth mentioning that Harrison (2016) derived $q \leq 0.071$ for WZ Sge ($P_{\text{orb}} = 0.056688$ d) by infrared spectroscopy of the secondary (not plotted in this figure). The present study has strengthened the concentration of WZ Sge-type dwarf novae around $q = 0.07$ just above the period minimum, as reported in Kato et al. (2015a).

Table 9. Superhump periods during stage A.

Object	Year	Period (d)	Error
EG Aqr	2015	0.08109	0.00022
V1006 Cyg	2015	0.10930	0.00030
V844 Her	2015	0.05703	0.00019
V493 Ser	2015	0.08377	0.00011
KK Tel	2015	0.09005	0.00012
ASASSN-15cl	2016	0.09613	0.00027
ASASSN-15dp	2015	0.06145	0.00013
ASASSN-15ee	2015	0.05794	0.00009
ASASSN-15gn	2015	0.06453	0.00003
ASASSN-15gq	2015	0.06748	0.00018
ASASSN-15hd	2015	0.05703	0.00024
ASASSN-15hm	2015	0.05662	0.00010
ASASSN-15hn	2015	0.06322	0.00016
ASASSN-15kh	2015	0.06155	0.00003
ASASSN-15lt	2015	0.06213	0.00024
ASASSN-15na	2015	0.06491	0.00012
ASASSN-15ni	2015	0.05673	0.00017
ASASSN-15po	2015	0.05178	0.00001
ASASSN-15pu	2015	0.05920	0.00030
ASASSN-15sc	2015	0.05867	0.00009
ASASSN-15uj	2015	0.05664	0.00008
ASASSN-15ux	2015	0.05743	0.00031
ASASSN-16bh	2016	0.05502	0.00010
ASASSN-16bu	2016	0.06159	0.00023
CRTS J095926	2015	0.09079	0.00090
CRTS J200331	2015	0.06058	0.00002
MASTER J073325	2016	0.06209	0.00017
PM J03338	2015	0.07067	0.00005

4.6 WZ Sge-type objects

In table 10, we list the parameters of WZ Sge-type dwarf novae (including likely ones).

It has been known that P_{dot} and P_{orb} are correlated with the rebrightening type [starting with figure 36 in Kato et al. (2009) and refined in Kato et al. (2010, 2012, 2013a, 2014a, 2014b, 2015a) and Kato (2015)]. The five types of outbursts based on rebrightenings are: type-A outbursts (long-duration rebrightening), type-B outbursts (multiple rebrightenings), type-C outbursts (single rebrightening), type-D outbursts (no rebrightening) and type-E outbursts (double superoutburst, with ordinary superhumps only during the second one). In figure 69, we show the updated result up to this paper. In this figure, we also added objects without known rebrightening types. These objects have been confirmed to follow the same trend, which we consider the evolutionary track.

ASASSN-16bh, the very noteworthy and well-observed WZ Sge-type dwarf nova in this study is located at the minimum period [$P_{\text{orb}} = 0.05346$ d, $P_{\text{dot}} = +3.7(3)$]. This object showed a typical type-A rebrightening, in agreement with the trend in other WZ Sge-type dwarf novae.

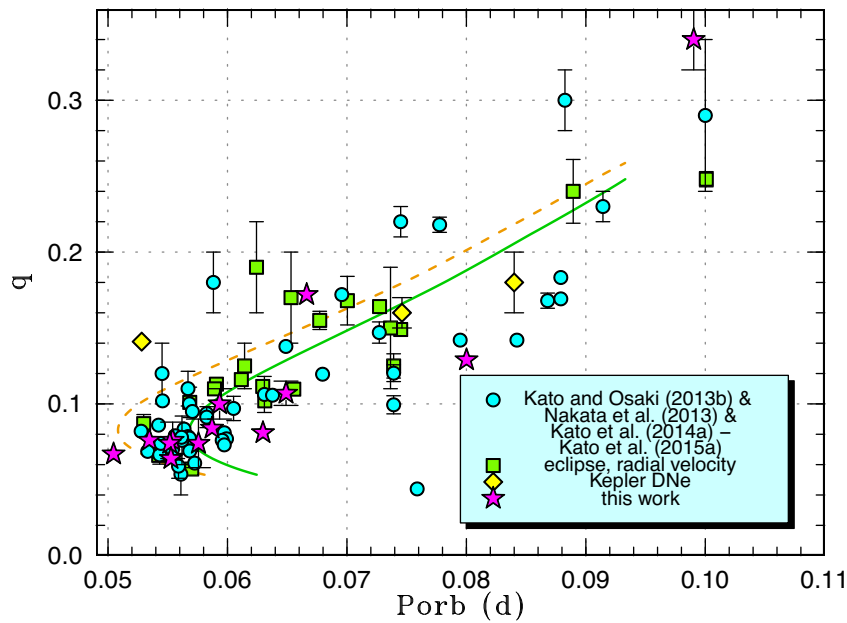


Fig. 68. Mass ratio versus orbital period. The dashed and solid curves represent the standard and optimal evolutionary tracks in Knigge, Baraffe, and Patterson (2011), respectively. The filled circles, filled squares, filled stars, and filled diamonds represent q values from a combination of the estimates from stage A superhumps published in four preceding sources (Kato & Osaki 2013b; Nakata et al. 2013; Kato et al. 2014a, 2014b, 2015a), known q values from quiescent eclipses or radial-velocity study (see Kato & Osaki 2013b for the data source), and q estimated in this work and dwarf novae in the Kepler data (see text for the complete reference), respectively. The objects in “this work” includes objects studied in other papers but listed in table 1. (Color online)

Table 10. Parameters of WZ Sge-type superoutbursts.

Object	Year	P_{SH}	P_{orb}	P_{dot}^*	Error*	ϵ	Type [†]	N_{reb}^{\ddagger}	Delay [§]	Max	Min
RZ Leo	2016	0.078675	0.076030	15.6	5.9	0.035	C	1	–]13.0	18.5
V2051 Oph	2015	0.064708	0.062428	–	–	0.037	–	–	–	–	–
ASASSN-15dp	2015	0.060005	–	0.4	1.1	–	–	–	–]14.1	19.4:
ASASSN-15ee	2015	0.057136	–	8.1	1.2	–	–	–	6	12.6	19.9:
ASASSN-15gq	2015	0.066726	0.06490	11.9	0.8	0.028	–	–	≥ 5]15.4	[21.6
ASASSN-15hd	2015	0.056105	0.05541	1.5	0.3	0.013	C?	≥ 1	11	14.0	21.7
ASASSN-15hn	2015	0.061831	–	–0.5	1.5	–	–	–	13–14	12.9	21.9:
ASASSN-15kh	2015	0.060480	–	1.2	1.6	–	–	–	13	13.2	[21.0
ASASSN-15na	2015	0.063720	0.06297	3.1	2.6	0.012	–	–	≥ 9]14.8	21.5:
ASASSN-15ni	2015	0.055854	0.05517	3.4	0.6	0.012	–	–	10	12.9	21.0:
ASASSN-15po	2015	0.050916	0.050457	1.1	0.1	0.009	A/B	≥ 5	11	13.7	21.6
ASASSN-15pu	2015	0.058254	0.05757	3.3	2.1	0.012	–	–	10	13.7	22.1:
ASASSN-15se	2015	0.063312	–	–	–	–	A/B or B	≥ 2	≥ 5]13.0	20.6
ASASSN-15sl	2015	0.091065	0.087048	9.1	2.6	0.046	–	–	–	–	–
ASASSN-15uj	2015	0.055805	0.055266	–1.1	1.6	0.010	–	–	10	14.3	21.0:
ASASSN-15ux	2015	0.056857	0.056109	–	–	0.013	–	–	14	14.4	[21.0
ASASSN-16bh	2016	0.054027	0.05346	3.7	0.3	0.011	A	1	7	12.7	20.3:
ASASSN-16bi	2016	–	0.05814	–	–	–	–	–	12:	14.3	[20.6
ASASSN-16bu	2016	0.060513	0.05934	–	–	0.020	–	–	9	14.5	22.1
CRTS J200331	2015	0.059720	0.058705	–	–	0.017	–	–	–	–	–
SDSS J074859	2015	0.05958	0.058311	–	–	0.022	–	–	–	–	–
SDSS J145758	2015	0.054912	0.054087	2.2	2.9	0.015	–	–	–	11.9	29.5

*In units of 10^{-5} .

[†]A: Long-lasting rebrightening; B: Multiple rebrightenings; C: Single rebrightening; A/B: intermediate type between A and B.

[‡]Number of rebrightenings.

[§]Days before ordinary superhumps appeared.

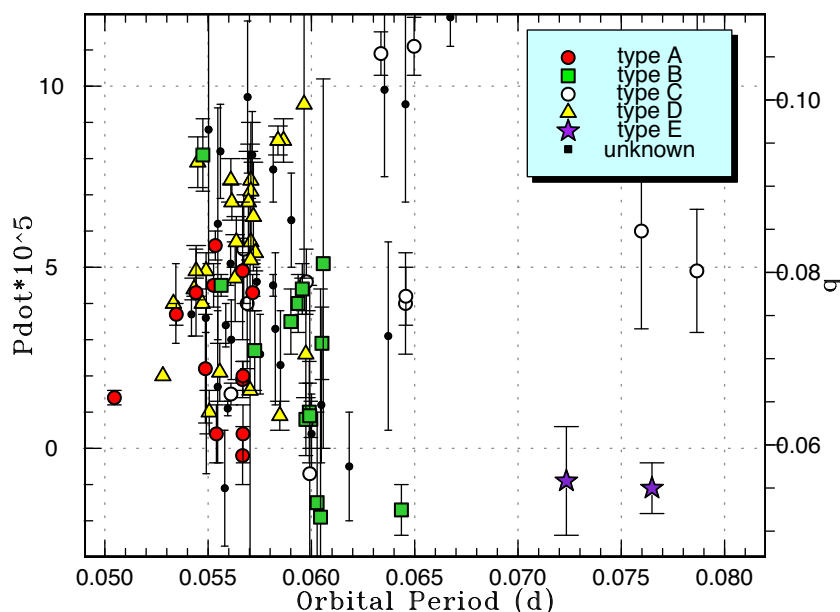


Fig. 69. P_{dot} versus P_{orb} for WZ Sge-type dwarf novae. Symbols represent the type of outburst: type-A (filled circles), type-B (filled squares), type-C (filled triangles), type-D (open circles), and type-E (filled stars) (see text for details). On the right-hand side, we show mass ratios estimated using equation (6) in Kato (2015). We can regard this figure as representing an evolutionary diagram. (Color online)

ASASSN-15po is an outlier ($P_{\text{orb}} = 0.05092$ d) in the figure below the period minimum of most of the objects. This object may be similar to OV Boo = SDSS J150722.33+523039.8, which has an orbital period of 0.046258 d (Littlefair et al. 2007; Patterson et al. 2008; Uthas et al. 2011). Although the spectroscopic features strongly suggest the dwarf nova-type (probably WZ Sge-type) nature, OV Boo has not been yet recorded in major outburst. ASASSN-15po is the first object below the period minimum which has undergone a typical WZ Sge-type superoutburst. The details of the outburst are discussed in Namekata et al. (2016).

4.7 Lessons from recent observations

Thanks to the increase of discoveries of new dwarf novae and detections of outbursts by modern surveys (such as ASAS-SN), the number of studied objects has dramatically increased in recent years. This increase has indeed improved our knowledge in the distribution of CVs below the period gap (e.g., subsection 4.1). The fraction of well-observed superoutbursts, however, largely decreased. For example, the number of “A” class (well-observed) observations decreased from 58 (out of 363 outbursts) in Kato et al. (2009) to six (out of 65 outbursts) in Kato et al. (2010) to five (out of 107 outbursts). Although such a qualification of observations is subjective and the criteria may have not necessarily been the same, the increase of “underobserved” outbursts is apparent despite the increase in observations (figure 70).

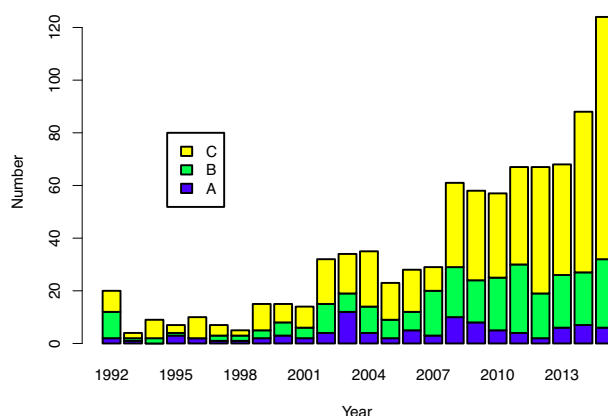


Fig. 70. Quality of observations (A: excellent, B: partial coverage or slightly low quality, C: insufficient coverage or observations with large scatter). The year represents the year of outburst. The year 1992 represents outbursts up to 1992, and the year 2015 includes the outbursts in 2016. (Color online)

The same trend is even more apparent in WZ Sge-type outbursts. In Kato et al. (2009, 2010, 2012, 2013a), 55 WZ Sge-type outbursts (out of 66) had observations to classify the rebrightening pattern. In the present study, only five WZ Sge-type outbursts (out of 18) have rebrightening classifications. Such a trend is fatal, since rebrightenings are one of the key elements in the study of WZ Sge-type dwarf novae (cf. Kato 2015).

These trends in observations probably reflect the increase in freshly discovered objects or outbursts, which would easily divert observers’ attention. In order that the observations will be more astrophysically beneficial and rewarding

to observers, we propose the following lessons from recent observations. Although some of the lessons may be evident, we list them as they will be useful for those who wish to start contributing to this field, and they are not usually written in practical textbooks (such as Hellier 2001).

- Single-night observations have very limited value (except for classification of the object and the initial detection of superhumps). If there are observations on more than two nights (hopefully consecutive nights), we can determine the superhump period to better than 0.2% (1σ error), necessary to make comparison with the orbital period. Periods from single-night observations have large errors, typically 1%–3%, which is completely insufficient to make comparison with the orbital one.
- Once the object is observed, do not lightly change the target. In general, fresh outbursts tend to be “overobserved” (observations are sometimes redundant) while they become underobserved as the outbursts progresses. There may not be many observations in the later phase and observations of such a phase can be relatively more important. We should note, however, that objects may become too faint or the amplitudes of superhumps become too small to make useful observations. In such cases, we recommend nightly snapshots.
- Even after the superoutburst ends, regularly visit the target and obtain snapshot observations. This is particularly apt for WZ Sge-type dwarf novae. If there is a major rebrightening, restart time-resolved photometry.
- For detecting stage A superhumps, which is very important to estimate mass ratios, early observations are very important. Even a 1-d gap in the observation could be fatal. In WZ Sge-type dwarf novae, there is usually a long waiting time (~ 10 d) before stage A superhumps appear. Although observations in this phase may not appear so appealing, since early superhumps may become less apparent and amplitudes of variations become smaller, this phase is astrophysically more important (compared to the phase after full growth of superhumps) and it is a waste to miss this phase.

5 Summary

In addition to the updated statistics of the period distribution, the $P_{\text{orb}}-P_{\text{dot}}$ relation, the updated evolutionary track using stage A superhumps, and the refined relationship between $P_{\text{orb}}-P_{\text{dot}}$ versus the rebrightening type in WZ Sge-type dwarf novae, the objects of special interest in this paper can be summarized as follows.

- V452 Cas ($P_{\text{SH}} \sim 0.0888$ d), KK Tel ($P_{\text{SH}} \sim 0.0876$ d), and ASASSN-15cl ($P_{\text{SH}} \sim 0.0946$ d) appear to have a long-lasting stage A. They would be members of a growing

group of long- P_{orb} objects with slowly growing superhumps. A slow growth of the 3 : 1 resonance near the stability border has been proposed (Kato et al. 2016a; also Kato et al. 2014b). If the mass ratios for these objects are determined by measuring P_{orb} , they would provide an excellent test for this interpretation.

- The WZ Sge-type object RZ Leo underwent a well-observed superoutburst in 2016. No clear evidence of early superhumps was detected. This object showed a strong beat phenomenon between the superhump and orbital periods.
- ASASSN-15cy is an object below the period minimum ($P_{\text{SH}} \sim 0.0500$ d). This object showed a superoutburst resembling the EI Psc-type object CSS J174033.5+414756.
- ASASSN-15hd is a WZ Sge-type dwarf nova showing large-amplitude early superhumps with a “saw-tooth”-like profile.
- ASASSN-15gn ($P_{\text{SH}} \sim 0.0636$ d), ASASSN-15hn ($P_{\text{SH}} \sim 0.0618$ d), ASASSN-15kh ($P_{\text{SH}} \sim 0.0605$ d), and ASASSN-16bu ($P_{\text{SH}} \sim 0.0609$ d) are possibly period bouncers as judged from the slow growth of ordinary superhumps and small amplitudes of superhumps.
- ASASSN-15na is a WZ Sge-type dwarf with a relatively long orbital period (0.06297 d). The object, however, appears to have a larger q than expected for a period bouncer.
- ASASSN-15ni is a WZ Sge-type dwarf nova showing a superoutburst typical for this class.
- ASASSN-15sl and SDSS J074859 are eclipsing systems and we have also determined the orbital periods using eclipse observations.
- ASASSN-15uj is a WZ Sge-type dwarf nova with a low $q = 0.064(4)$, indicating its relatively evolved state.
- ASASSN-15ux is a rare eclipsing WZ Sge-type dwarf nova.
- ASASSN-16bh is a WZ Sge-type dwarf nova showing a relatively rare plateau-type, long rebrightening (without small rebrightenings in it). This object also showed early superhumps with three maxima in one cycle.
- CRTS J200331 is an eclipsing SU UMa-type or WZ Sge-type dwarf nova, probably near the border between SU UMa-type and WZ Sge-type objects.

Acknowledgements

This work was supported by the Grant-in-Aid “Initiative for High-Dimensional Data-Driven Science through Deepening of Sparse Modeling” (25120007) from the Ministry of Education, Culture, Sports, Science and Technology (MEXT) of Japan. The authors are grateful to observers of VSNET Collaboration and VSOLJ observers who supplied vital data. We acknowledge with thanks the variable star observations from the AAVSO International Database

contributed by observers worldwide and used in this research. We are also grateful to the VSOLJ database. This work is deeply indebted to outburst detections and announcement by a number of variable star observers worldwide, including participants of CVNET and BAA VSS alert. The CCD operation of the Bronberg Observatory is partly sponsored by the Center for Backyard Astrophysics. We are grateful to the Catalina Real-time Transient Survey team for making their real-time detection of transient objects available to the public. This research has made use of the SIMBAD database, operated at CDS, Strasbourg, France. This research has made use of the International Variable Star Index (VSX) database, operated at AAVSO, Cambridge, Massachusetts, USA.

Supporting information

Additional supporting information can be found in the online version of this article:

E-tables 1–109

E-figures 1–92

[Supplementary data is available at PASJ Journal online.](#)

References

- Abazajian, K. N., et al. 2009, *ApJS*, 182, 543
- Ahn, C. P., et al. 2012, *ApJS*, 203, 21
- Ahnert-Rohlfs, E. 1952, *Mitteil. Veränderl. Sterne*, 158
- Andrade, E. L., & Baptista, R. 2014, *Rev. Mex. Astron. Astrofis., Ser. Conf.*, 44, 145
- Angel, R., Liebert, J., & Stockman, H. 1977, *IAU Circ.*, 3065, 3
- Antipin, S. V. 1996a, *IBVS*, 4343
- Antipin, S. V. 1996b, *IBVS*, 4360
- Antipin, S. V. 1999, *IBVS*, 4673, 1
- Baba, H., Kato, T., Nogami, D., Hirata, R., Matsumoto, K., & Sadakane, K. 2000, *PASJ*, 52, 429
- Bakowska, K., Olech, A., Zloczewski, K., & Wisniewski, M. 2010, *Acta Astron.*, 60, 137
- Balayan, S. K. 1997, *Astrophysics*, 40, 211
- Baptista, R. 2012, *Mem. Soc. Astron. Ital.*, 83, 530
- Baptista, R., Borges, B. W., Bond, H. E., Jablonski, F., Steiner, J. E., & Grauer, A. D. 2003, *MNRAS*, 345, 889
- Baptista, R., & Bortoletto, A. 2004, *AJ*, 128, 411
- Baptista, R., Catalán, M. S., Horne, K., & Zilli, D. 1998, *MNRAS*, 300, 233
- Baptista, R., Santos, R. F., Faúndez-Abans, M., & Bortoletto, A. 2007, *AJ*, 134, 867
- Barentsen, G., et al. 2014, *MNRAS*, 444, 3230
- Bateson, F. M. 1982, *Publ. Variable Stars Sect., R. Astron. Soc. New Zealand*, 9, 1
- Bateson, F., McIntosh, R., & Stubbings, R. 2000, *Publ. Variable Stars Sect., R. Astron. Soc. New Zealand*, 24, 48
- Berardi, P. 2015, *Astronomer's Telegram*, 7854
- Bertaud, C. 1951, *Ann. Astrophys.*, 14, 199
- Bond, H. E. 1978, *PASP*, 90, 526
- Bond, H. E. 1979, in *IAU Colloq. 53, White Dwarfs and Variable Degenerate Stars*, ed. H. M. van Horn & V. Weidemann (University of Rochester), 495
- Bond, H. E., Wagner, R. L., & Tapia, S. 1977, *IAU Circ.*, 3049
- Boyd, D., Graham, K., Kato, T., Koff, R., Miller, I., Oksanen, A., Pickard, R., & Poyner, G. 2009, *J. Br. Astron. Assoc.*, 119, 251
- Boyle, B. J., Shanks, T., Croom, S. M., Smith, R. J., Miller, L., Loaring, N., & Heymans, C. 2000, *MNRAS*, 317, 1014
- Breedt, E., et al. 2014, *MNRAS*, 443, 3174
- Bruch, A. 2000, *A&A*, 359, 998
- Bruch, A., Fischer, F.-J., & Wilmens, U. 1987, *A&AS*, 70, 481
- Bruch, A., & Schimpke, T. 1992, *A&AS*, 93, 419
- Brun, A., & Petit, M. 1957, *Perem. Zvezdy*, 12, 18
- Busch, H., Häußler, K., & Splittgerber, E. 1979, *Veröff. Sternw. Sonneberg*, 9, 125
- Cannizzo, J. K., Still, M. D., Howell, S. B., Wood, M. A., & Smale, A. P. 2010, *ApJ*, 725, 1393
- Cao, Y., & Kulkarni, S. R. 2014, *Astronomer's Telegram*, 6221
- Cleveland, W. S. 1979, *J. Amer. Statist. Assoc.*, 74, 829
- Cook, M. C., & Brunt, C. C. 1983, *MNRAS*, 205, 465
- Cristiani, H., Duerbeck, H. W., & Seitter, W. C. 1985, *IAU Circ.*, 4027
- Cutri, R. M., et al. 2003, *2MASS All Sky Catalog of Point Sources (NASA/IPAC Infrared Science Archive)*
- Dai, Z., Szkody, P., Garnavich, P. M., & Kennedy, M. 2016, *AJ*, 152, 5
- Danilet, A. B., et al. 2015, *Astronomer's Telegram*, 7260
- Davis, A. B., et al. 2014, *Astronomer's Telegram*, 6211
- Davis, A. B., Shappee, B. J., & Archer Shappee, B. 2015, *AAS Meeting*, 225, 344.02
- Denisenko, D. V. 2012, *Astron. Lett.*, 38, 249
- Denisenko, D., et al. 2013a, *Astronomer's Telegram*, 5065
- Denisenko, D., et al. 2013b, *Astronomer's Telegram*, 5111
- Dong, S., et al. 2015, *Astronomer's Telegram*, 7850
- Downes, R. A. 1990, *AJ*, 99, 339
- Downes, R., Webbink, R. F., & Shara, M. M. 1997, *PASP*, 109, 345
- Drake, A. J., et al. 2009, *ApJ*, 696, 870
- Drake, A. J., et al. 2014, *MNRAS*, 441, 1186
- Drew, J. E., et al. 2005, *MNRAS*, 362, 753
- Echevarria, J., & Alvarez, M. 1993, *A&A*, 275, 187
- Fernie, J. D. 1989, *PASP*, 101, 225
- Goranskij, V. P. 1972, *Astron. Tsirk.*, 696
- Gorbovskoy, E. S., et al. 2013, *Astron. Rep.*, 57, 233
- Green, R. F., Ferguson, D. H., Liebert, J., & Schmidt, M. 1982, *PASP*, 94, 560
- Greiss, S., et al. 2012, *AJ*, 144, 24
- Gress, O., et al. 2015a, *Astronomer's Telegram*, 7237
- Gress, O., et al. 2015b, *Astronomer's Telegram*, 7972
- Gress, O., et al. 2016a, *Astronomer's Telegram*, 8596
- Gress, O., et al. 2016b, *Astronomer's Telegram*, 8730
- Hamilton, R. T., Harrison, T. E., Tappert, C., & Howell, S. B. 2011, *ApJ*, 728, 16
- Haro, G., & Chavira, E. 1960, *Bol. Obs. Tonantzintla y Tacubaya*, 2, 11
- Harrison, T. E. 2016, *ApJ*, 816, 4
- Hellier, C. 2001, *Cataclysmic Variable Stars: How And Why They Vary* (Berlin: Springer)
- Herbig, G. H. 1958, *PASP*, 70, 605
- Hirose, M., & Osaki, Y. 1990, *PASJ*, 42, 135
- Hirose, M., & Osaki, Y. 1993, *PASJ*, 45, 595
- Hoffleit, D. 1935, *Harvard Coll. Obs. Bull.*, 901, 20
- Hoffmeister, C. 1949, *Erg. Astron. Nachr.*, 12, 1
- Hoffmeister, C. 1957, *Mitteil. Veränderl. Sterne*, 245
- Hoffmeister, C. 1963a, *IBVS*, 24

- Hoffmeister, C. 1963b, *Veröff. Sternw. Sonneberg*, 6, 1
- Hoffmeister, C. 1966, *Astron. Nachr.*, 289, 139
- Hoffmeister, C. 1967, *Astron. Nachr.*, 290, 43
- Hoppe, J. 1935, *Astron. Nachr.*, 254, 369
- Howell, S. B., De Young, J., Mattei, J. A., Foster, G., Szkody, P., Cannizzo, J. K., Walker, G., & Fierce, E. 1996, *AJ*, 111, 2367
- Howell, S. B., Dobrzycka, D., Szkody, P., & Kreidl, T. J. 1991, *PASP*, 103, 300
- Howell, S. B., Harrison, T. E., Szkody, P., & Silvestri, N. M. 2010, *AJ*, 139, 1771
- Howell, S., & Szkody, P. 1988, *PASP*, 100, 224
- Hurst, G. M., Lubbock, S., & McNaught, R. H. 1987, *IAU Circ.*, 4504
- Imada, A., et al. 2008, *PASJ*, 60, 1151
- Imada, A., Kato, T., Monard, L. A. G., Retter, A., Liu, A., & Nogami, D. 2006, *PASJ*, 58, 383
- Ishioka, R., et al. 2001, *PASJ*, 53, 905
- Ishioka, R., et al. 2002, *A&A*, 381, L41
- Ishioka, R., Uemura, M., Kato, T., Iwamatsu, H., Matsumoto, K., Billings, G., Masi, G., & Kiyota, S. 2000, *IAU Circ.*, 7552
- Isogai, K., et al. 2016, *PASJ*, 68, 64
- Kato, T. 1991, *IBVS*, 3671
- Kato, T. 1995, *IBVS*, 4239
- Kato, T. 2001a, *IBVS*, 5107
- Kato, T. 2001b, *IBVS*, 5110
- Kato, T. 2002, *PASJ*, 54, L11
- Kato, T. 2015, *PASJ*, 67, 108
- Kato, T., et al. 2003b, *MNRAS*, 339, 861
- Kato, T., et al. 2009, *PASJ*, 61, S395
- Kato, T., et al. 2010, *PASJ*, 62, 1525
- Kato, T., et al. 2012, *PASJ*, 64, 21
- Kato, T., et al. 2013a, *PASJ*, 65, 23
- Kato, T., et al. 2014a, *PASJ*, 66, 30
- Kato, T., et al. 2014b, *PASJ*, 66, 90
- Kato, T., et al. 2014c, *PASJ*, 66, L7
- Kato, T., et al. 2015a, *PASJ*, 67, 105
- Kato, T., et al. 2016a, *PASJ*, 68, L4
- Kato, T., et al. 2016b, *PASJ*, 68, 49
- Kato, T., Fujino, S., & Iida, M. 1989, *VSOLJ Variable Star Bull.*, 9, 33
- Kato, T., Hamsch, F.-J., & Monard, B. 2015b, *PASJ*, 67, L2
- Kato, T., Kunjaya, C., Okyudo, M., & Takahashi, A. 1994, *PASJ*, 46, L199
- Kato, T., & Matsumoto, K. 1999a, *IBVS*, 4765
- Kato, T., & Matsumoto, K. 1999b, *IBVS*, 4767
- Kato, T., Monard, B., Hamsch, F.-J., Kiyota, S., & Maehara, H. 2013b, *PASJ*, 65, L11
- Kato, T., & Nogami, D. 1995, *IBVS*, 4260
- Kato, T., Nogami, D., Baba, H., Matsumoto, K., Arimoto, J., Tanabe, K., & Ishikawa, K. 1996a, *PASJ*, 48, L21
- Kato, T., Nogami, D., Moilanen, M., & Yamaoka, H. 2003a, *PASJ*, 55, 989
- Kato, T., Nogami, D., Masuda, S., & Hirata, R. 1996b, *PASJ*, 48, 45
- Kato, T., & Osaki, Y. 2013a, *PASJ*, 65, 97
- Kato, T., & Osaki, Y. 2013b, *PASJ*, 65, 115
- Kato, T., Stubbings, R., Monard, B., Butterworth, N. D., Bolt, G., & Richards, T. 2004a, *PASJ*, 56, S89
- Kato, T., Stubbings, R., Nelson, P., Pearce, A., Garradd, G., & Kiyota, S. 2001, *IBVS*, 5159
- Kato, T., & Uemura, M. 2000, *IBVS*, 4902
- Kato, T., Uemura, M., Ishioka, R., Nogami, D., Kunjaya, C., Baba, H., & Yamaoka, H. 2004b, *PASJ*, 56, S1
- Kazarovets, E. V., Kireeva, N. N., Samus, N. N., & Durlevich, O. V. 2003, *IBVS*, 5422
- Kazarovets, E. V., Samus, N. N., Durlevich, O. V., Kireeva, N. N., & Pastukhova, E. N. 2011, *IBVS*, 5969
- Kazarovets, E. V., Samus, N. N., Durlevich, O. V., Kireeva, N. N., & Pastukhova, E. N. 2015a, *IBVS*, 6151
- Kazarovets, E. V., Samus, N. N., Durlevich, O. V., Kireeva, N. N., & Pastukhova, E. N. 2015b, *IBVS*, 6155
- Kepler Mission Team 2009, *VizieR Online Data Catalog*, V/133
- Khatsov, A. Sh. 1971, *Abastumanskaya Astrofiz. Obs. Byull.*, 40, 13
- Kholopov, P. N., et al. 1985, *General Catalogue of Variable Stars*, 4th edition (Moscow: Nauka Publishing House)
- Khruslov, A. V. 2005, *Perem. Zvezdy, Prilozh.*, 5, 4
- Kimura, M., et al. 2016a, *PASJ*, 68, L2
- Kimura, M., et al. 2016b, *PASJ*, 68, 55
- Kiyota, S., & Kato, T. 1998, *IBVS*, 4644
- Knigge, C., Baraffe, I., & Patterson, J. 2011, *ApJS*, 194, 28
- Koch, D. G., et al. 2010, *ApJ*, 713, L79
- Kryachko, T. V. 2001, *IBVS*, 5058
- Kukarkin, B. V., et al. 1982, *New Catalogue of Suspected Variable Stars* (Moscow: Nauka Publishing House)
- Kurochkin, N. E. 1977, *Astron. Tsirk.*, 974, 4
- Lasker, B., et al. 2007, *VizieR Online Data Catalog*, I/305
- Levitan, D., Groot, P. J., Prince, T. A., Kulkarni, S. R., Laher, R., Ofek, E. O., Sesar, B., & Surace, J. 2015, *MNRAS*, 446, 391
- Littlefair, S. P., Dhillon, V. S., Marsh, T. R., Gänsicke, B. T., Baraffe, I., & Watson, C. A. 2007, *MNRAS*, 381, 827
- Liu, Wu., Hu, J. Y., Zhu, X. H., & Li, Z. Y. 1999, *ApJS*, 122, 243
- Longa-Peña, P., Steeghs, D., & Marsh, T. 2015, *MNRAS*, 447, 149
- Lubow, S. H. 1991, *ApJ*, 381, 259
- Lubow, S. H. 1992, *ApJ*, 401, 317
- Luyten, W. J., & Haro, G. 1959, *PASP*, 71, 469
- McAllister, M. J., et al. 2015, *MNRAS*, 451, 4633
- McNaught, R. H. 1985, *IAU Circ.*, 4036
- Mattei, J., Ducoty, R., Stanton, R., & Scovill, C. 1985, *IAU Circ.*, 4026
- Mattei, J., Isles, J., & Lubbock, S. 1987, *IAU Circ.*, 4506
- Mattei, J. A., Stubbings, R., & Dubovsky, P. 2000, *IAU Circ.*, 7547
- Mayall, M. W. 1968, *JRASC*, 62, 141
- Mayall, M. W. 1970, *JRASC*, 64, 205
- Mennicken, R., & Vogt, N. 1993, *Rev. Mexicana Astron. Astrof.*, 26, 111
- Mennickent, R. E., & Diaz, M. P. 2002, *MNRAS*, 336, 767
- Mennickent, R. E., Sterken, C., Gieren, W., & Unda, E. 1999, *A&A*, 352, 239
- Mennickent, R. E., & Tappert, C. 2001, *A&A*, 372, 563
- Meyer, F., & Meyer-Hofmeister, E. 2015, *PASJ*, 67, 52
- Monet, D. B. A., et al. 1998, *VizieR Online Data Catalog*, I/252
- Montgomery, M. M. 2001, *MNRAS*, 325, 761
- Morgenroth, O. 1934, *Astron. Nachr.*, 253, 441
- Motch, C., et al. 1998, *A&AS*, 132, 341
- Munari, U., & Zwitter, T. 1998, *A&AS*, 128, 277

- Murray, J. R. 1998, *MNRAS*, 297, 323
- Nakata, C., et al. 2013, *PASJ*, 65, 117
- Nakata, C., et al. 2014, *PASJ*, 66, 116
- Namekata, K., et al. 2016, *PASJ* submitted
- Narumi, H., Korh, S., Dyck, G., Iida, M., & Hurst, G. 1989, *IAU Circ.*, 4757
- Nesci, R., Caravano, A., Falasca, V., & Villani, L. 2013, *IBVS*, 6059
- Nogami, D., et al. 2003, *A&A*, 404, 1067
- Nogami, D., & Kato, T. 1997, *PASJ*, 49, 109
- Nogami, D., Kato, T., Baba, H., Matsumoto, K., Arimoto, J., Tanabe, K., & Ishikawa, K. 1997, *ApJ*, 490, 840
- Nogami, D., Monard, B., Retter, A., Liu, A., Uemura, M., Ishioka, R., Imada, A., & Kato, T. 2004, *PASJ*, 56, L39
- Nogami, D., Uemura, M., Ishioka, R., Kato, T., & Pietz, J. 2004, *PASJ*, 56, S155
- Novák, R. 1997, *IBVS*, 4489
- O'Donoghue, D., Chen, A., Marang, F., Mittaz, J. P. D., Winkler, H., & Warner, B. 1991, *MNRAS*, 250, 363
- Ohshima, T., et al. 2014, *PASJ*, 66, 67
- Oizumi, S., et al. 2007, *PASJ*, 59, 643
- Olech, A., Schwarzenberg-Czerny, A., Kędzierski, P., Złoczewski, K., Mularczyk, K., & Wiśniewski, M. 2003, *Acta Astron.*, 53, 175
- Osaki, Y. 1989, *PASJ*, 41, 1005
- Osaki, Y. 1996, *PASP*, 108, 39
- Osaki, Y., & Kato, T. 2013a, *PASJ*, 65, 50
- Osaki, Y., & Kato, T. 2013b, *PASJ*, 65, 95
- Osaki, Y., & Kato, T. 2014, *PASJ*, 66, 15
- Osaki, Y., & Meyer, F. 2002, *A&A*, 383, 574
- Osaki, Y., & Meyer, F. 2003, *A&A*, 401, 325
- Papadaki, C., Boffin, H. M. J., Steeghs, D., & Schmidtobreick, L. 2008, *A&A*, 487, 611
- Parsamyan, E. S., Oganyan, G. B., Kazaryan, E. S., & Yankovich, I. I. 1983, *Astron. Tsirk.*, 1269, 7
- Patterson, J. 1980, *J. American Assoc. Variable Star Obs.*, 9, 49
- Patterson, J. 1998, *PASP*, 110, 1132
- Patterson, J., et al. 2003, *PASP*, 115, 1308
- Patterson, J., Thorstensen, J. R., & Knigge, C. 2008, *PASP*, 120, 510
- Patterson, J., Augusteijn, T., Harvey, D. A., Skillman, D. R., Abbott, T. M. C., & Thorstensen, J. 1996, *PASP*, 108, 748
- Pavlenko, E. P., et al. 2014, *PASJ*, 66, 111
- Pearson, K. J. 2006, *MNRAS*, 371, 235
- Petit, M. 1960, *J. Obs.*, 43, 17
- Pinto, G., & Romano, G. 1972, *Mem. Soc. Astron. Ital.*, 43, 135
- Pinto, G., & Romano, G. 1976, *Mem. Soc. Astron. Ital.*, 47, 229
- Pojmański, G. 2002, *Acta Astron.*, 52, 397
- Prieto, J. L., et al. 2013, *Astronomer's Telegram*, 4999
- Prieto, J. L., et al. 2014, *Astronomer's Telegram*, 6249
- Richter, G. A. 1969, *Mitteil. Veränderl. Sterne*, 5, 69
- Richter, G. A. 1985, *IBVS*, 2714
- Ritter, H., & Kolb, U. 2003, *A&A*, 404, 301
- Romano, G., & Minello, S. 1976, *IBVS*, 1140
- Rosino, L., & Candeo, G. 1989, *IAU Circ.*, 4900
- Rutkowski, A., Olech, A., Mularczyk, K., Boyd, D., Koff, R., & Wisniewski, M. 2007, *Acta Astron.*, 57, 267
- Rutkowski, A., Pietrukowicz, P., Olech, A., Ak, T., Złoczewski, K., Poleski, R., Tappert, C., & Eker, Z. 2011, *Acta Astron.*, 61, 345
- Saito, R. K., & Baptista, R. 2006, *AJ*, 131, 2185
- Sanduleak, N. 1972, *IBVS*, 663
- Shappee, B. J., et al. 2013, *Astronomer's Telegram*, 5052
- Shappee, B. J., et al. 2014, *ApJ*, 788, 48
- Shears, J., Lloyd, C., Boyd, D., Brady, S., Miller, I., & Pickard, R. 2009, *J. Br. Astron. Assoc.*, 119, 31
- Shears, J., Wils, P., Bolt, G., Hamsch, F.-J., Krajci, T., Miller, I., Sabo, R., & Staels, B. 2011, *J. Br. Astron. Assoc.*, 121, 155
- Sheets, H. A., Thorstensen, J. R., Peters, C. J., Kapusta, A. B., & Taylor, C. J. 2007, *PASP*, 119, 494
- Shurpakov, S., et al. 2013, *Astronomer's Telegram*, 5083
- Simonian, G., et al. 2015, *Astronomer's Telegram*, 7809
- Simonian, G., et al. 2016, *Astronomer's Telegram*, 8648
- Skiff, B. A. 1999, *IBVS*, 4675
- Skinner, J. N., Thorstensen, J. R., & Lépine, S. 2014, *AJ*, 148, 115
- Smak, J. I. 1991, *Acta Astron.*, 41, 269
- Smart, R. L. 2013, *VizieR Online Data Catalog*, I/324
- Southworth, J., et al. 2008, *MNRAS*, 391, 591
- Stanek, K. Z., et al. 2013, *Astronomer's Telegram*, 5082
- Stanek, K. Z., et al. 2015, *Astronomer's Telegram*, 8068
- Steeghs, D., O'Brien, K., Horne, K., Gomer, R., & Oke, J. B. 2001, *MNRAS*, 323, 484
- Stellingwerf, R. F. 1978, *ApJ*, 224, 953
- Szkody, P. 1987, *ApJS*, 63, 685
- Szkody, P., et al. 2002, *AJ*, 123, 430
- Szkody, P., et al. 2005, *AJ*, 129, 2386
- Szkody, P., et al. 2009, *AJ*, 137, 4011
- Szkody, P., & Howell, S. B. 1992, *ApJS*, 78, 537
- Tappert, C., Mennickent, R. E., Arenas, J., Matsumoto, K., & Hanuschik, R. W. 2003, *A&A*, 408, 651
- Tchäpe, R. 1963, *Mitteil. Veränderl. Sterne*, 2, 3
- Thorstensen, J. R., & Fenton, W. H. 2003, *PASP*, 115, 37
- Thorstensen, J. R., Patterson, J. O., Kemp, J., & Vennes, S. 2002, *PASP*, 114, 1108
- Thorstensen, J. R., Patterson, J. O., Shambrook, A., & Thomas, G. 1996, *PASP*, 108, 73
- Uemura, M., et al. 2008, *IBVS*, 5815, 1
- Uthas, H. 2011, PhD thesis, University of Southampton ([arXiv:1105.1164](https://arxiv.org/abs/1105.1164))
- Uthas, H., et al. 2012, *MNRAS*, 420, 379
- Uthas, H., Knigge, C., Long, K. S., Patterson, J., & Thorstensen, J. 2011, *MNRAS*, 414, L85
- Voges, W., et al. 1999, *A&A*, 349, 389
- Vogt, N. 1983, *A&A*, 118, 95
- Vogt, N., & Bateson, F. M. 1982, *A&AS*, 48, 383
- Vriellmann, S., & Offutt, W. 2000, *New Astron. Rev.*, 44, 39P
- Vriellmann, S., & Offutt, W. 2003, *MNRAS*, 338, 165
- Vriellmann, S., Stiening, R. F., & Offutt, W. 2002, *MNRAS*, 334, 608
- Warner, B. 1995a, *Cataclysmic Variable Stars* (Cambridge: Cambridge University Press)
- Warner, B. 1995b, *Ap&SS*, 226, 187
- Warner, B., & Cropper, M. 1983, *MNRAS*, 203, 909
- Warner, B., & O'Donoghue, D. 1987, *MNRAS*, 224, 733
- Watts, D. J., Bailey, J., Hill, P. W., Greenhill, J. G., McCowage, C., & Carty, T. 1986, *A&A*, 154, 197
- Webbink, R. F., Hazen, M. L., & Hoffleit, D. 2002, *IBVS*, 5298
- Wenzel, W. 1984, *IBVS*, 2481

- Whitehurst, R. 1988, MNRAS, 232, 35
- Wils, P., Gänsicke, B. T., Drake, A. J., & Southworth, J. 2010, MNRAS, 402, 436
- Witham, A. R., Knigge, C., Drew, J. E., Greimel, R., Steeghs, D., Gänsicke, B. T., Groot, P. J., & Mampaso, A. 2008, MNRAS, 384, 1277
- Wojcikiewicz, E., & Baptista, R. 2014, Rev. Mex. Astron. Astrofis. Ser. Conf., 44, 170
- Wolf, M. 1919, Astron. Nachr., 209, 85
- Wood, M. A., Still, M. D., Howell, S. B., Cannizzo, J. K., & Smale, A. P. 2011, ApJ, 741, 105
- Woudt, P. A., & Warner, B. 2010, MNRAS, 403, 398
- Yamaoka, H., Itagaki, K., Maehara, H., & Nakano, S. 2008, Cent. Bur. Electron. Telegrams, 1535
- Zacharias, N., et al. 2015, AJ, 150, 101